

Molecular Studies of Surfaces under Reaction Conditions; Sum
Frequency Generation Vibrational Spectroscopy, Scanning
Tunneling Microscopy and Ambient Pressure X-ray
Photoelectron Spectroscopy

Gabor A. Somorjai

Department of Chemistry and
Lawrence Berkeley National Laboratory
University of California, Berkeley

Evolution of Surface Science

Nanosciences

Monodispersed nanoparticles 2D and 3D

Applications in Catalysis, Tribology, Polymers,
Biointerfaces, Microelectronics, Energy Conversions,
Environmental Chemistry, Electrochemistry, Corrosion

Surface Instruments at High Pressures, Liquid Interfaces
(STM, SFG, AFM, QCM, RAIRS)

Surface Dynamics

Rapid energy transfer between incident and product molecules
Mobility of the adsorbed molecules along surfaces during catalytic turnover

Surface Thermodynamics

Adsorbate coverage dependent heats of adsorption
Coadsorption induced ordering
Surface segregation

Surface Structure and Bonding

Clean surface reconstruction
Adsorbate induced restructuring
Surface defects (steps, kinks) are chemically active

Model Surfaces - Single Crystals, (Metals, Semiconductors)

Surface Instruments in Vacuum (XPS, AES, LEED, SIMS)

Surface Science Techniques for Gas/Solid or Liquid/Solid Interfaces

Photon-in and Photon-out:

IR spectroscopy, Raman spectroscopy, Sum-frequency generation vibrational spectroscopy, X-ray emission spectroscopy, Surface X-ray diffraction, X-ray absorption fine structure

Surface probe microscopy:

Scanning Tunneling Microscopy, Atomic Force Microscopy

Photon-in and Electron-out:

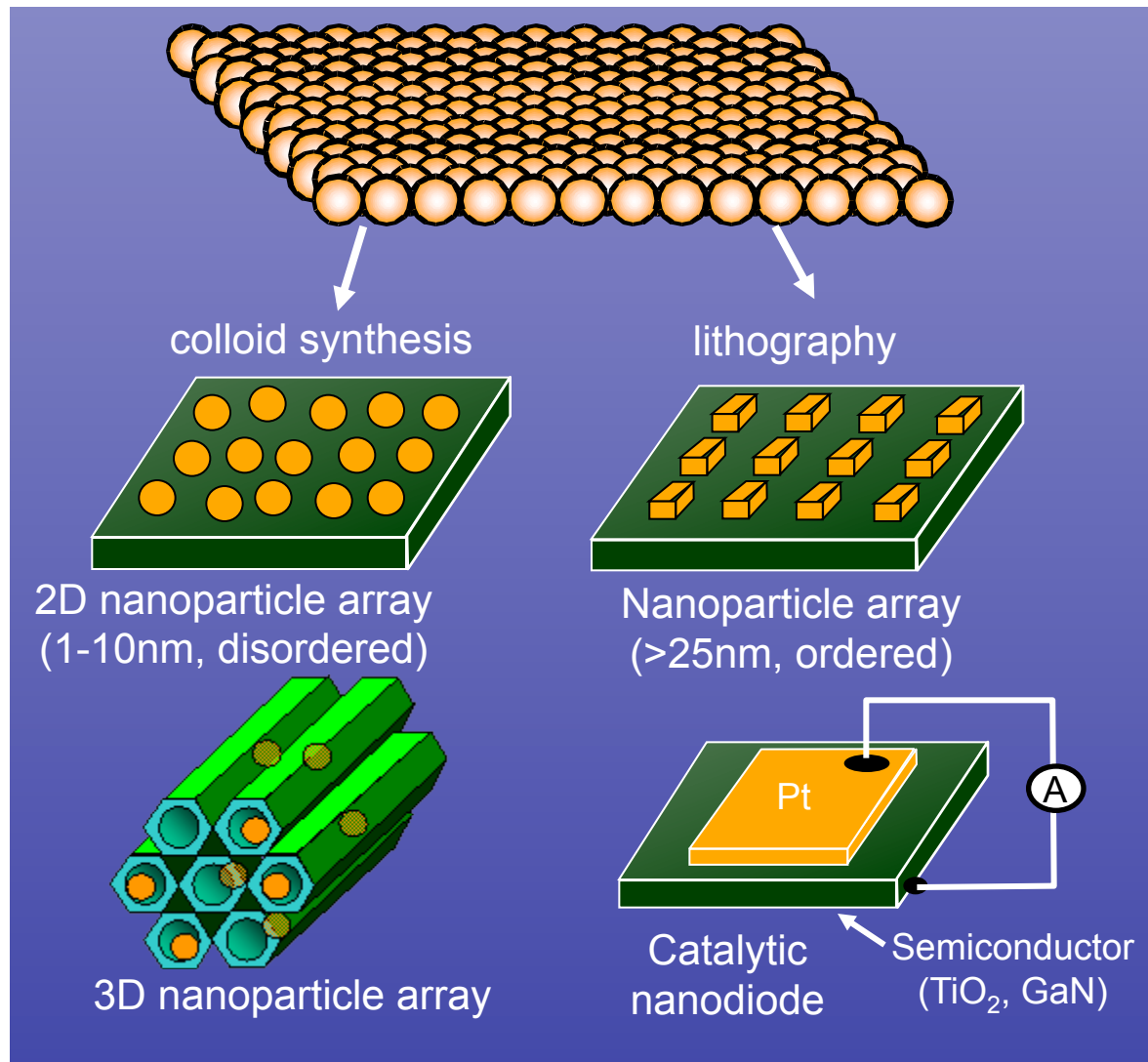
Ambient pressure X-ray Photoelectron Spectroscopy

Electron-in and Electron-out:

Transmission Electron Microscopy
Electron Flow During Catalytic Reactions

Model Catalytic Surfaces for Identifying Active Sites

From Single Crystal Surfaces to Monodispersed Nanoparticles



Biointerfaces

Catalysts

Nanomaterials

Tribology

Coatings

Surfaces

Electrochemistry

Corrosion

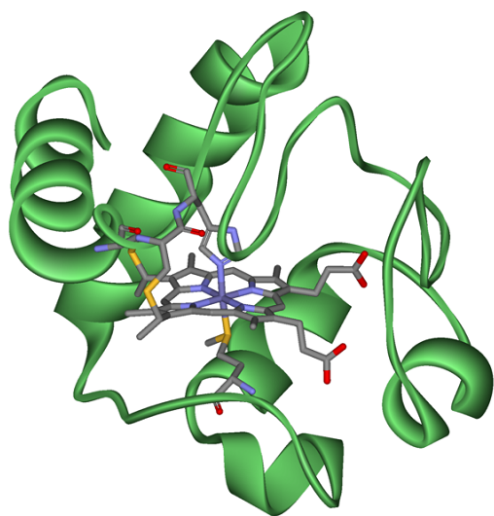
Magnetic Information
Storage

Integrated Circuitry

Sensors

Catalysts are Nanoparticles

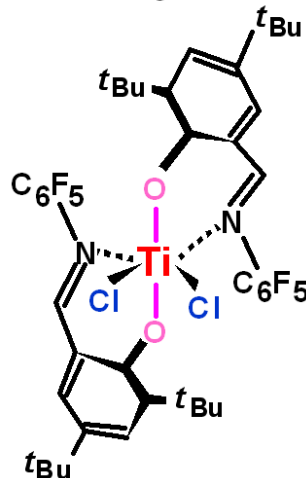
(a) Enzyme



Cytochrome C

Size: ~4 nm, 100 amino acids
Molecular weight: ~12,000 daltons

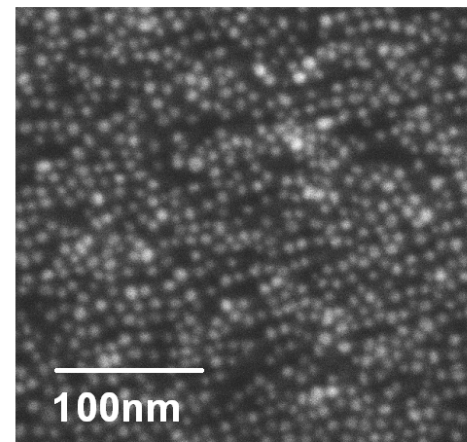
(b) Homogeneous catalysis



**Single-site olefin
polymerization catalyst**

Size : ~1.6 nm

(c) Heterogeneous catalysis

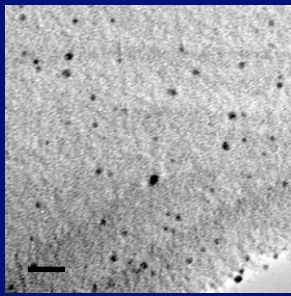


**Pt/Rh bimetallic
nanoparticles**

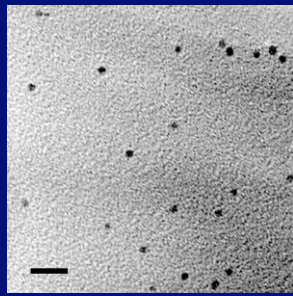
Size : 8 nm

Synthesis of Pt Nanoparticles with Size and Shape Control

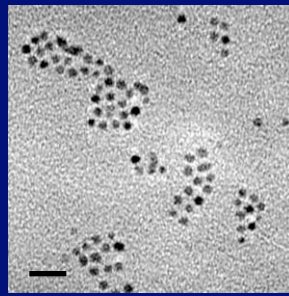
- PVP: Poly(vinylpyrrolidone), surface regulating polymer
- Particle size control in the range of 1.7 ~ 7.1 nm



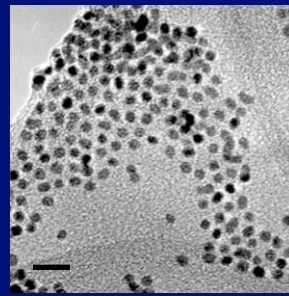
1.73 ± 0.26 nm



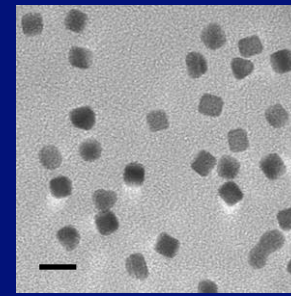
2.48 ± 0.22 nm



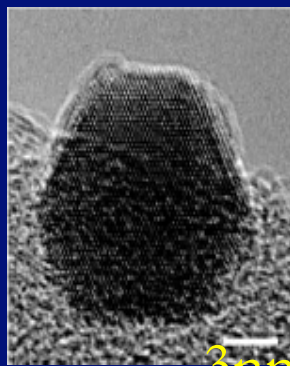
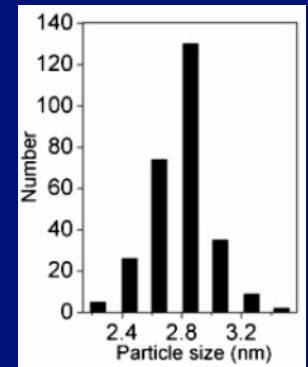
2.80 ± 0.21 nm



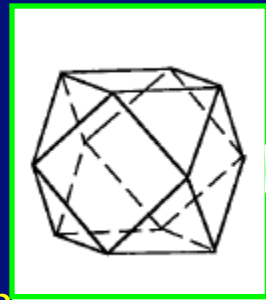
3.39 ± 0.26 nm



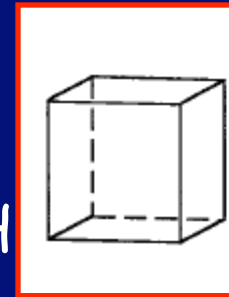
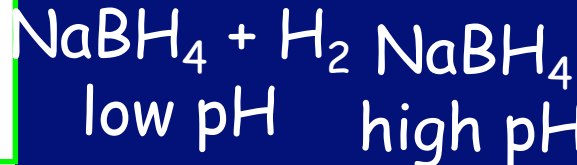
7.16 ± 0.37 nm



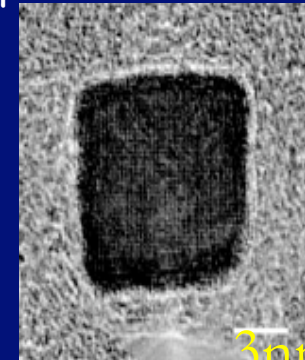
3nm



Cuboctahedra



Cubes {100}

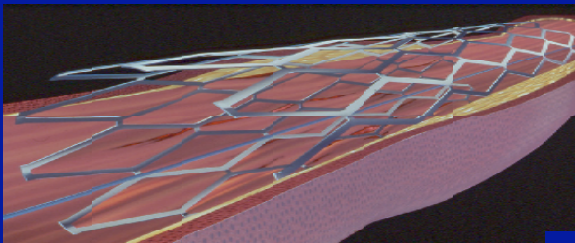


3nm

Biointerfaces and Medical Devices

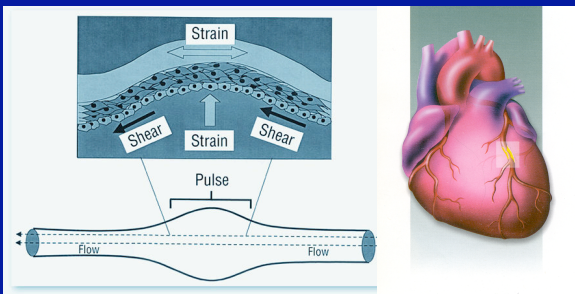
- Biomaterials improve our everyday quality of life
 - NIH estimates 8-10% of Americans have medical implants¹
- Biological Compatibility of Materials
 - Non-Specific Protein Adsorption²

Heart Stent



Polyurethane Under Reversible Loading (Fatigue Test)

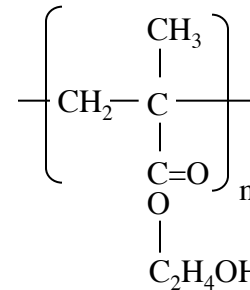
3.2 billion heart valve loading cycles in ~80 years of normal heart function



Soft Contact Lens



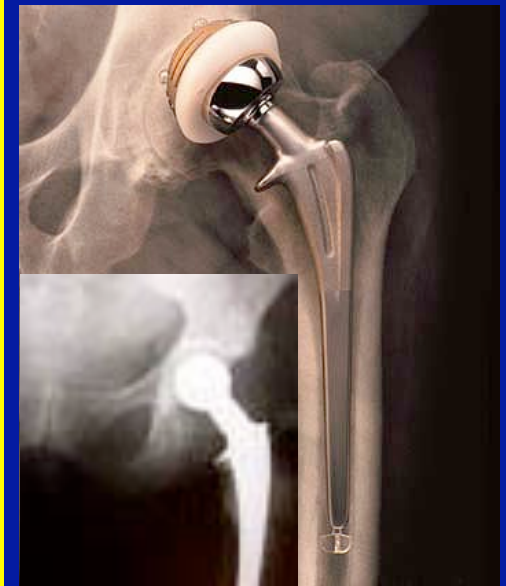
Soft contact lens:
crosslinked pHEMA



In water, pHEMA swells & forms hydrogel

pHEMA = poly(2-hydroxyethyl methacrylate)

Prosthesis

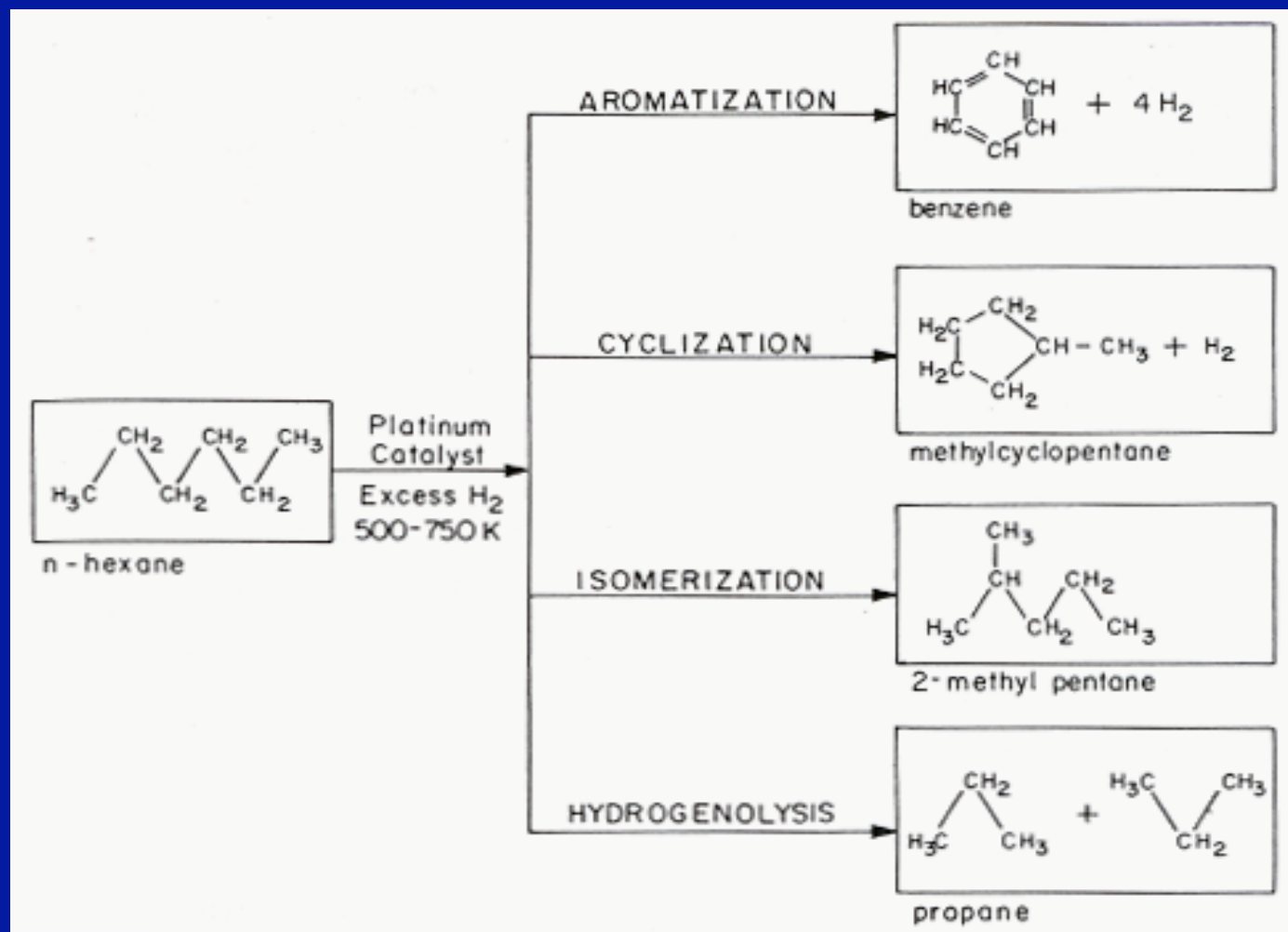


<http://www.biotronik.de/sixcms/detail.php/346>

1. <http://consensus.nih.gov/2000/2000MedicalImplantsta019html.htm>
2. Ratner, B.D., Bryant S.J., *Annu. Rev. Biomed. Eng.* (6) 41-75, 2004.

Catalysis by Metals

Industrial Hydrocarbon Reforming with Pt Catalyst



Octane
Rating

110

93

78

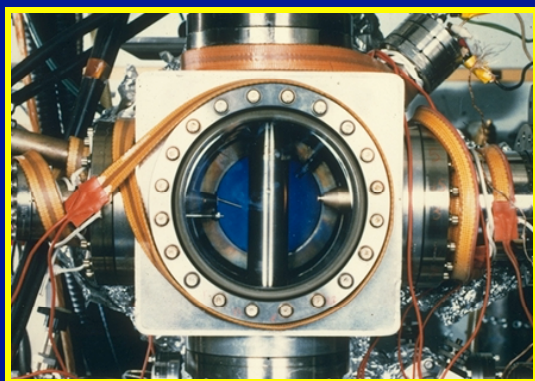
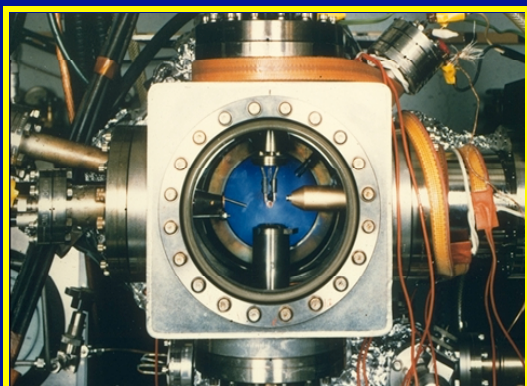
N/A

Reaction Selectivity Minimizes Waste Byproducts → Green Chemistry

Prenatal and Postmortem Studies of Metal Catalysis Before SFG Techniques

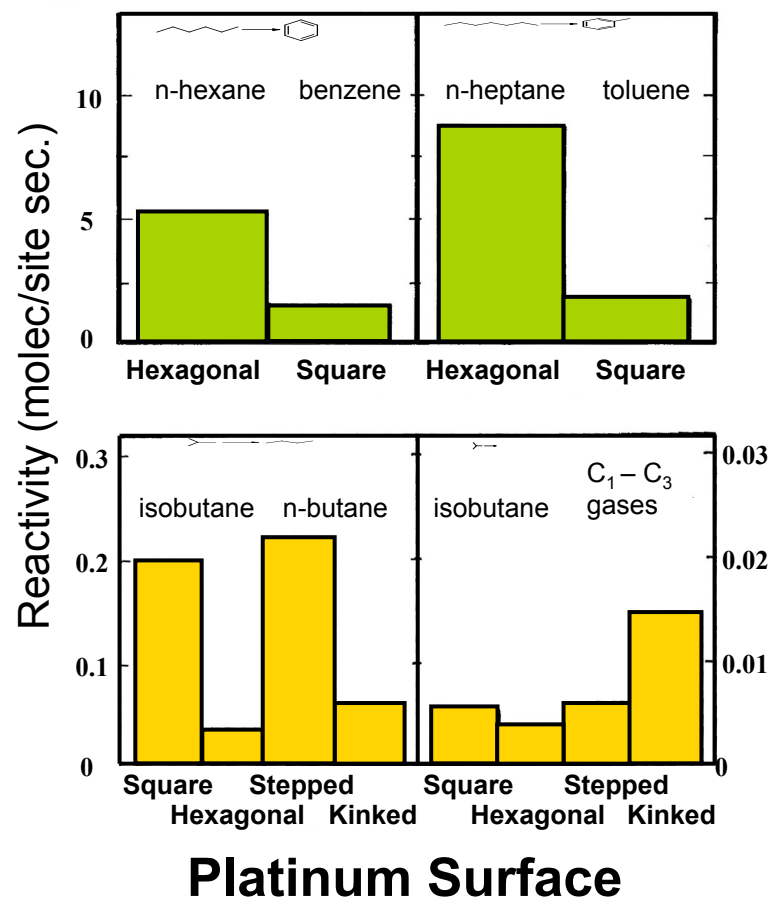
Ultra High Vacuum (UHV) Reactor Combined w/ High Pressure Reaction Cell

1. Low Pressure Catalyst Characterization



2. High Pressure Catalyst Reaction

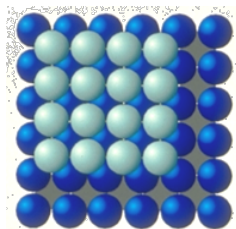
3. Selectivity & Reaction Product Study



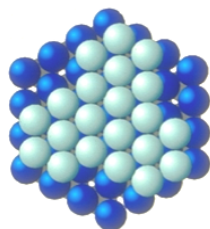
Benzene Hydrogenation on Pt Nanoparticles

Pt(111) & Cuboctahedra Nanoparticles show similar selectivity

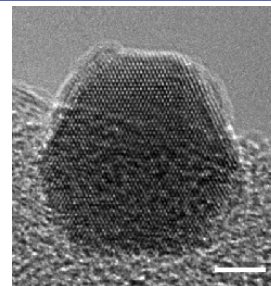
Pt(100) & Cubic Nanoparticles show similar selectivity



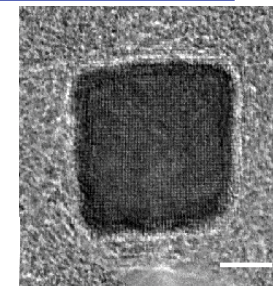
Pt (100)



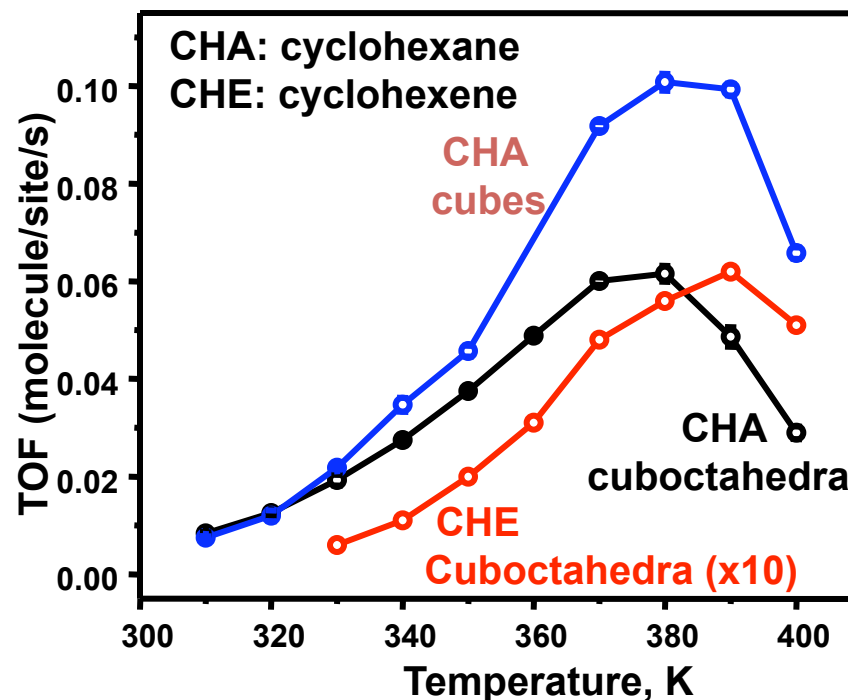
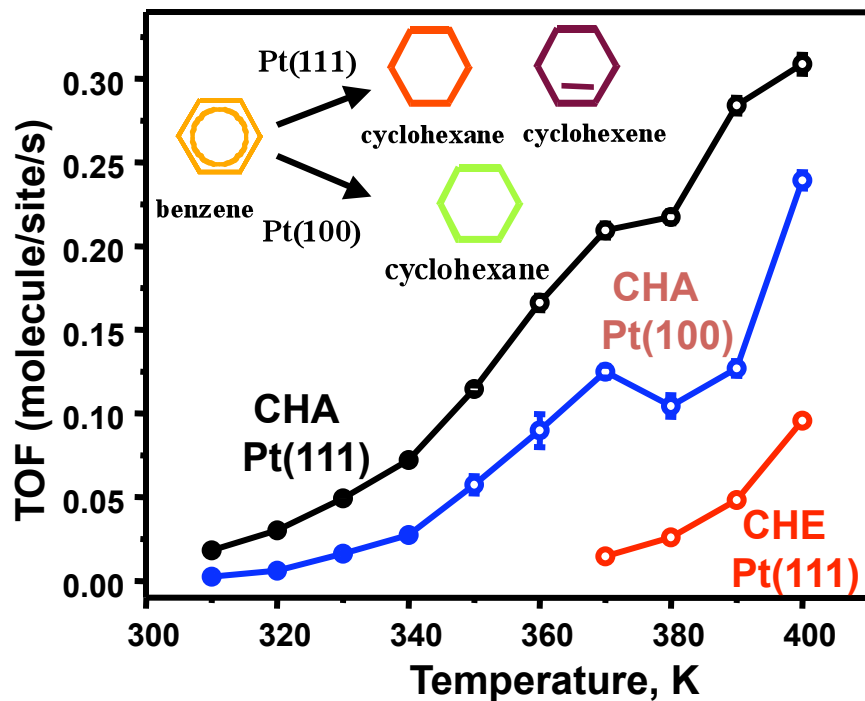
Pt (111)



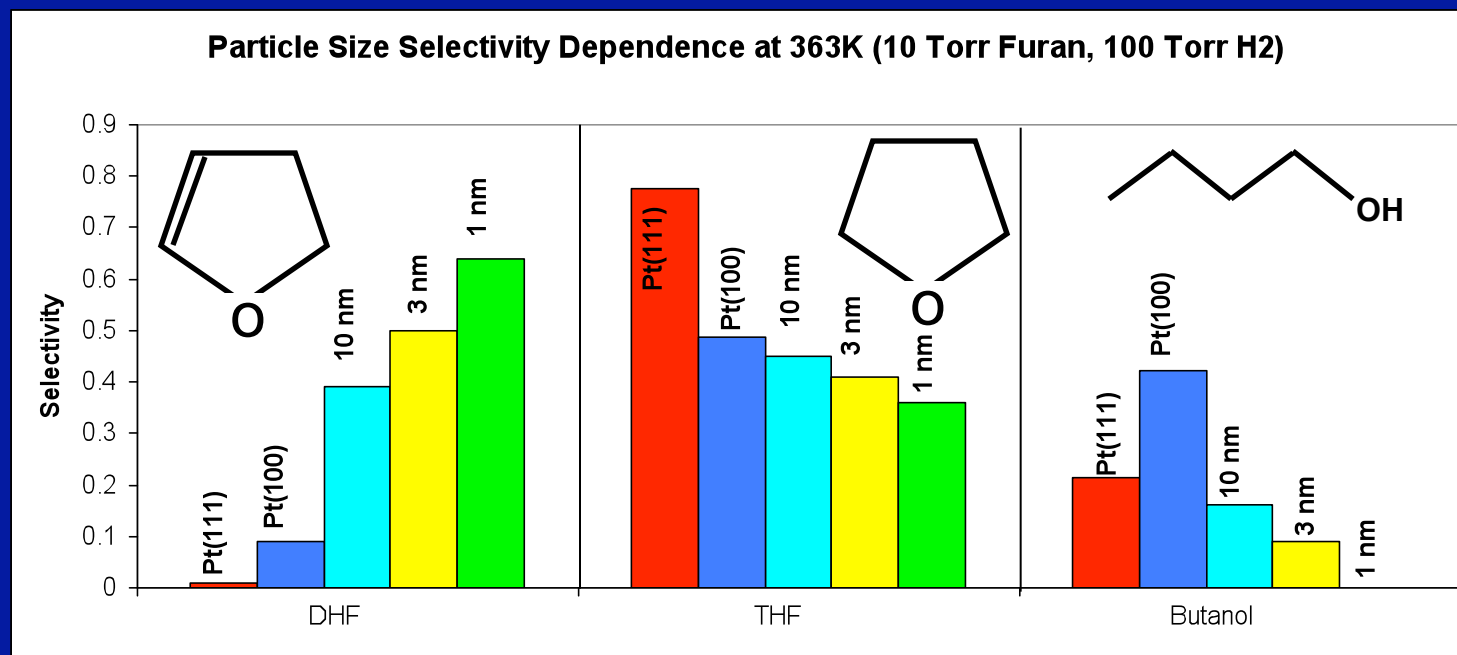
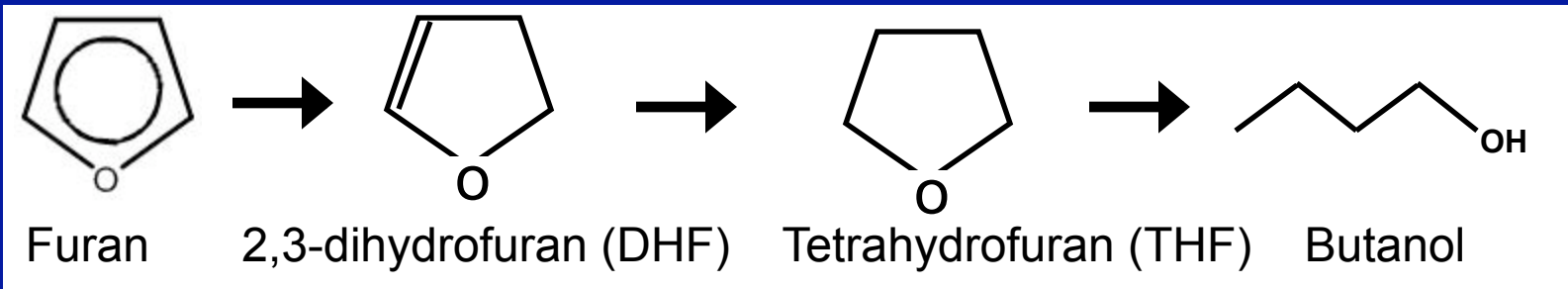
Cuboctahedra
(12.6 nm)



Cube
(13.4 nm)



Using SFG to Investigate Furan Hydrogenation: Selectivity Dependence on Pt Nanoparticle Size



All Runs: 10 Torr Furan, 100 Torr Hydrogen, 363K

Why are Catalytic Selectivity
and Turnover Rates
Nanoparticle Size and Shape
Sensitive?

Prenatal and Postmortem Studies of Metal Catalysis

Revolution in Molecular Studies of Catalysts During Reactions

High Pressure In-situ Surface Techniques

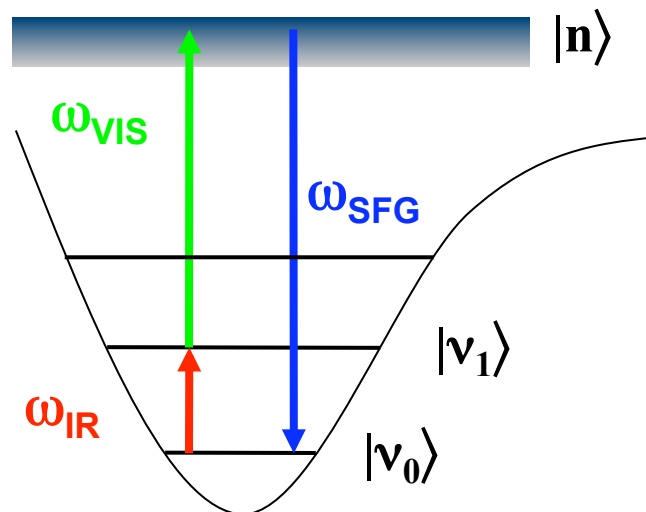
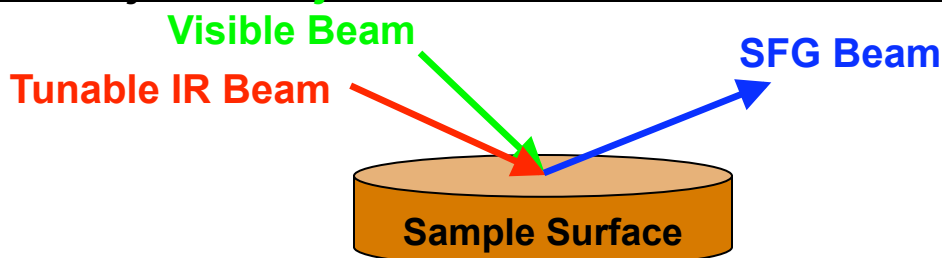
- Sum Frequency Generation Vibrational Spectroscopy (SFG)
- High Pressure Scanning Tunneling Microscopy (HPSTM)
- X-ray Absorption Spectroscopies (XAS)
- Ambient Pressure X-ray Photoelectron Spectroscopy (APXPS)
- Catalytic Nanodiode (CND)

Sum Frequency Generation Vibrational Spectroscopy

SFG: Surface-Specific Vibrational Spectroscopy

► Two Laser Beams Overlapped:

$$E = [E_j \cos(\omega_j t) + E_k \cos(\omega_k t)]$$



$$\omega_{\text{SFG}} = (\omega_{\text{VIS}} + \omega_{\text{IR}})$$

► Intense E-field Induces 2nd Order Non-linear Polarization:

$$P = P^{(0)} + P^{(1)} + P^{(2)} + \dots$$

$$P^{(0)} = \chi^{(0)} \quad \text{Permanent Dipole}$$

$$P^{(1)} = \chi^{(1)} [E_j \cos(\omega_j t) + E_k \cos(\omega_k t)] \quad \text{Linear (Raman, IR)}$$

$$P^{(2)} = \chi^{(2)} [E_j \cos(\omega_j t) + E_k \cos(\omega_k t)]^2 \quad \text{Non-linear (SFG, SHG, \dots)}$$



$$P^{(2)} = \chi^{(2)} [E_j E_k [\cos(\omega_j + \omega_k)t] + \dots]$$

(SFG)

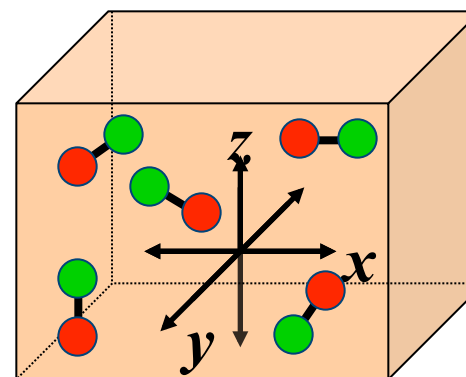
► Total SFG intensity:

$$I(\omega_{\text{SFG}}) \propto |\chi^{(2)}|^2 I(\omega_{\text{VIS}}) I(\omega_{\text{IR}})$$

SFG: Surface-Specific Vibrational Spectroscopy

Centrosymmetric Distribution:

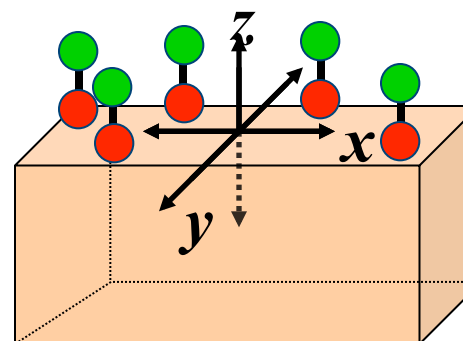
Selection Rule: $\chi^{(2)}_{xyz} = -\chi^{(2)}_{(-x)(-y)(-z)}$
BUT
 $x = -x$
 $y = -y \rightarrow \chi^{(2)}_{xyz} = \chi^{(2)}_{(-x)(-y)(-z)}$
 $z = -z$
 $\rightarrow \chi^{(2)}_{xyz} = 0$



$\chi^{(2)}$ is zero \rightarrow **No SFG Signal!***

Chemical Species at Interface:

Selection Rule: $\chi^{(2)}_{xyz} = -\chi^{(2)}_{(-x)(-y)(-z)}$
AND
 $x = -x$
 $y = -y \rightarrow \chi^{(2)}_{xyz} \neq \chi^{(2)}_{(-x)(-y)(-z)}$
 $z \neq -z$
 $\rightarrow \chi^{(2)}_{xyz} \neq 0$



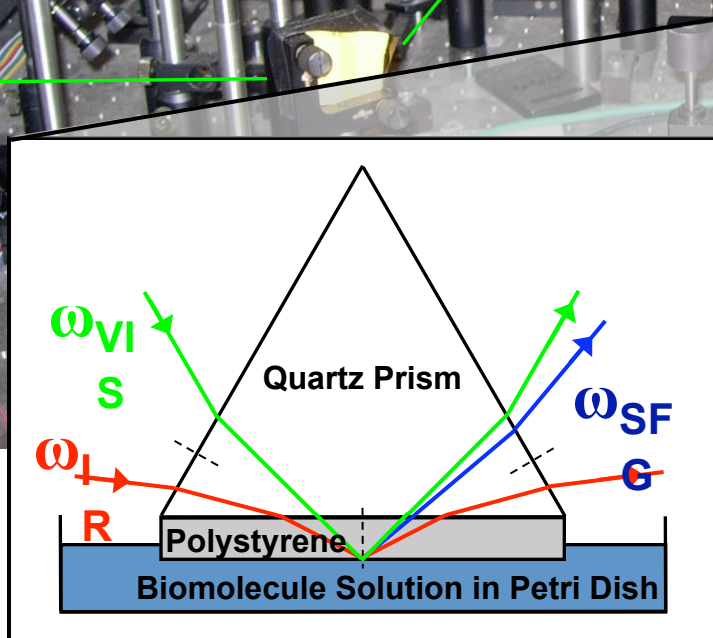
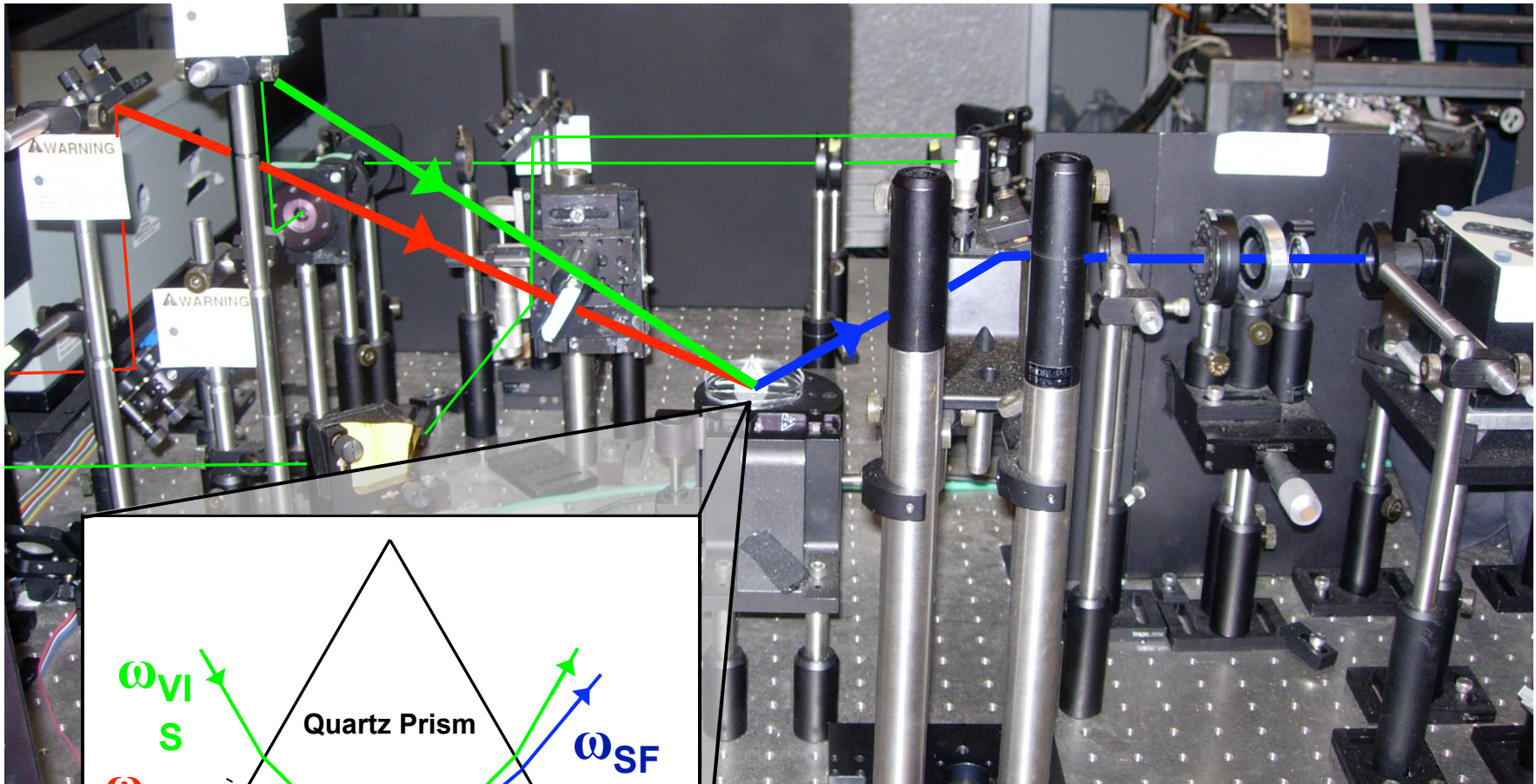
$\chi^{(2)}$ is nonzero \rightarrow **Surface-Specific SFG Signal!**

Experimental SFG Setup

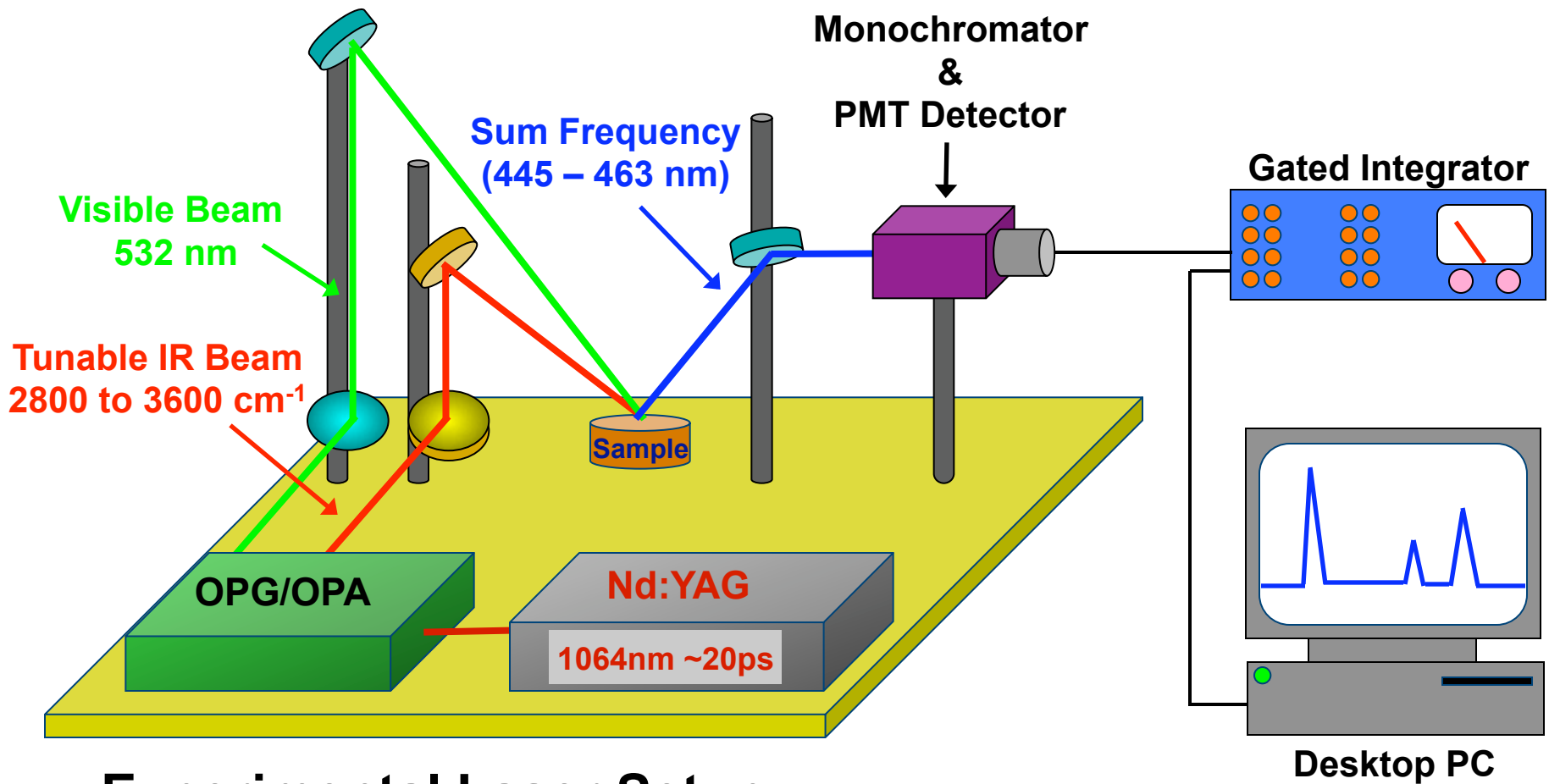
— Visible (532 nm)

— IR (2800-3600 cm^{-1})

— SFG (445-463 nm)



SFG: Surface-Specific Vibrational Spectroscopy

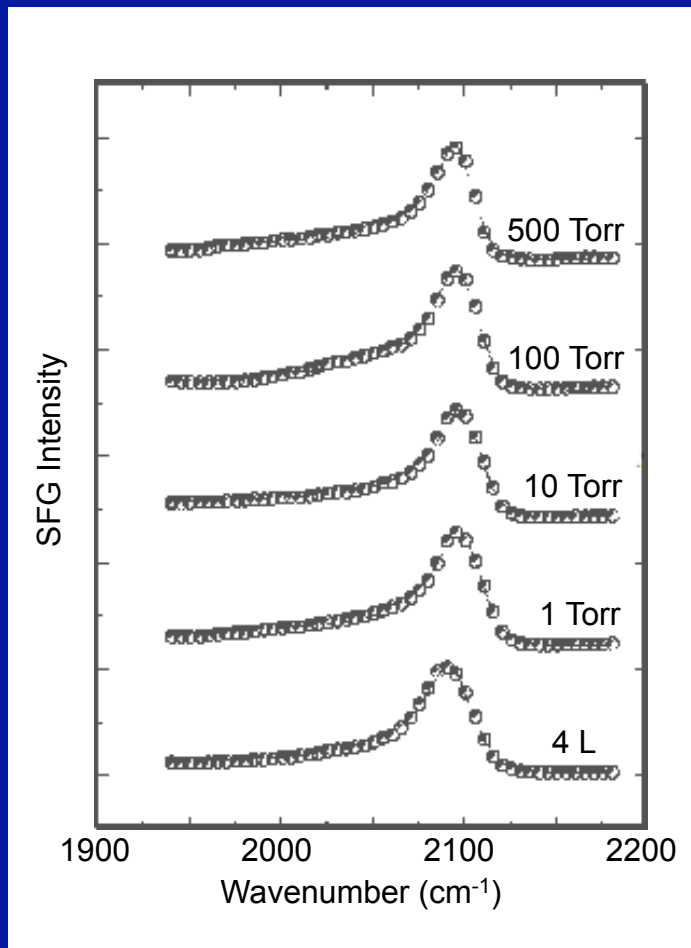


Experimental Laser Setup

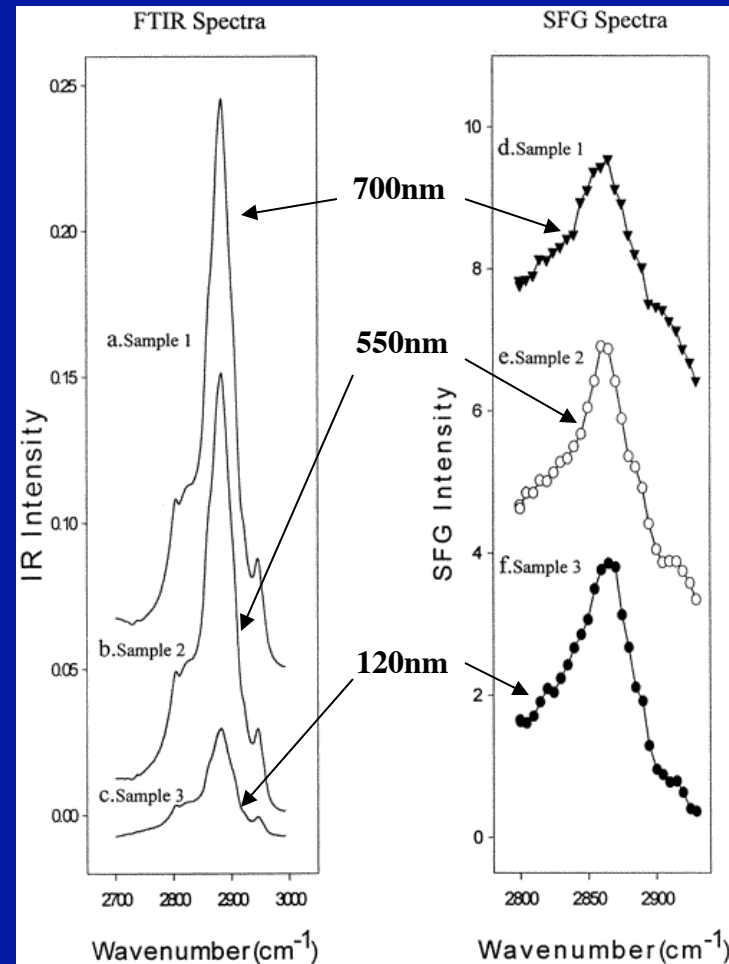
Surfaces Under Pressure and at Liquid Interfaces

Experimental Evidence for the Surface Sensitivity of SFG

The pressure independence of the SFG spectra of CO on Pt (557)

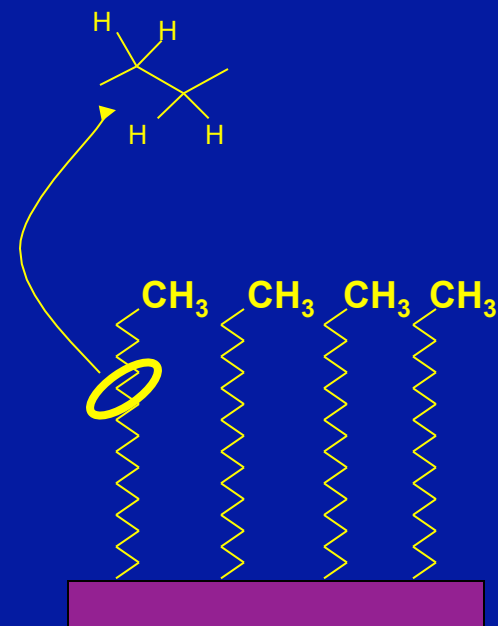
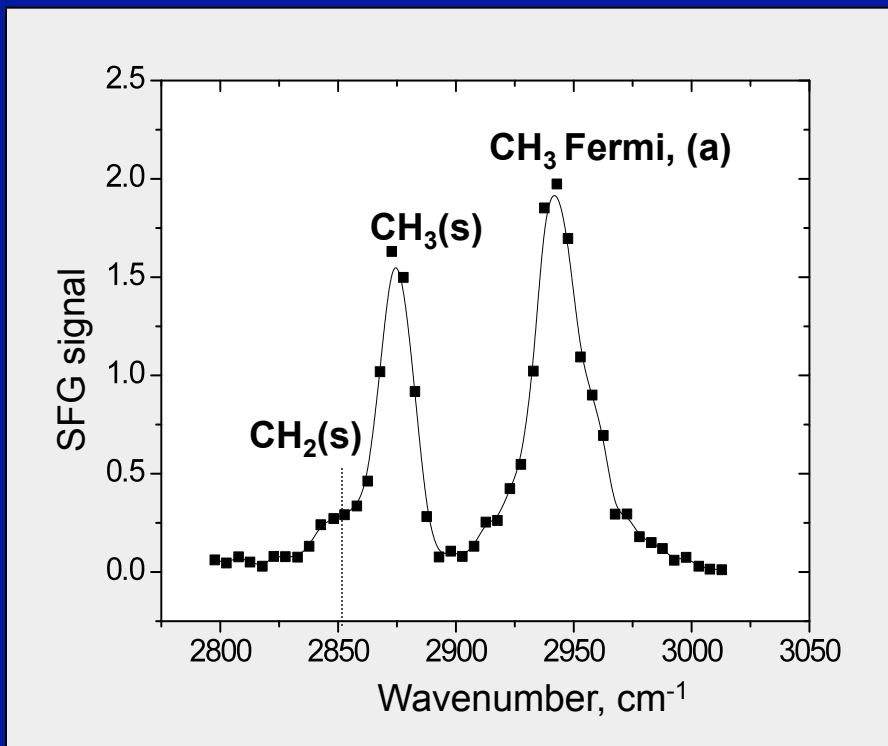


The thickness independence of the SFG spectra of polyethylene glycol films



Example of SFG Surface Sensitivity: Alkanethiol self-assembled monolayer (SAM)

SFG spectra: C-H stretching region

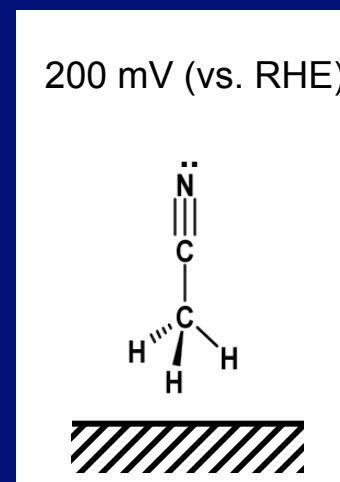
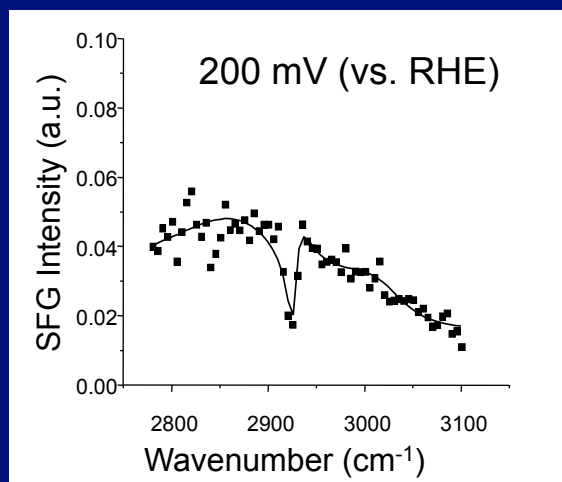
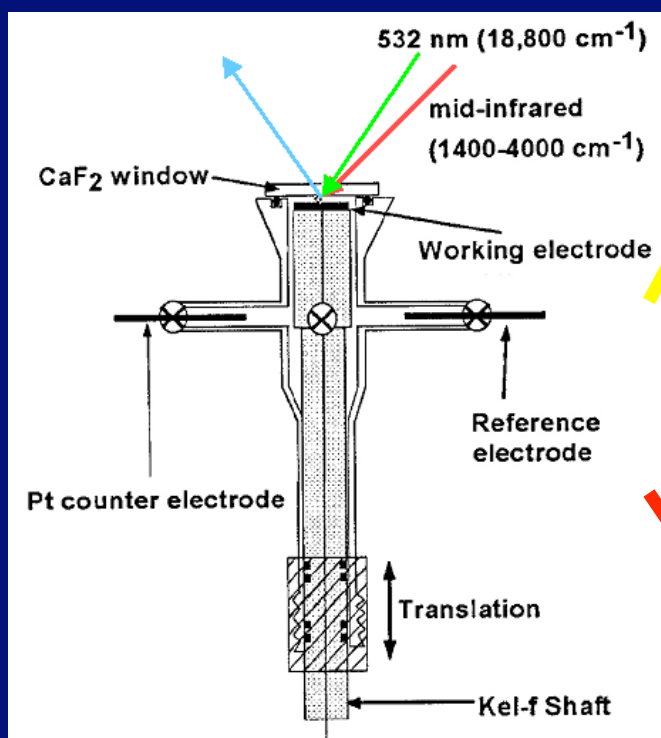


Surface Science at Liquid Interfaces

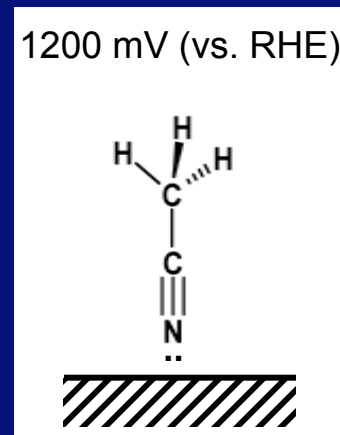
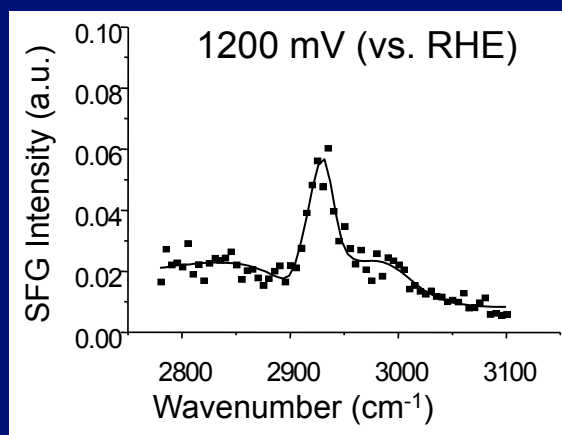
- Surface Electrochemistry
- Biointerfaces

SFG Sensitive to Orientation of Acetonitrile on Pt(111) with Varying Surface Potential

SFG Electrochemical Cell

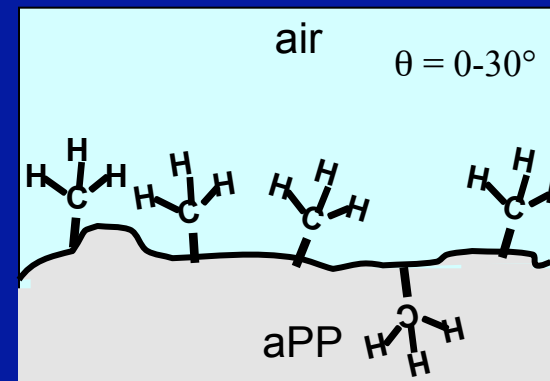
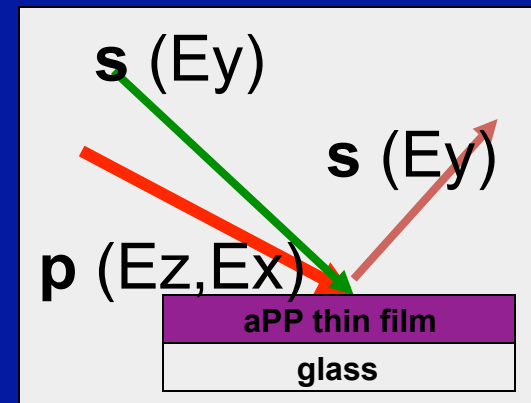
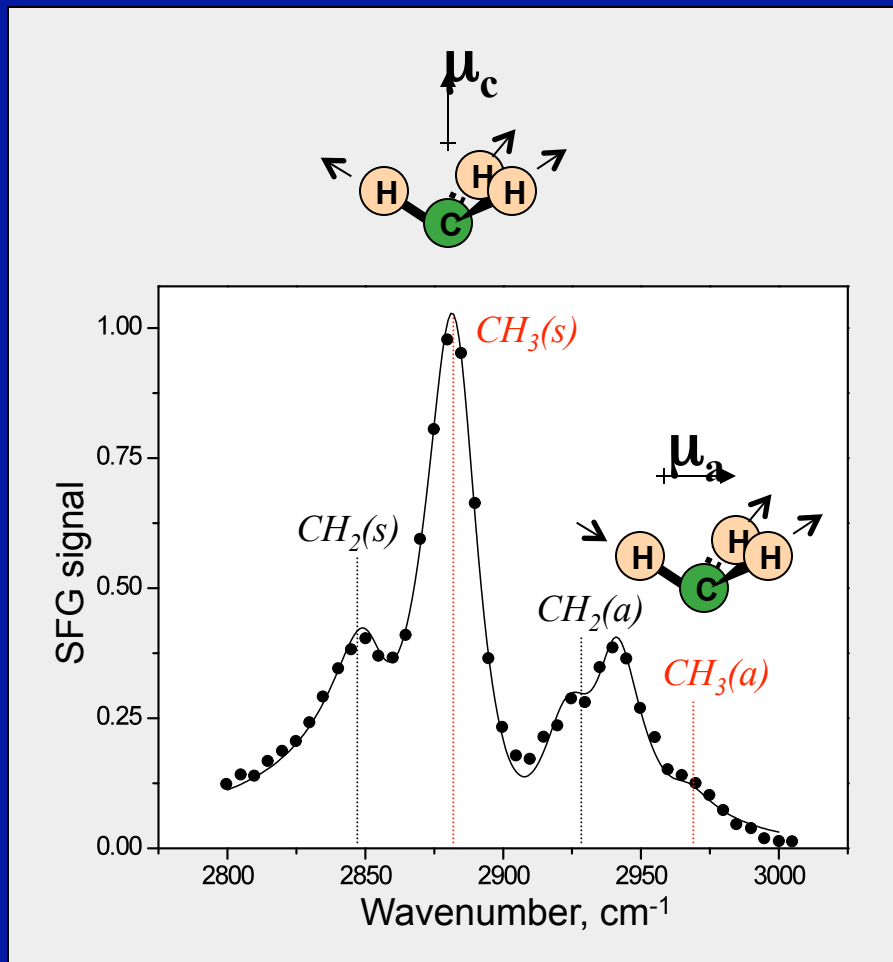


Low (+) Potential
VS.
High (+) Potential

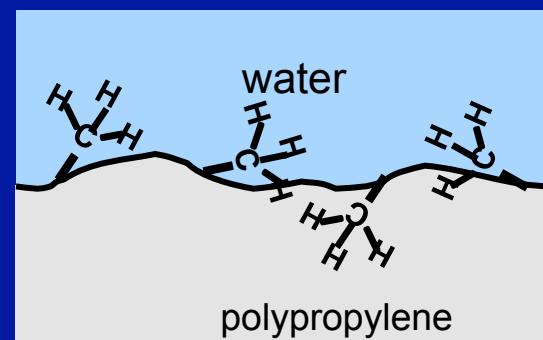
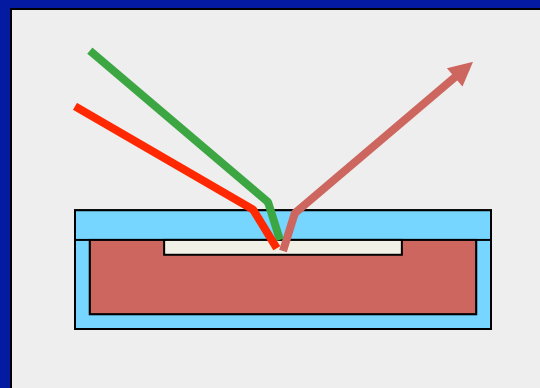
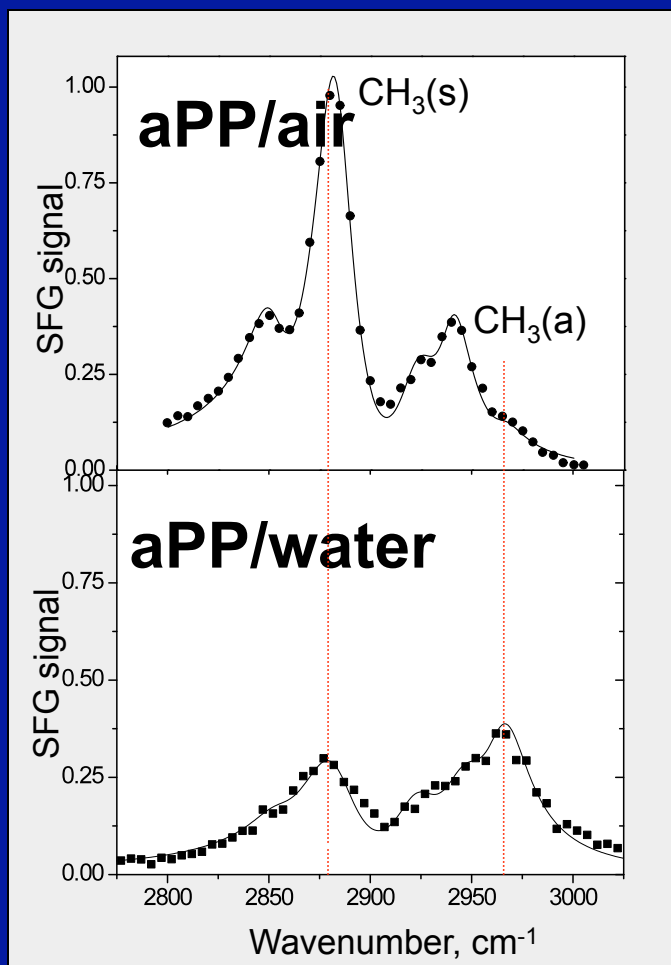


Changes of Polymers at Solid- Gas and Solid-Liquid Interfaces

SFG spectrum of atactic polypropylene

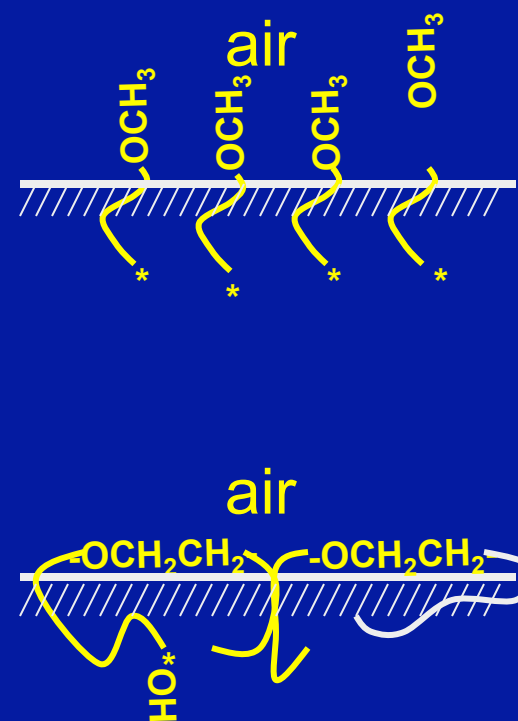
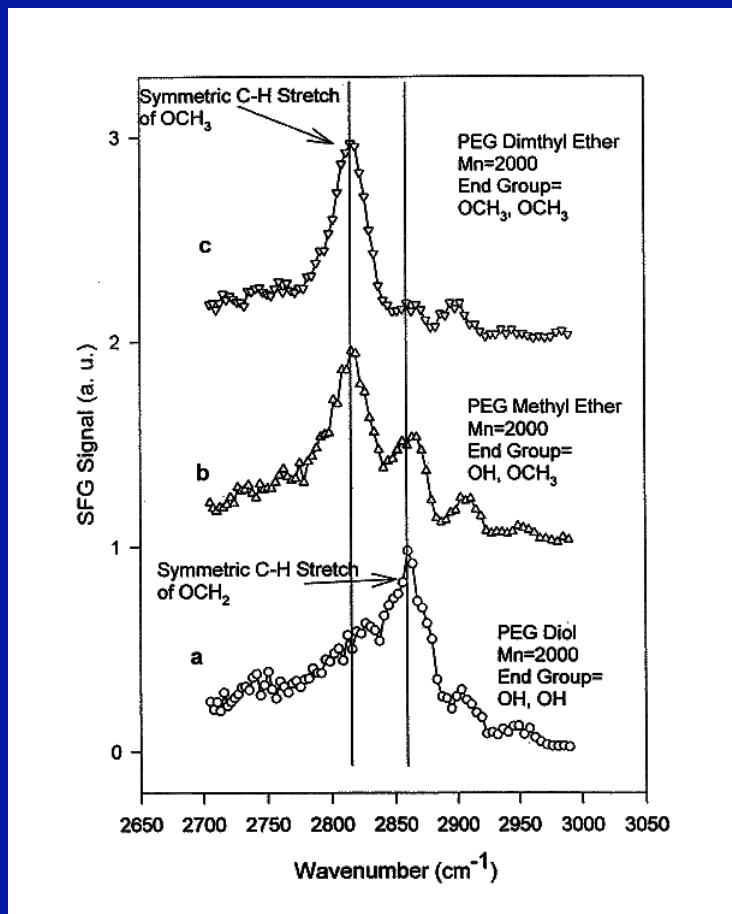


Polypropylene/water interface



Polypropylene CH₃ side branches tilt and/or disorder

Hydrophobic endgroup segregation at the air interface in polyethylene glycol (PEG) oligomers

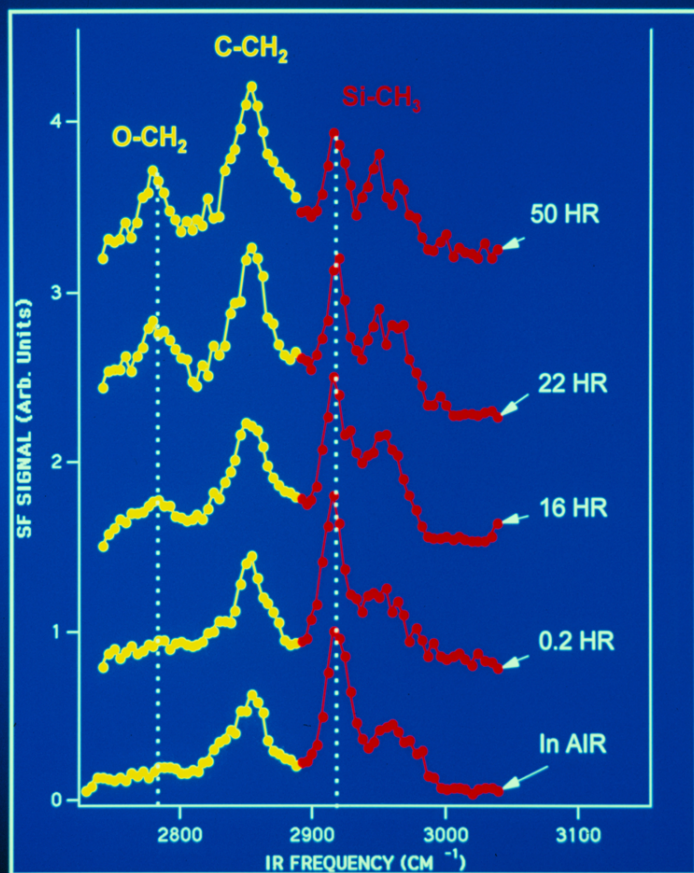


Detection of Hydrophobic End Groups on Polymer Surfaces by Sum-Frequency Generation Vibrational Spectroscopy

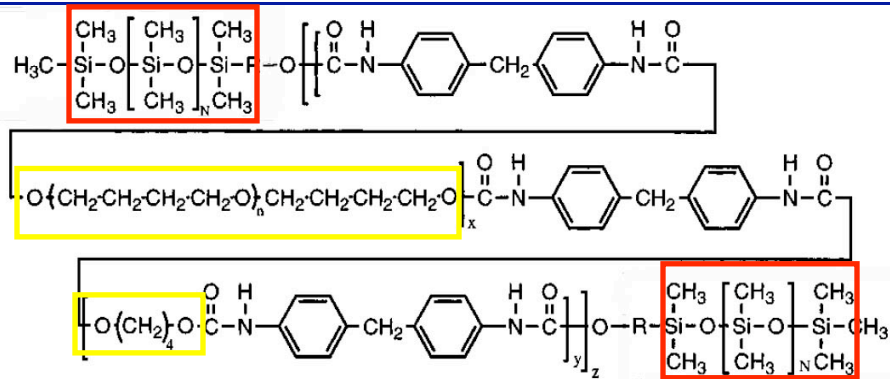
Chen, Z.; Ward, R.; Tian, Y.; Baldelli, S.; Opdahl, A.; Shen, Y.-R.; Somorjai, G. A.;
J. Am. Chem. Soc.; **2000**; 122(43); 10615-10620.

SFG Sensitivity to Polymer Surface Hydration

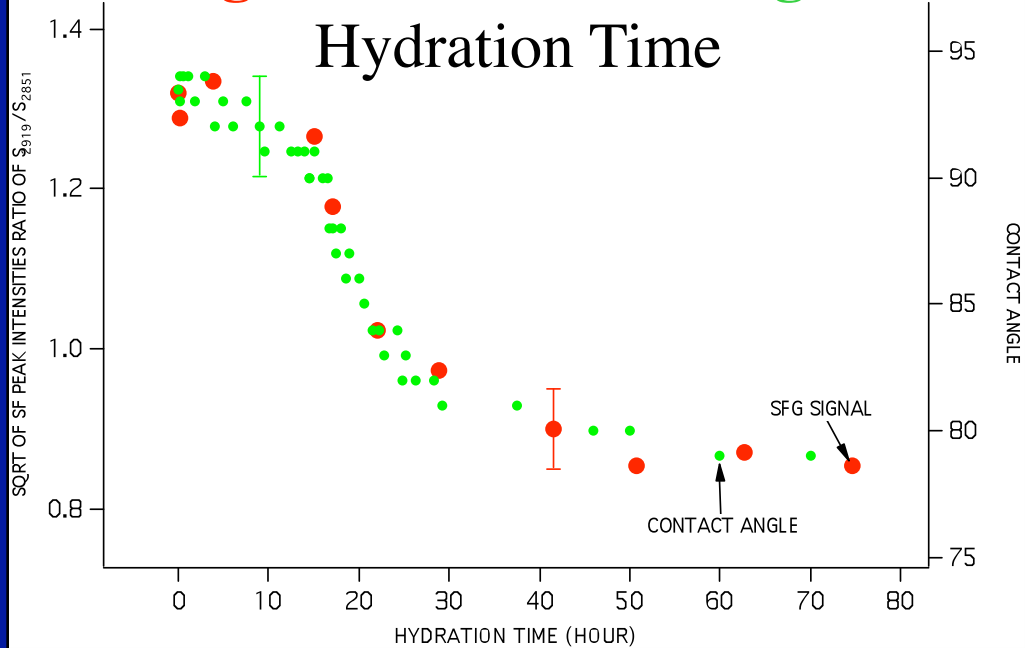
Time Evolution of SFG Spectra at the Biospan-S/Water Interface



Biospan-S Polymer



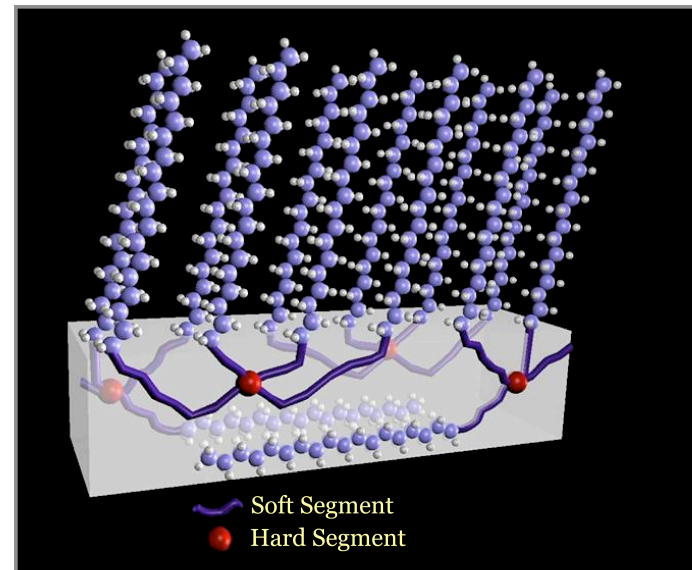
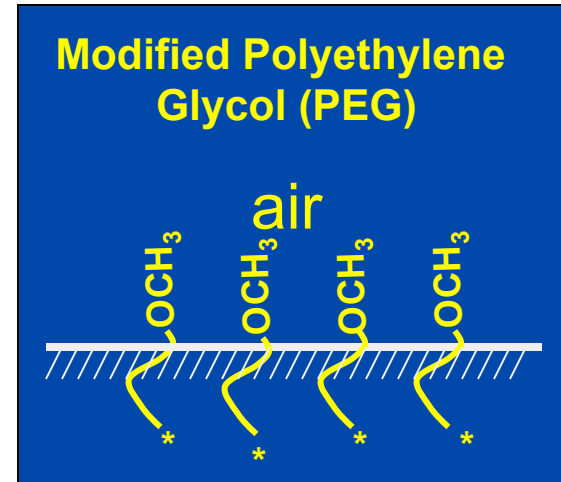
SF Signal and Contact Angle vs. Hydration Time



Surface Modification Technology

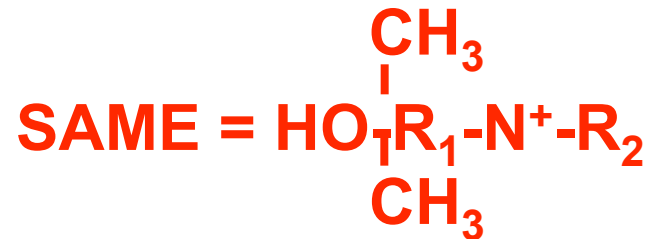
- **SME™ = Surface Modifying End Group**
 - Surface-active end group covalently bonded to a base polymer during synthesis

- **SAME™ = Self Assembling Monolayer End Group**
 - Self-assembling end group covalently bonded to a base polymer during synthesis

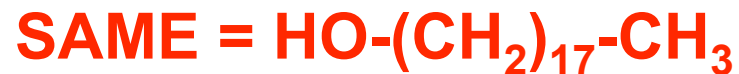


Utilizing End Groups to Modify Surface Chemistry

1. Antimicrobial Activity



2. Enhanced Thrombo-resistance



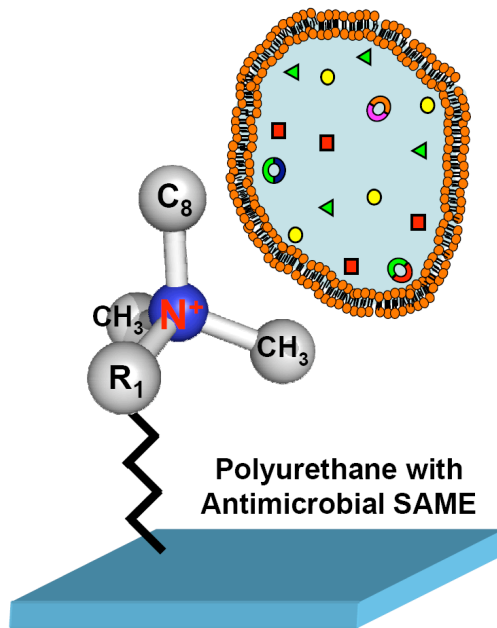
3. Improved Biostability



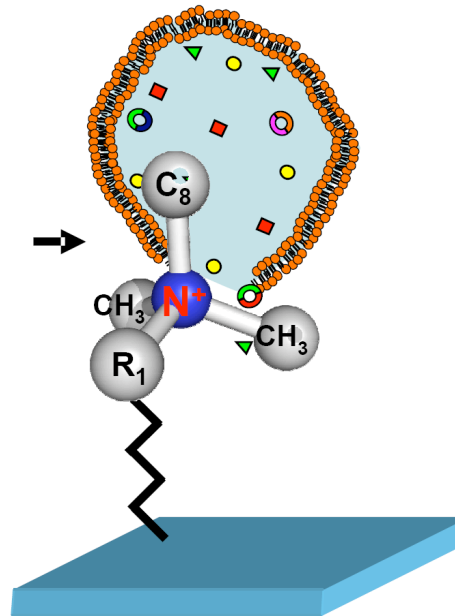
Example 1: Antimicrobial SAME Surfaces

- Ionic Interaction with Bacterium Cell Membranes¹
 - Membranes Disrupted
 - Permeability Increased

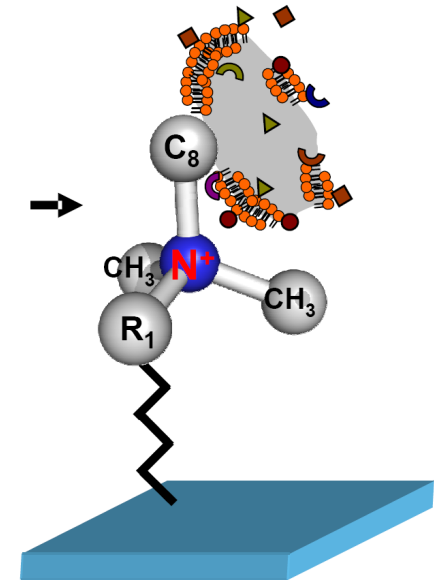
SAME and Bacterium Associate



Membrane Compromised



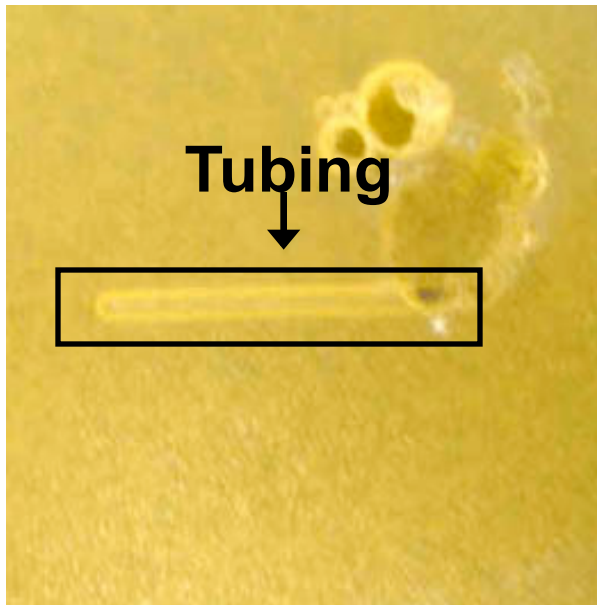
Bacterium Dies



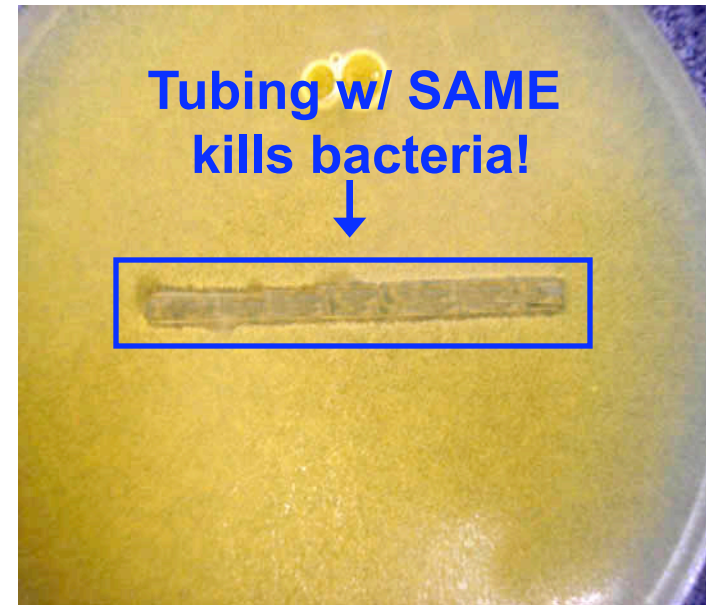
1. Denyer, S. P. and Stewart, G. S. A. B., *Int. Biodev. Biodegrad.* (41) 261-268, 1998.

Antimicrobial SAME Resists Staphylococcus Bacteria

PU Tubing Control



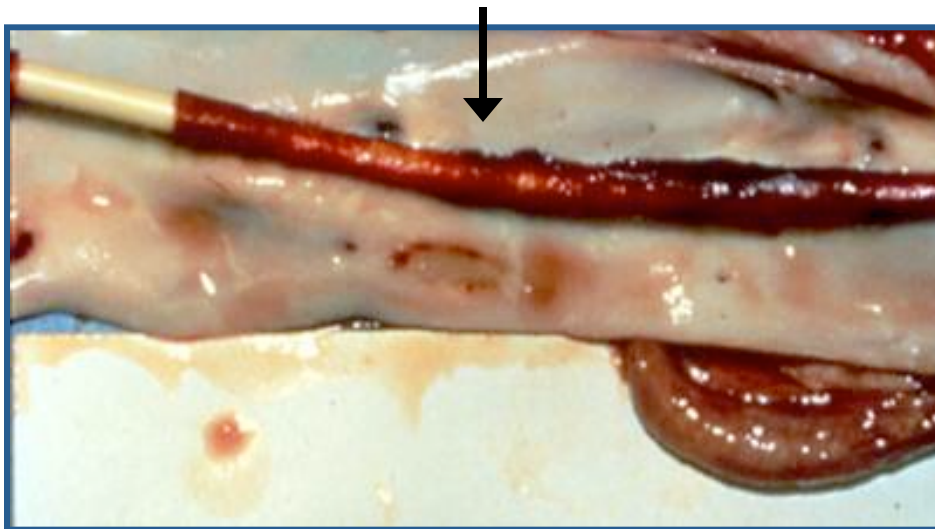
PU tubing with 0.5 wt%
Antimicrobial SAME



Test Organism: *Staphylococcus aureus* (ATCC 6538)

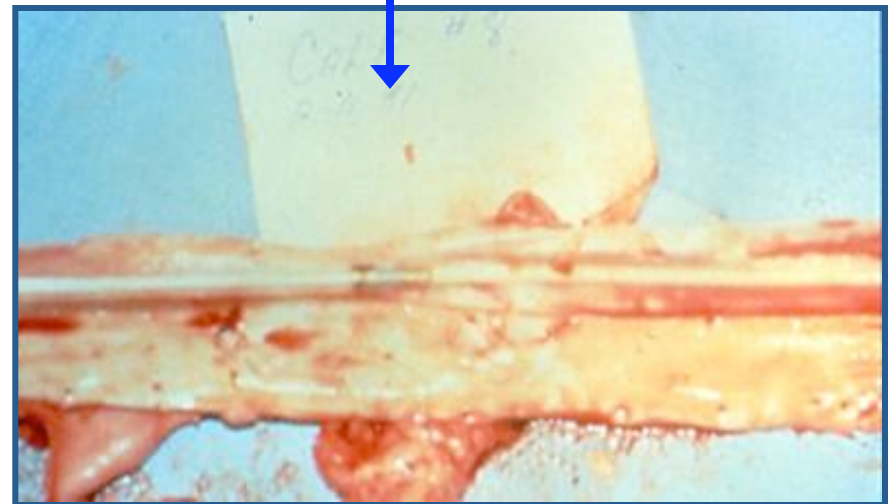
Enhanced Thrombo-resistance

Without surface modifier/wax



Blood clots line balloon surface

With surface modifier/wax



Enhanced thrombo-resistance

Example 3: Biostability of Fluorocarbon SMEs

**Polyether-urethane control
no fluorocarbon**



Polymer Degradation

**Polyether-urethane
with fluorocarbon SME**



No Polymer Degradation

SFG Molecular Studies of Metal Catalysts and Reaction Intermediates

Catalysis in the 20th Century

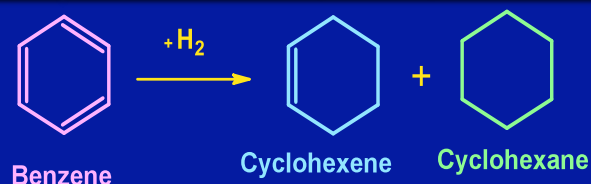
Focus on Catalytic Activity

Catalysis in the 21st Century

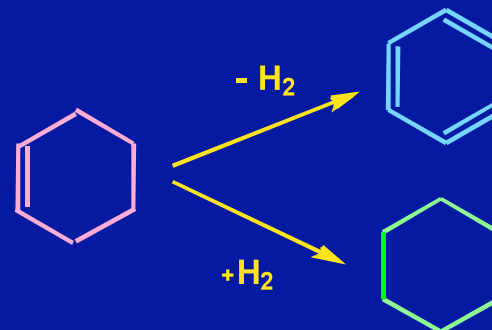
Focus on Catalytic Selectivity

Catalytic Reactions Studied By SFG

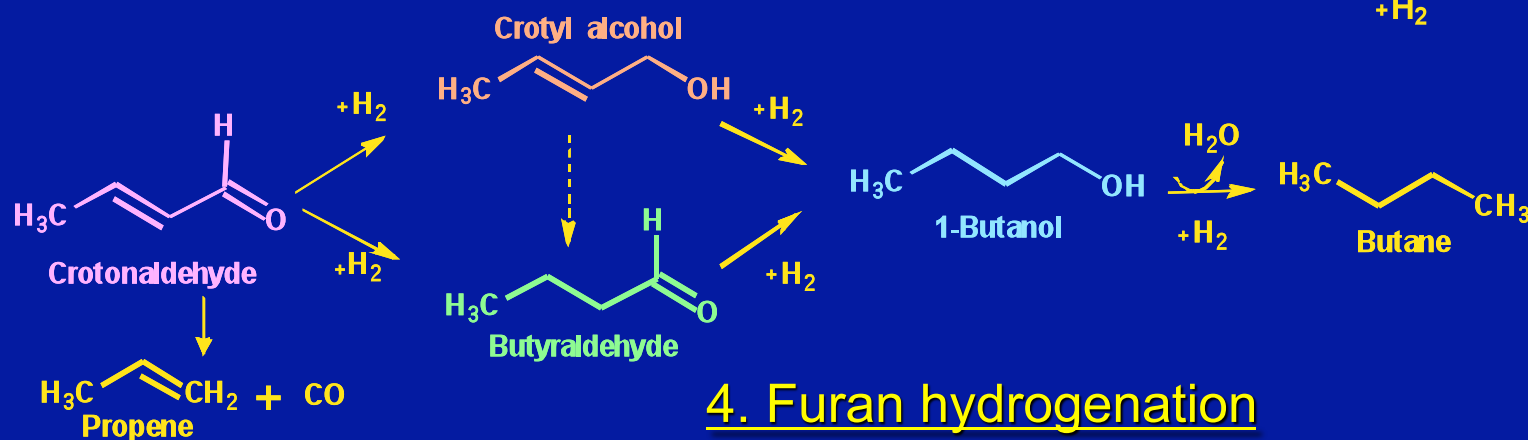
1. Benzene hydrogenation



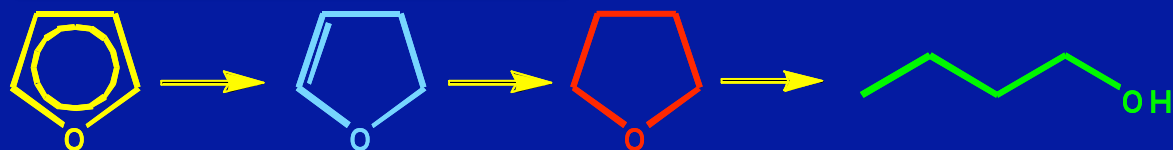
2. Cyclohexene hydrogenation/dehydrogenation



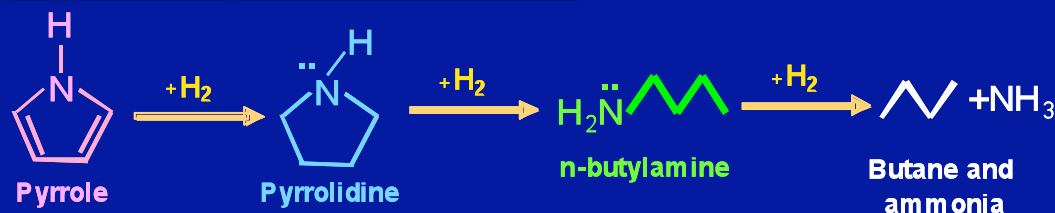
3. Crotonaldehyde hydrogenation



4. Furan hydrogenation

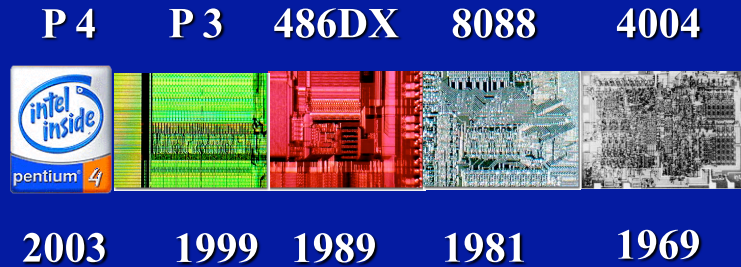


5. Pyrrole hydrogenation

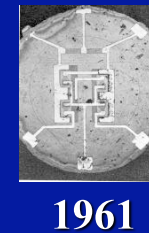


Technically and Biologically Important Length Scales

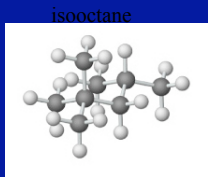
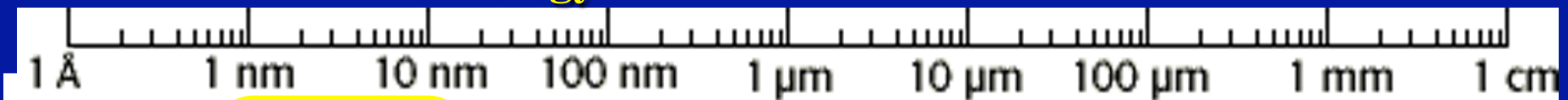
Intel Processors



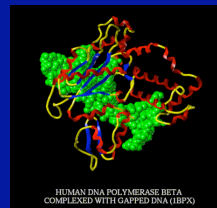
First Fairchild IC



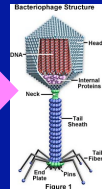
Nanotechnology



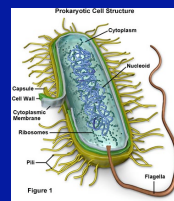
Hydrocarbon
Fuel of today



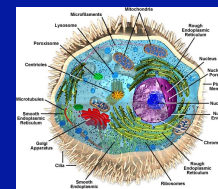
Enzyme



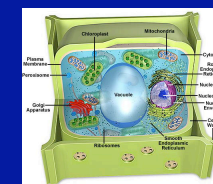
Virus



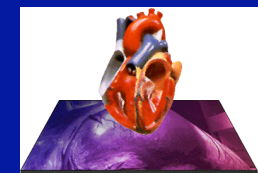
Bacterium



Animal Cell



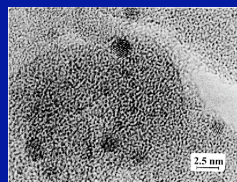
Plant Cell



Tissue & Organ



H₂ - Fuel
of tomorrow



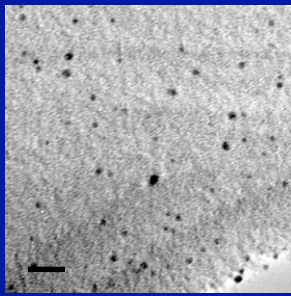
Pt/SiO₂ catalyst

Catalysis

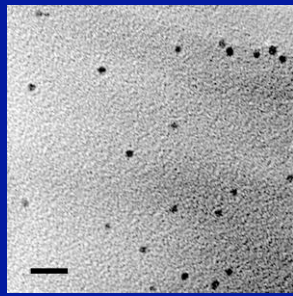
Catalysis is an integral part of nanotechnology. Biological catalysts – enzymes – are the foundation of biological systems, while synthetic heterogeneous catalysts – metal or metal oxide nanoparticles supported on oxides – are the foundation of the chemical industry.

Synthesis of Pt Nanoparticles with Size and Shape Control

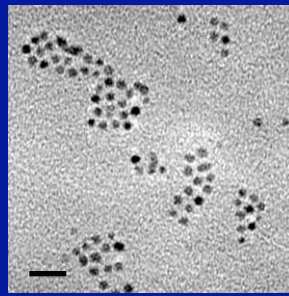
- PVP: Poly(vinylpyrrolidone), surface regulating polymer
- Particle size control in the range of 1.7 ~ 7.1 nm



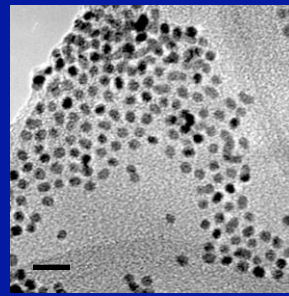
1.73 ± 0.26 nm



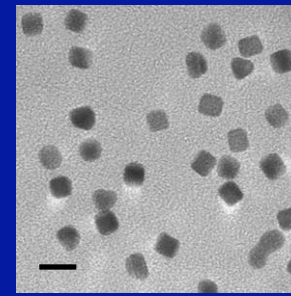
2.48 ± 0.22 nm



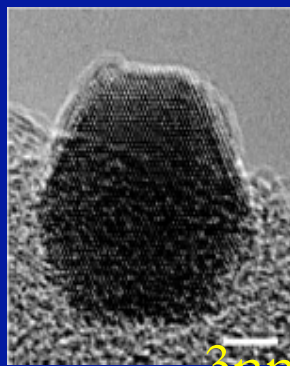
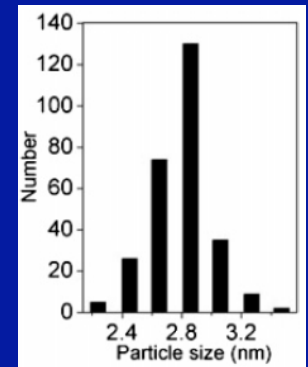
2.80 ± 0.21 nm



3.39 ± 0.26 nm

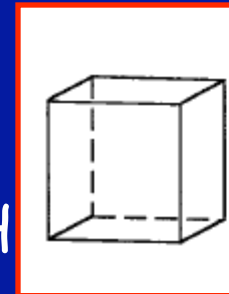
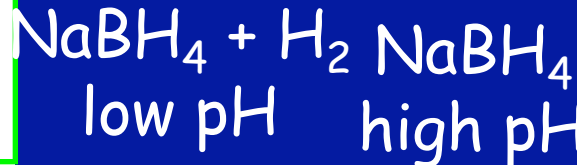
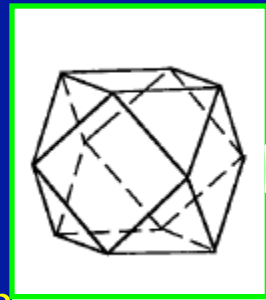


7.16 ± 0.37 nm

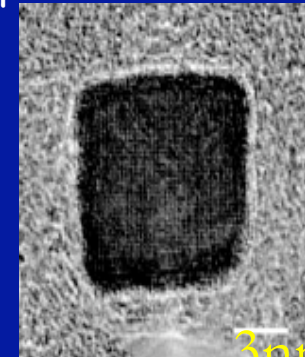


3nm

Cuboctahedra



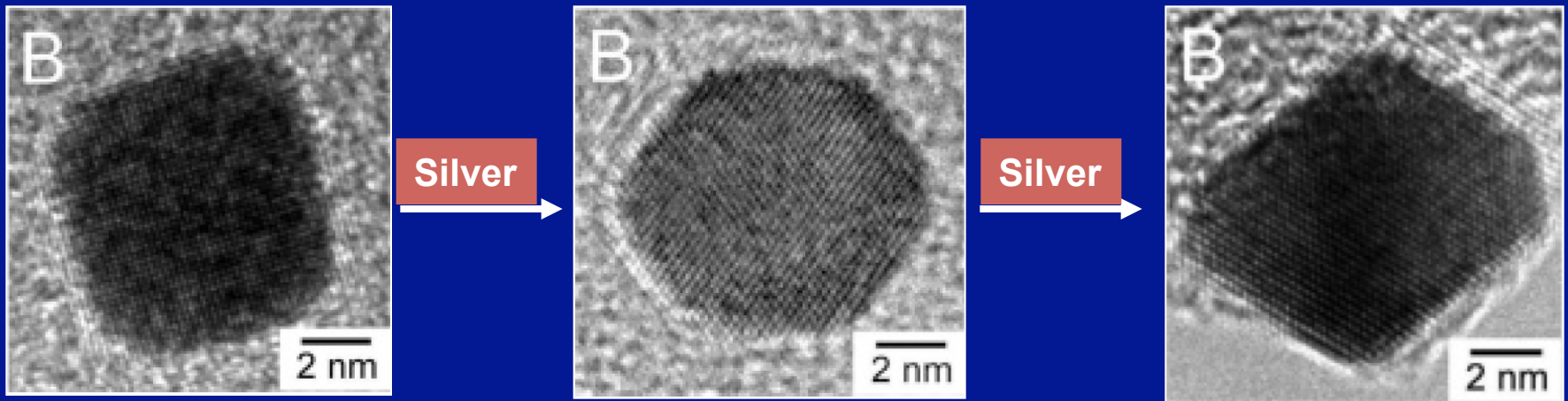
Cubes {100}



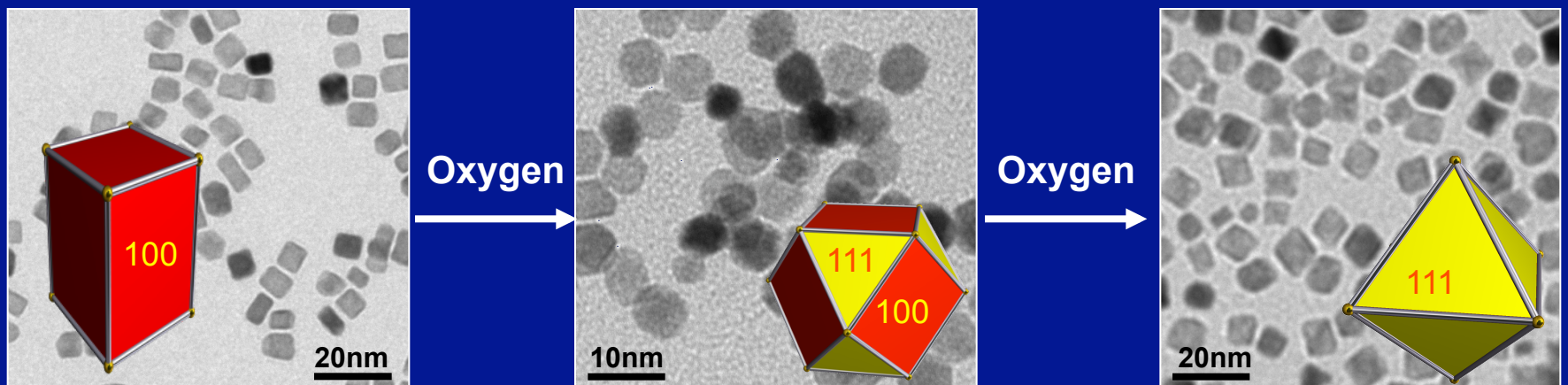
3nm

Pt and PdPt Alloy Nanocrystal Shape Control

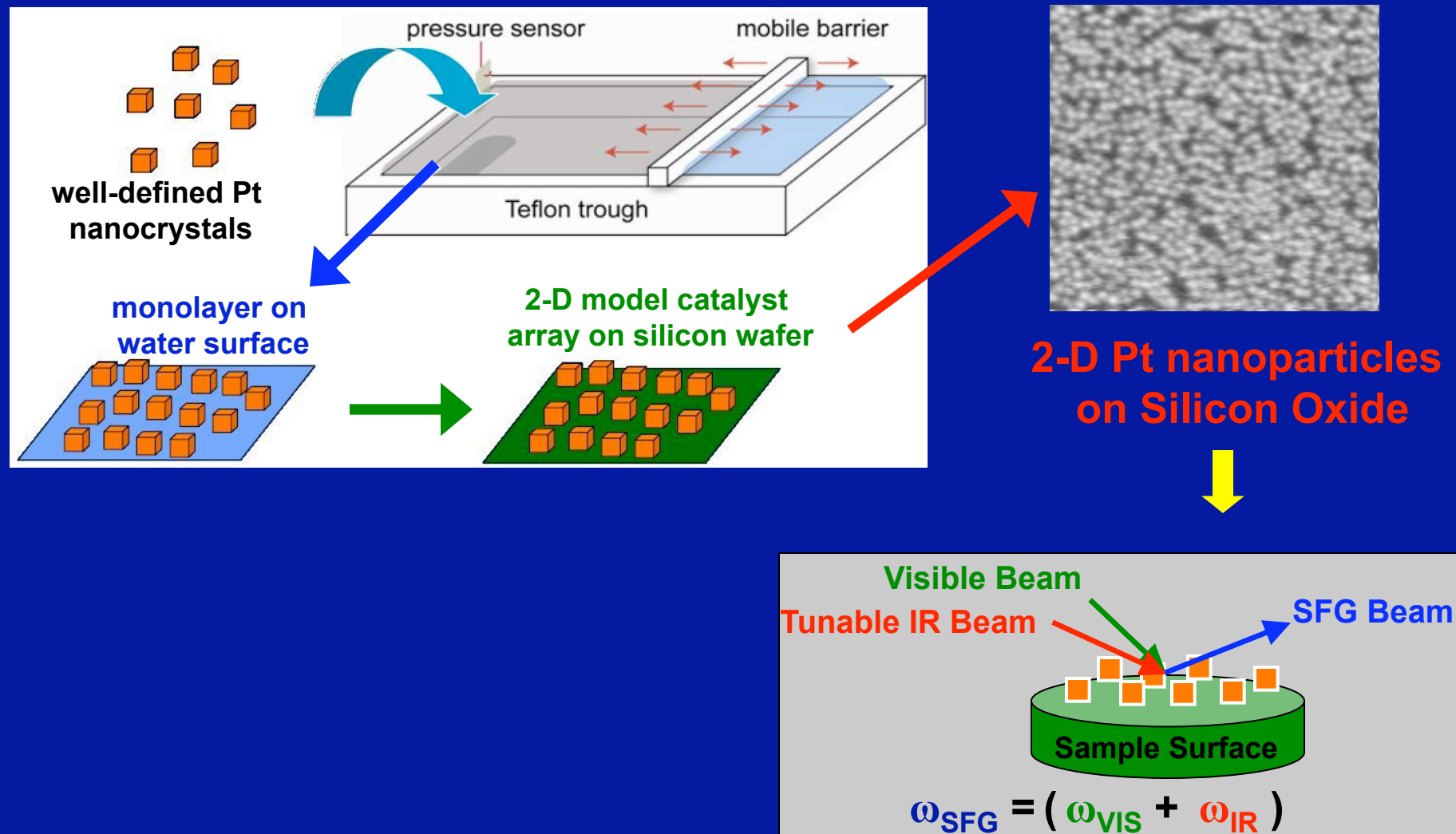
Pt nanocrystal shape control – silver ion



PdPt alloy nanocrystal shape control – oxygen

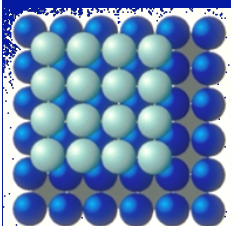


SFG Catalysis Study of 2-Dimensional Pt Nanoparticle Array

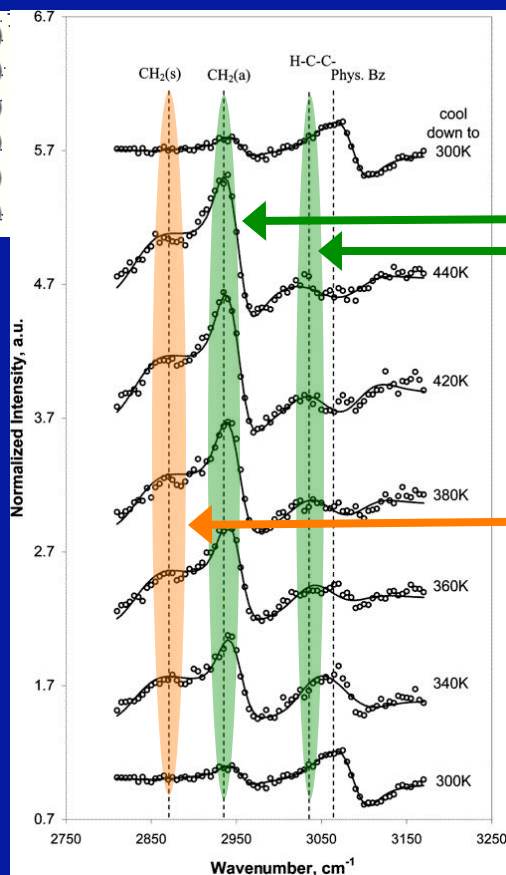


SFG of Benzene Hydrogenation on Pt(111) and Pt (100)

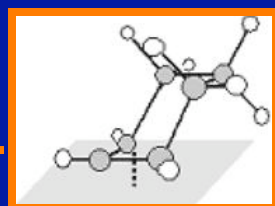
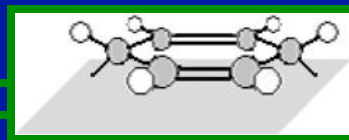
SFG of Pt (100)



Pt (100)

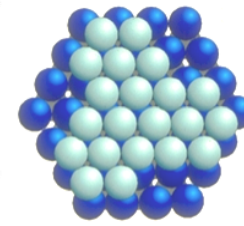


dienyl C_6H_6

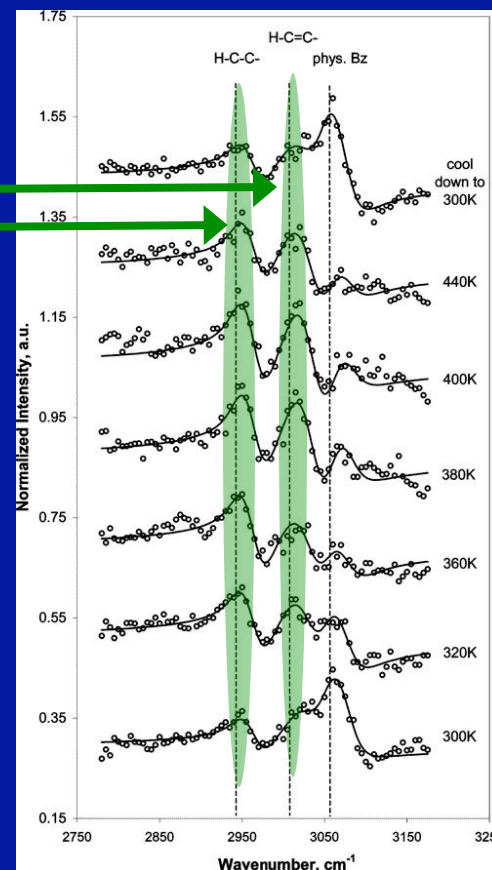


π -allyl *c*- C_6H_9

SFG of Pt (111)



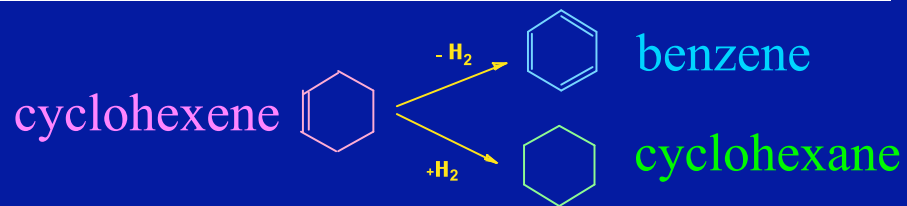
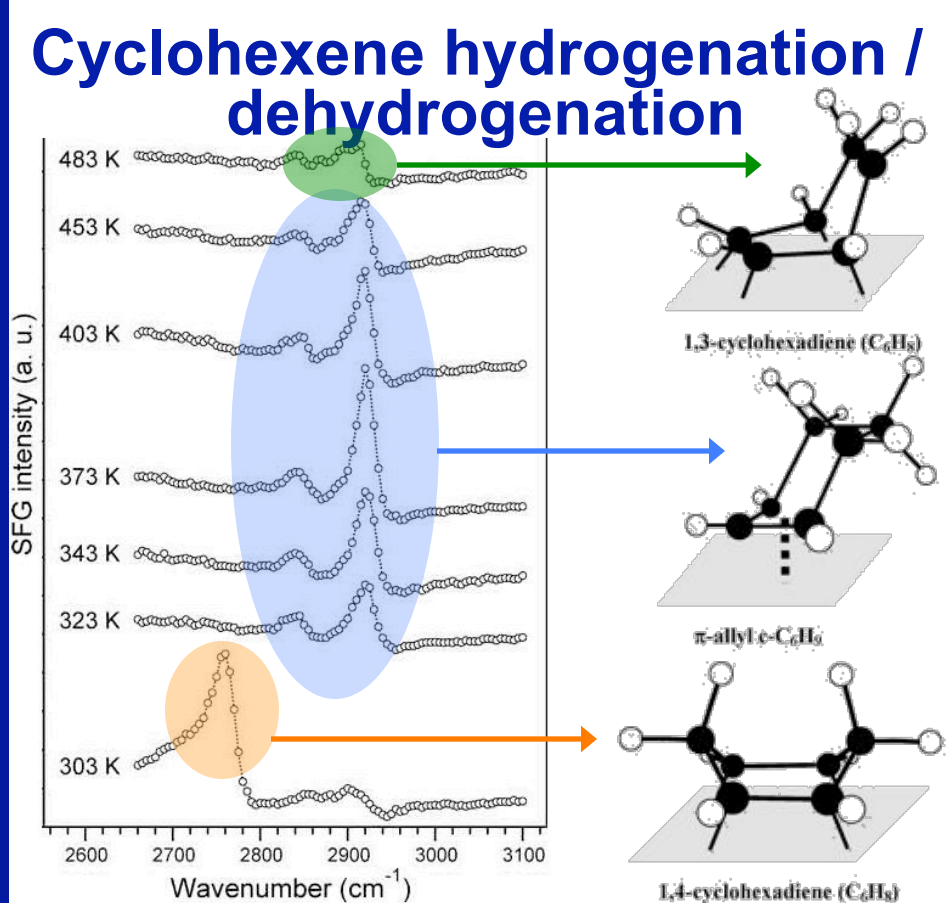
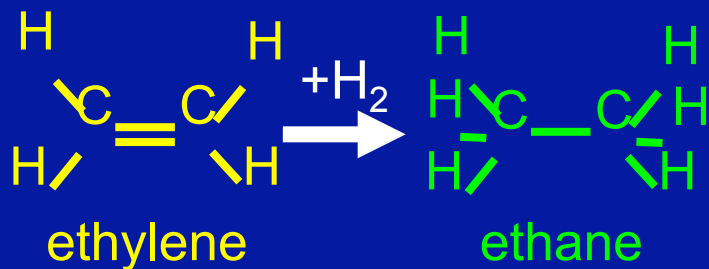
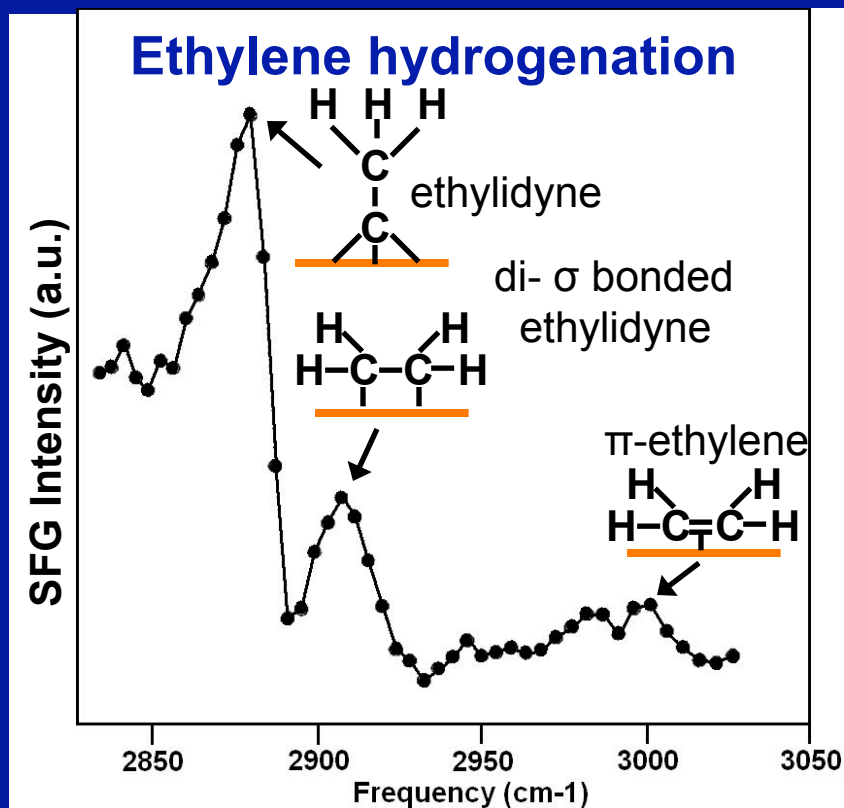
Pt (111)



- SFG shows π -allyl *c*- C_6H_9 benzene hydrogenation intermediate on Pt(100) only at high temperatures

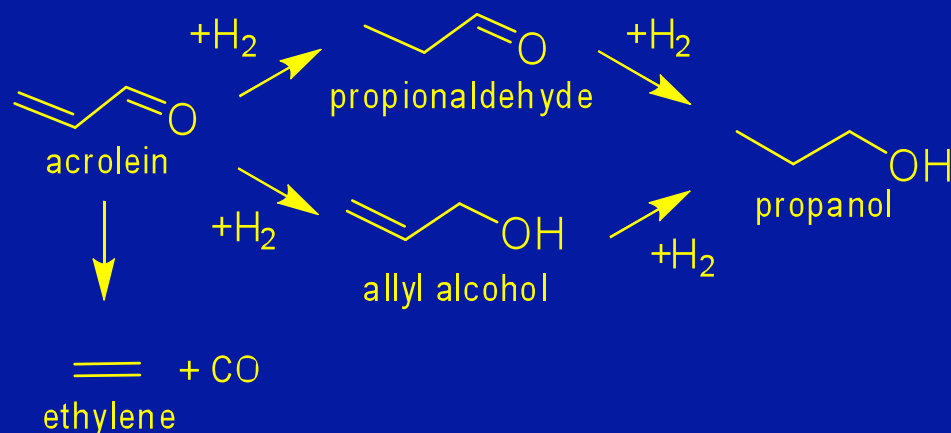
SFG Allows Study of Single Crystal Metal Catalysts *In-Situ*

SFG of Catalytic Reaction Intermediates During Reaction on Platinum

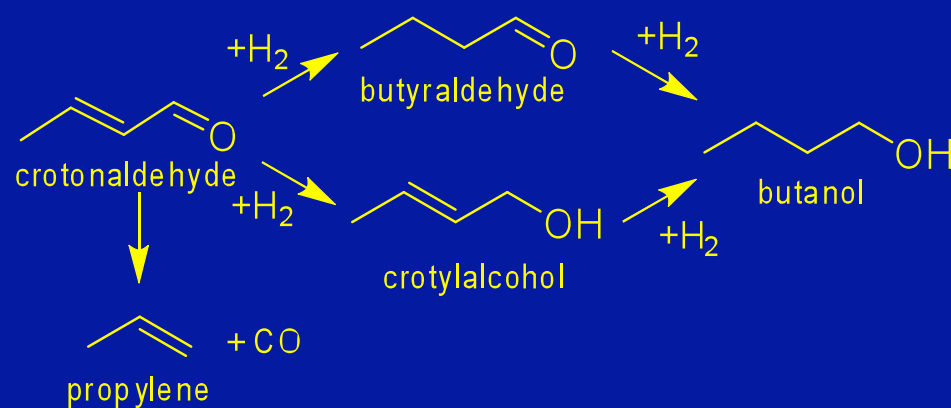


SFG of Hydrogenation of Bifunctional Molecules over Pt(111)

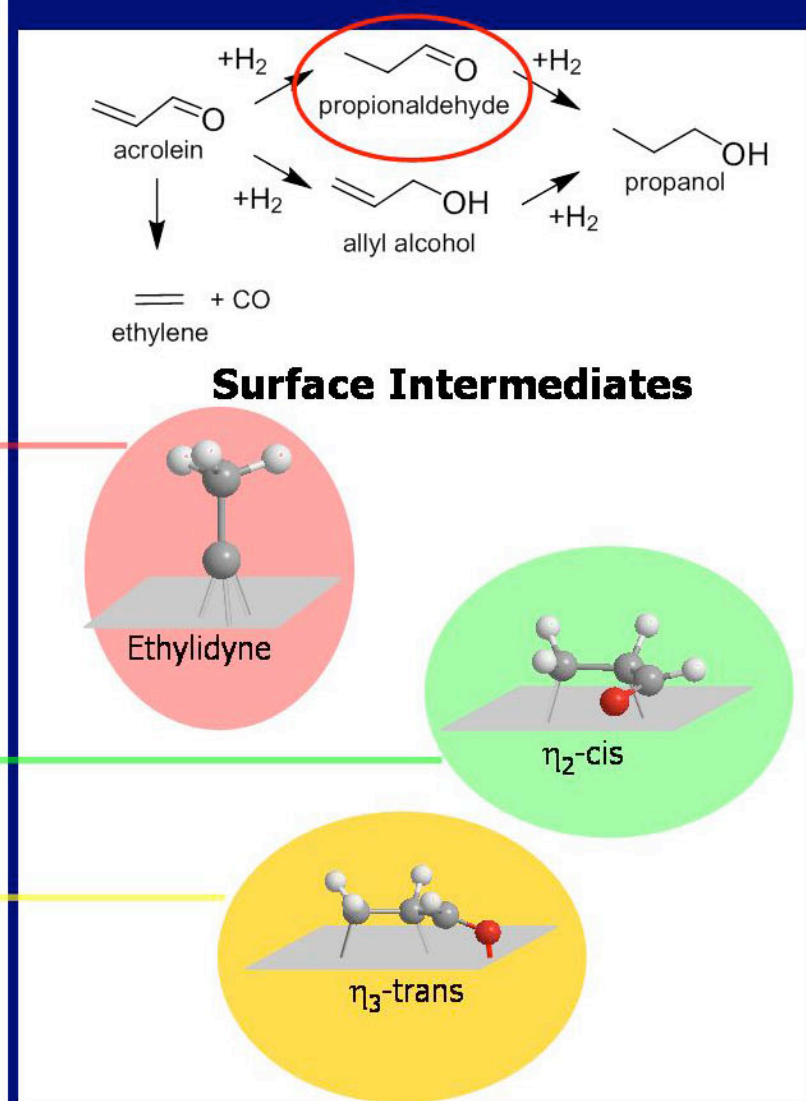
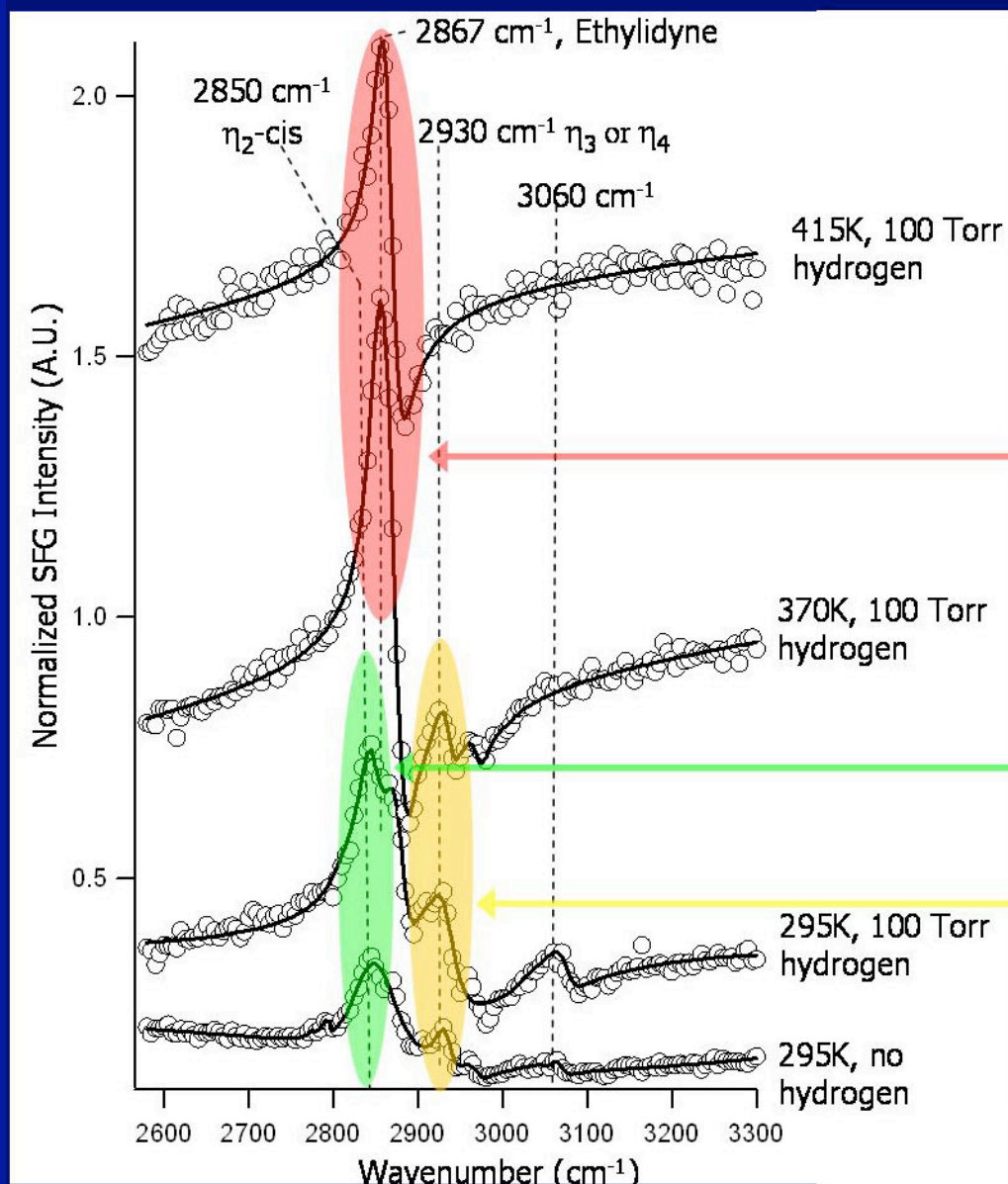
Acrolein Hydrogenation



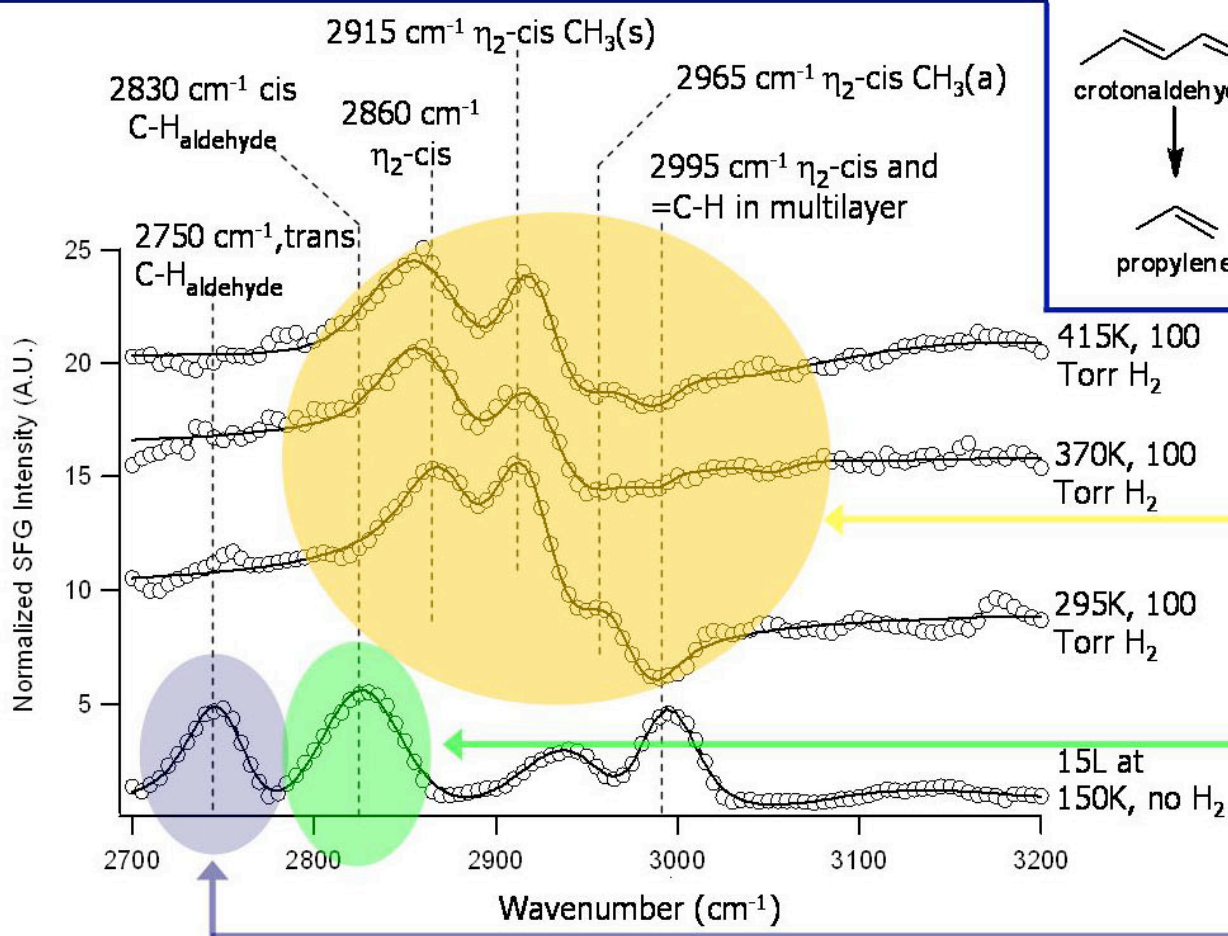
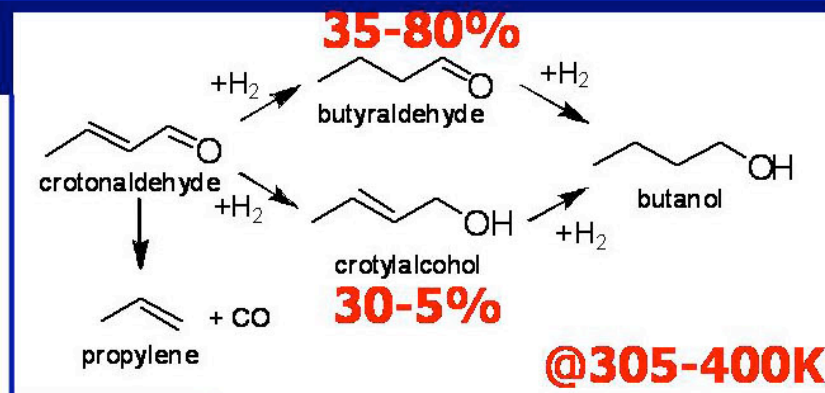
Crotonaldehyde Hydrogenation



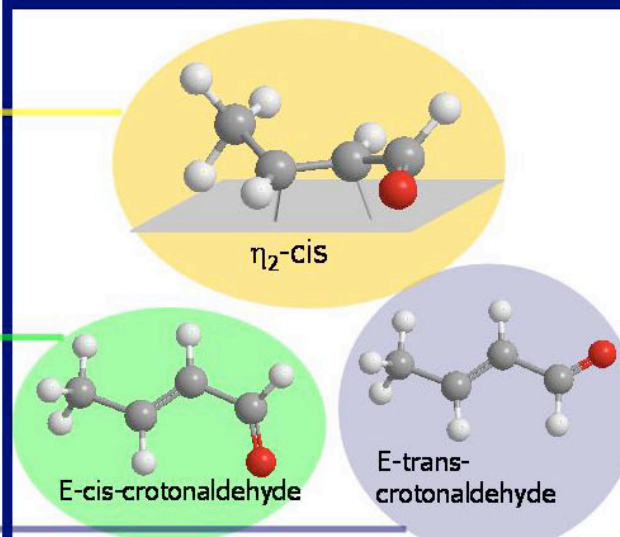
Acrolein Hydrogenation over Pt(111) Temperature Dependence



Crotonaldehyde Hydrogenation on Pt(111) (1 Torr Crotonaldehyde)

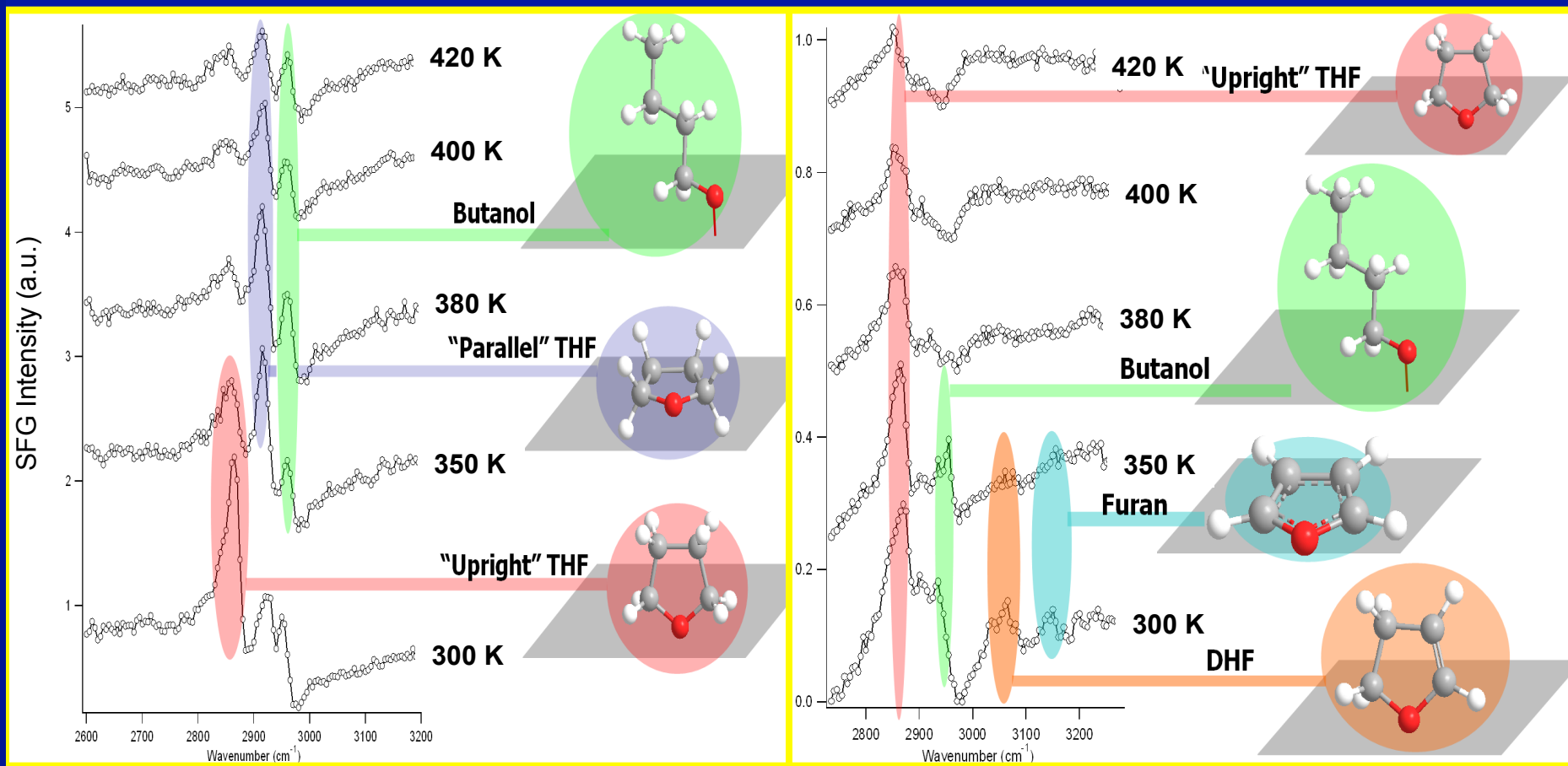


Surface Intermediates



Furan Hydrogenation over Pt(111) vs 10 nm Pt Nanoparticles

10 Torr Furan and 100 Torr Hydrogen

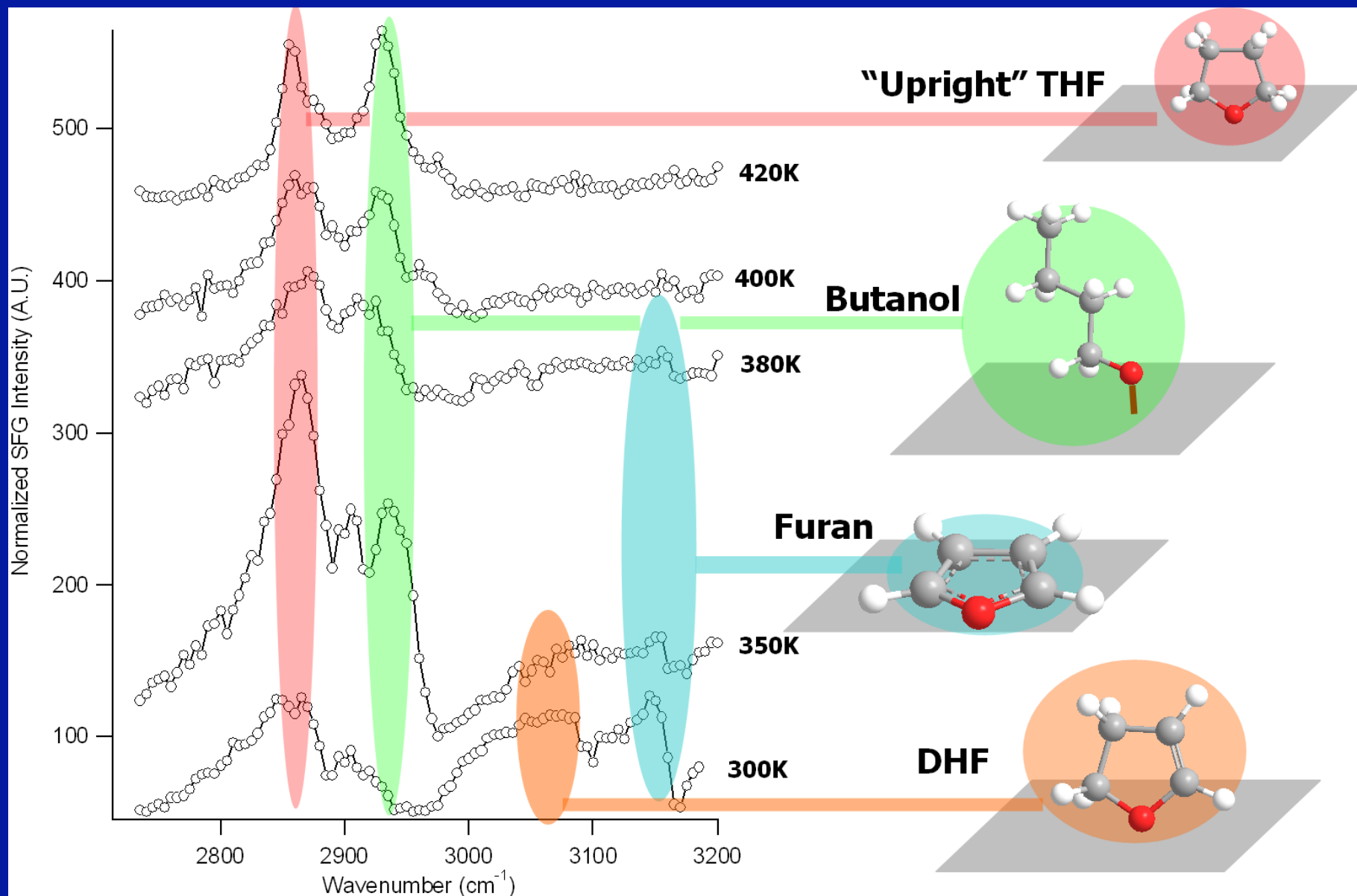


Pt(111) Single Crystal

10 nm Pt Nanoparticles

Furan Hydrogenation on 1 nm Pt Nanoparticles

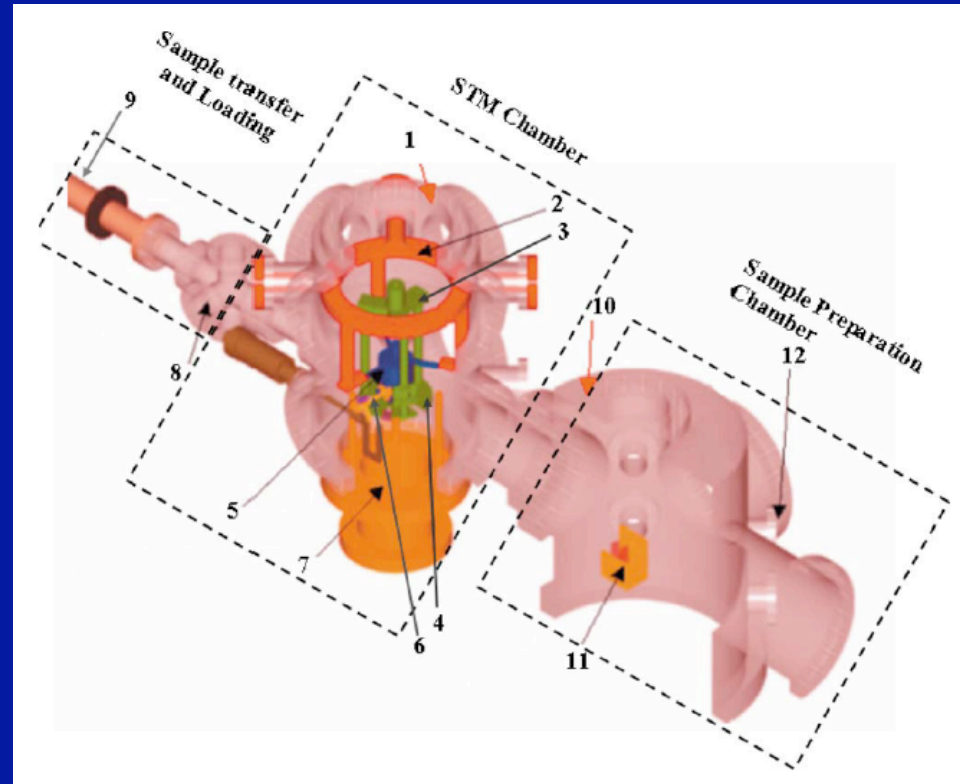
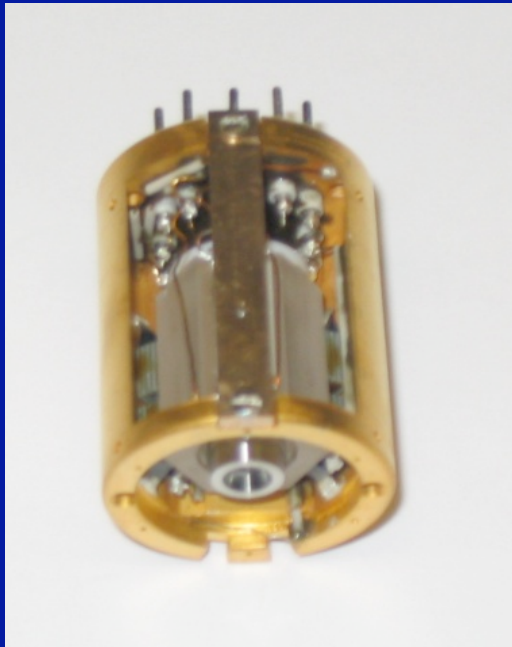
10 Torr Furan / 100 Torr H₂



High Pressure STM

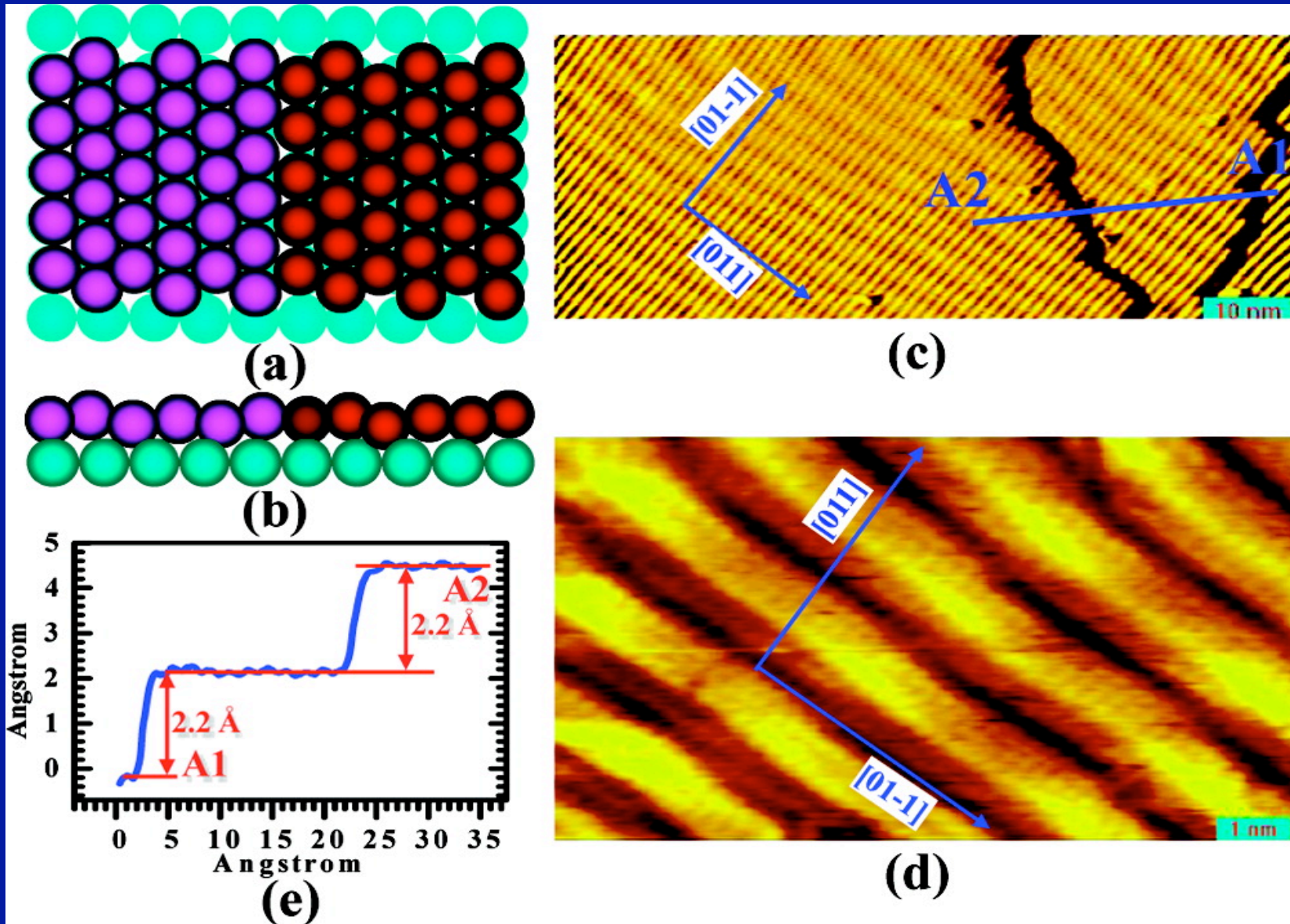
Substrate Mobility

Scanning tunneling microscopy working under high pressure conditions



CO on Pt(100)

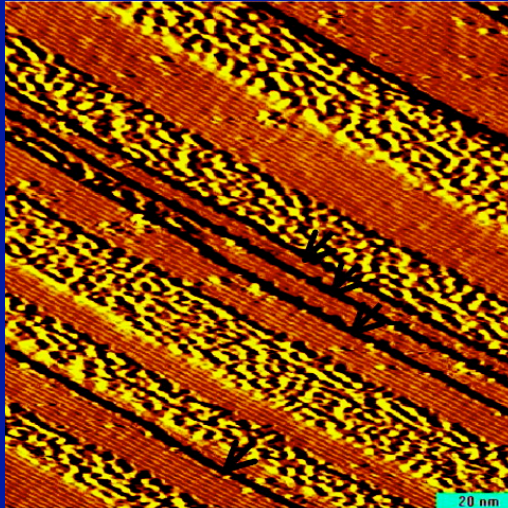
STM of Pt(100) Hex Reconstruction



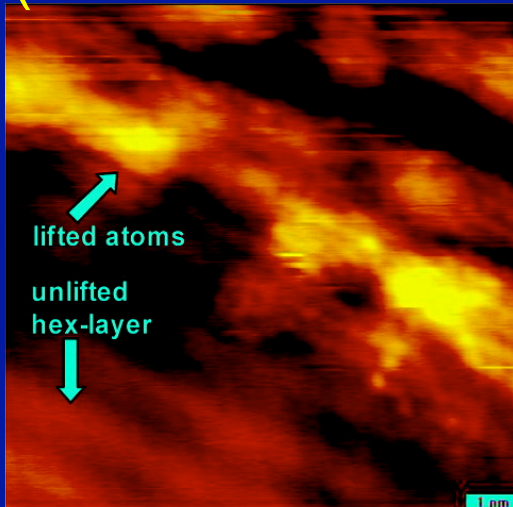
Feng Tao; Sefa Dag; Lin-Wang Wang; Zhi Liu; Derek R. Butcher; Miquel Salmeron; Gabor A. Somorjai; *Nano Lett.* **2009**, 9, 2167-2171.

Pt(100) Restructuring

10^{-9} Torr CO

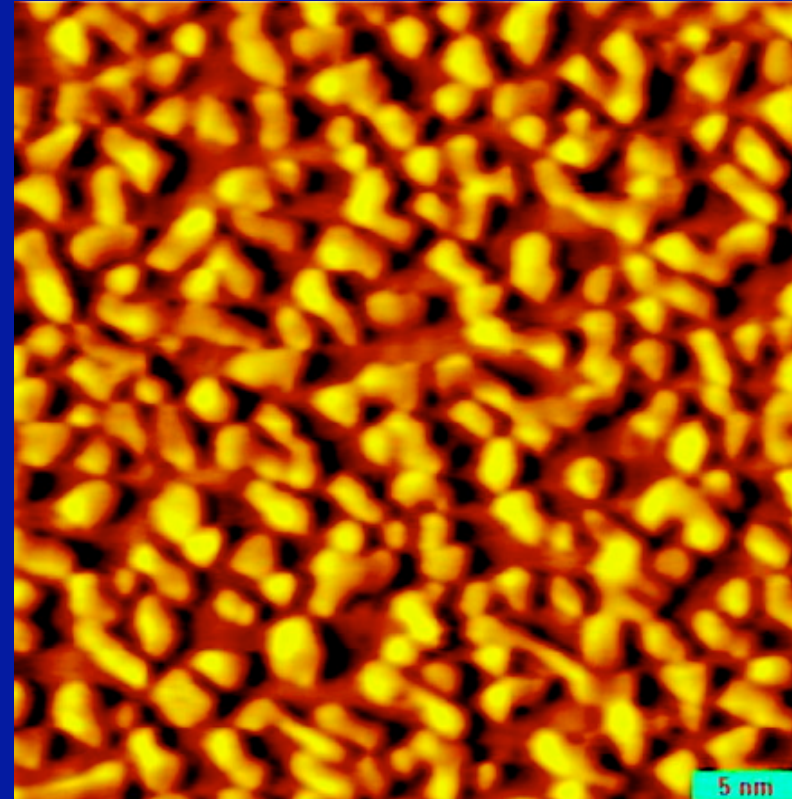


(100 nm x 100 nm)



(10 nm x 10 nm)

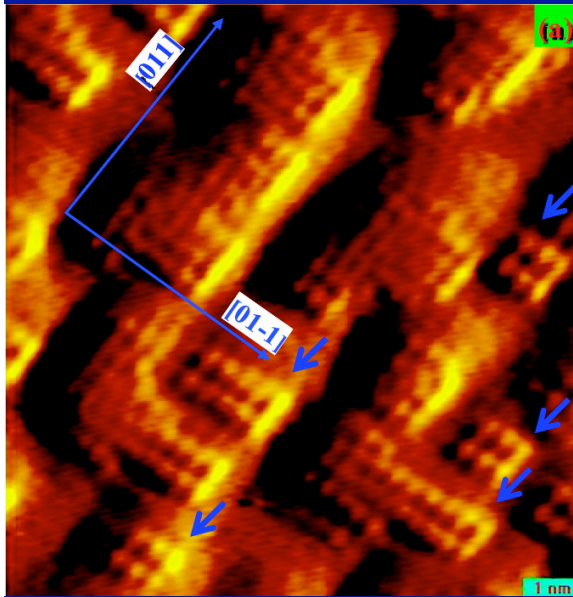
10^{-5} Torr CO



(38 nm x 36 nm)

CO lifts the hex Reconstruction resulting in clusters

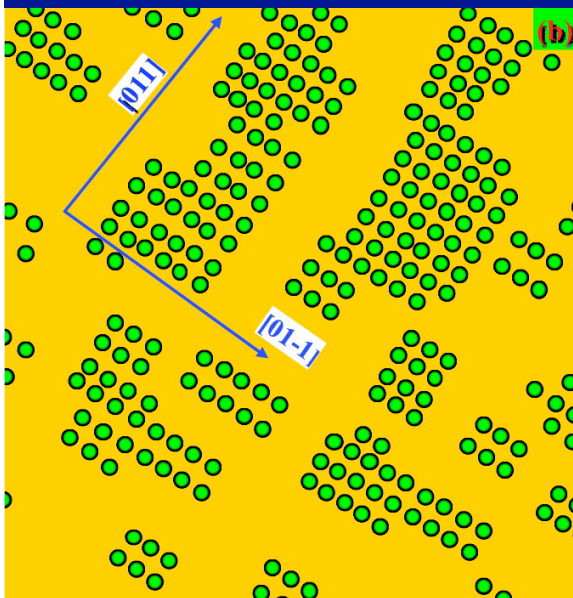
CO/Pt(100) Cluster Structure



Atomic resolution images

CO nearest neighbor
O-O distance: 3.7-4.1 Å

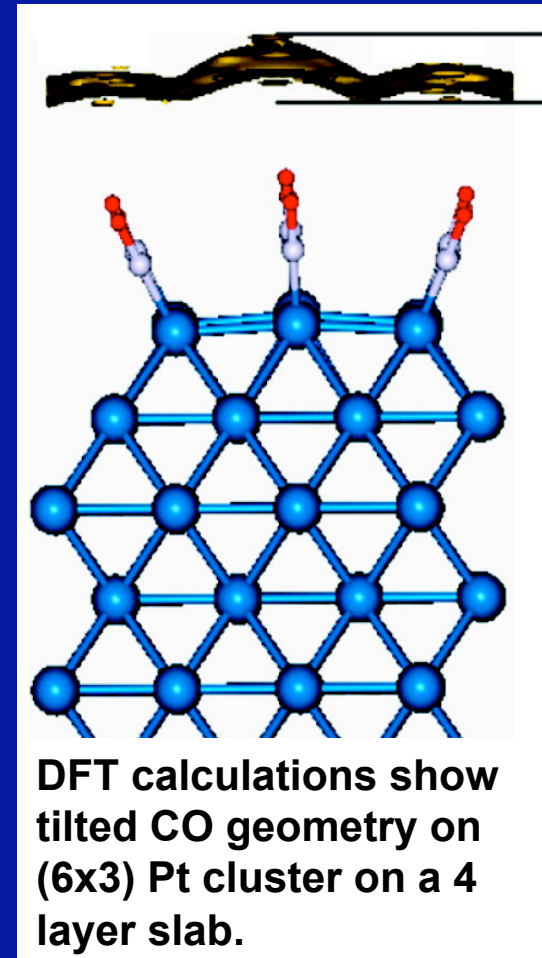
Compared to
Pt-Pt 2.75 Å



DFT Calculations

CO-CO repulsion results
in tilting expanding CO-
CO distance.

Energy gain 3.2 eV per
Pt-CO pair

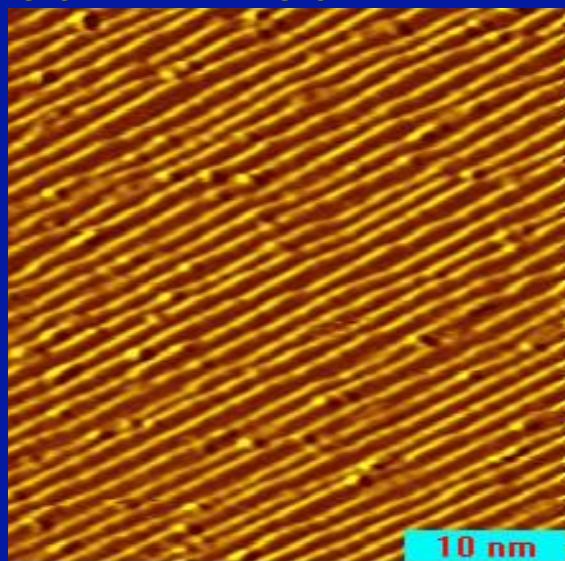


DFT calculations show
tilted CO geometry on
(6x3) Pt cluster on a 4
layer slab.

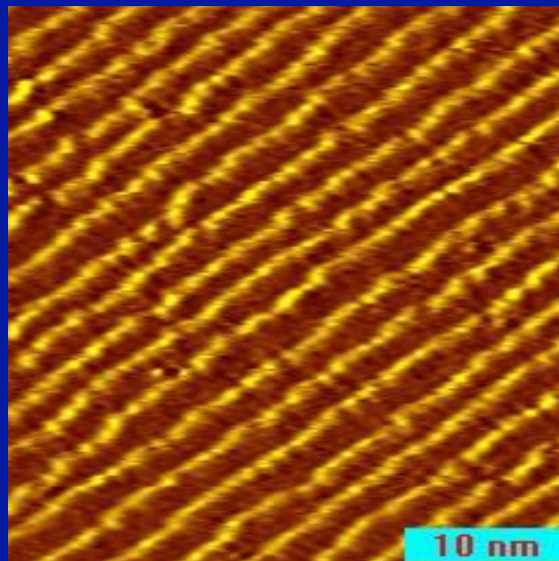
CO on Stepped Pt

Reversible Cluster Formation on Pt(557)

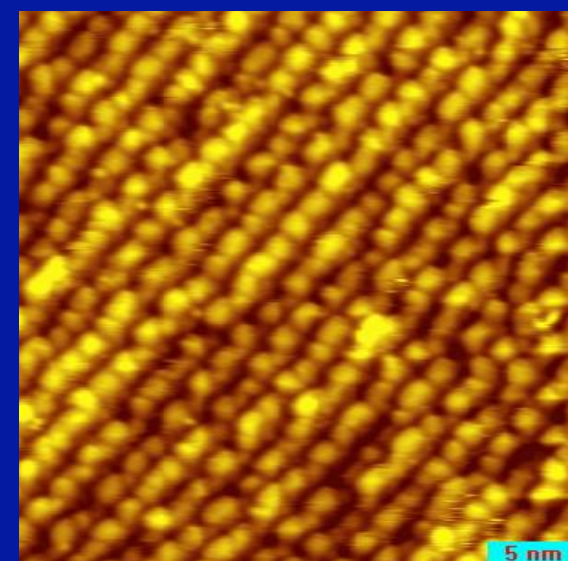
30 nm x 30 nm



10^{-10} Torr

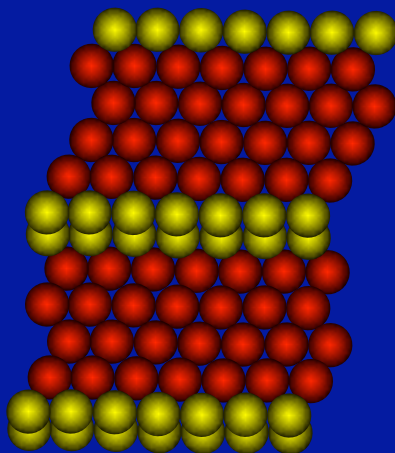


5×10^{-8} Torr CO



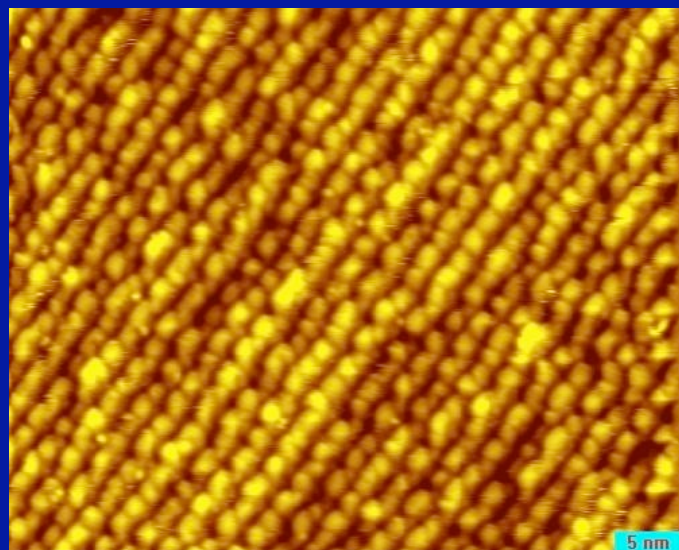
1 Torr CO

Pt(557):
6(111)x(100)



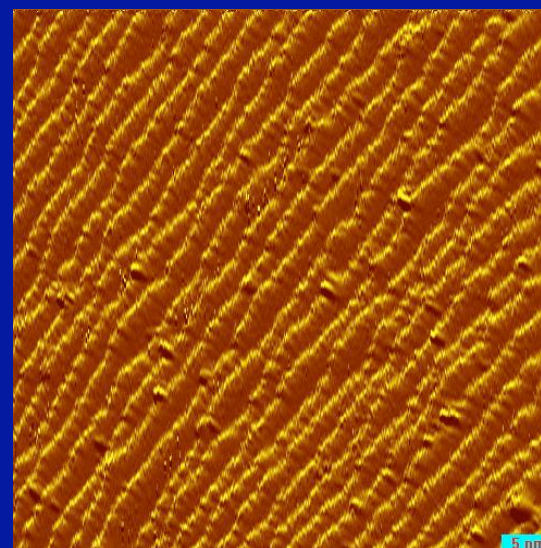
- Low pressure CO induces step doubling
- High pressure CO causes the step terraces to break up into ~ 2 nm clusters

Reversible CO-induced Restructuring of Pt(557)



1 Torr CO

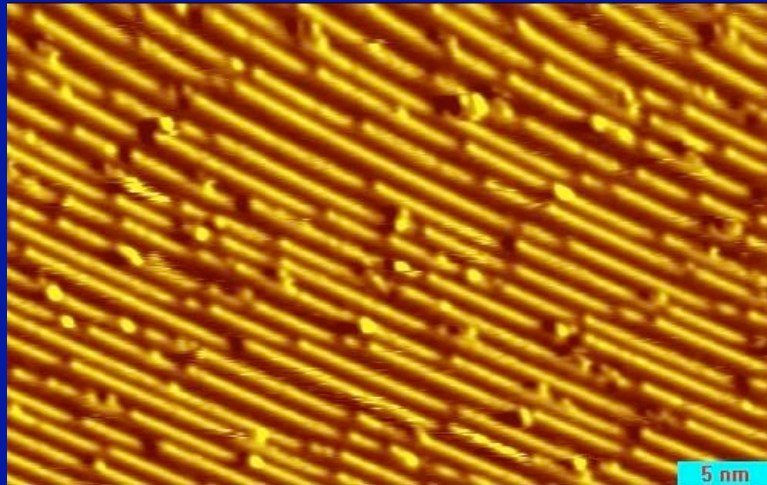
Pump out
to 10^{-8} Torr
CO



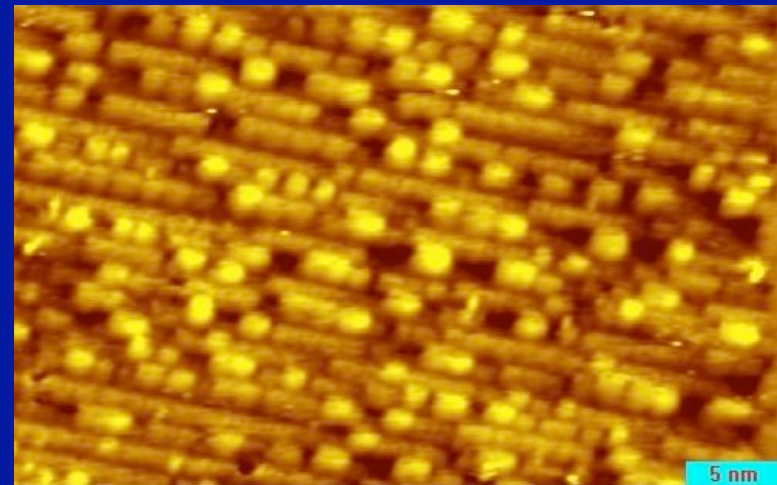
$\sim 10^{-8}$ Torr CO

- Low pressure structure has regular terraces
- High pressure CO causes the step terraces to break up into ~ 2 nm clusters
- Cluster formation is reversible: Pump out reforms terraces with increased kink sites
- CO-CO repulsion causes clustering

Reversible CO-induced clustering on Pt(332)

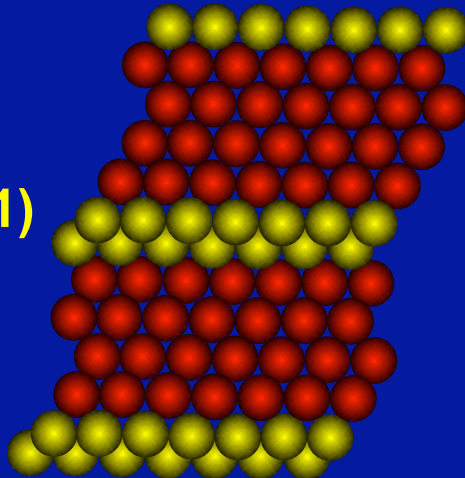


10^{-8} Torr CO



1 Torr CO

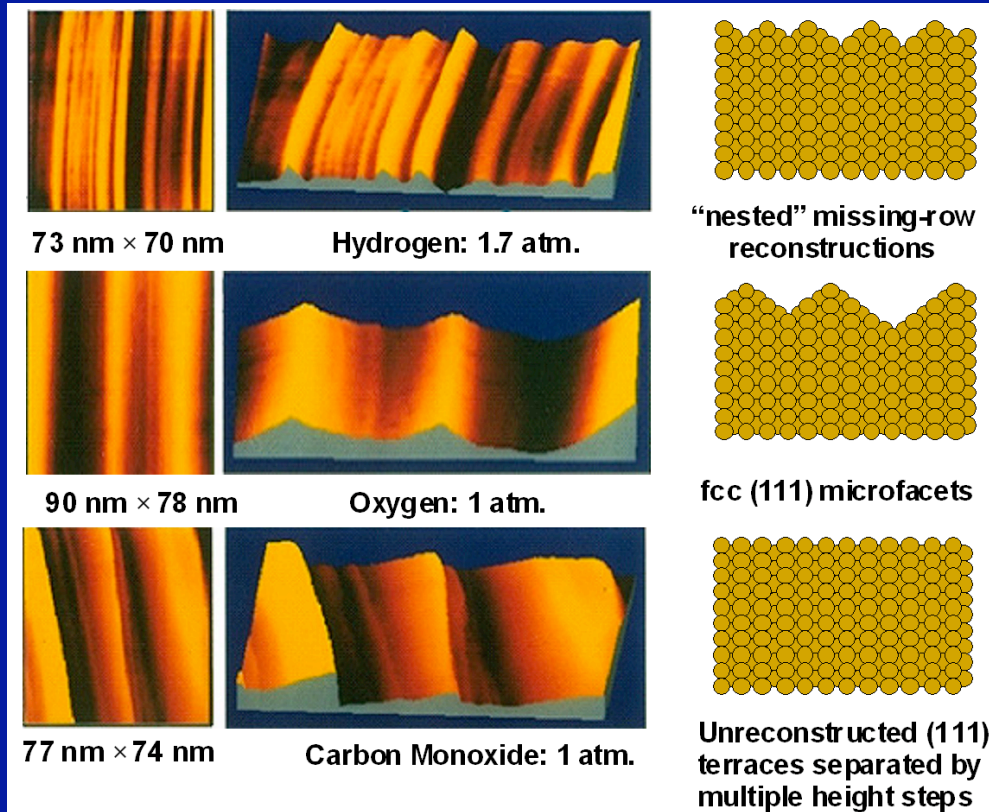
Pt(332):
6(111)x(111)



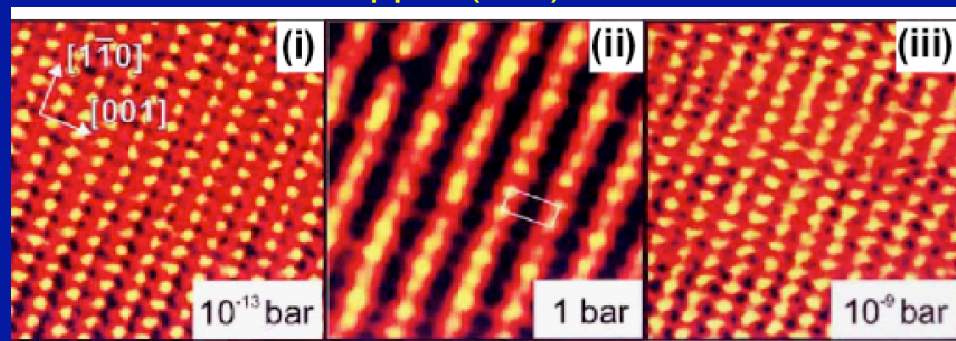
- Cluster Structure on (332) consists of rectangular blocks and depressions
- Clustering is also reversible upon pump out.

Pressure Enhanced
Adsorbate-Induced Restructuring

Platinum (110)



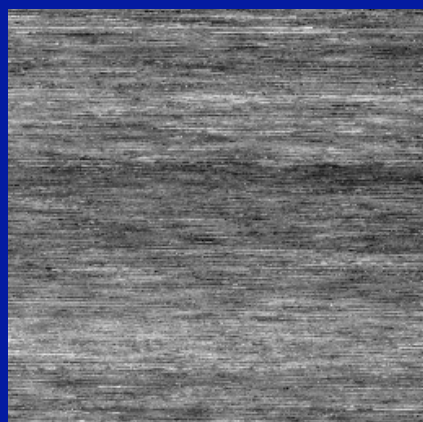
Copper (110)



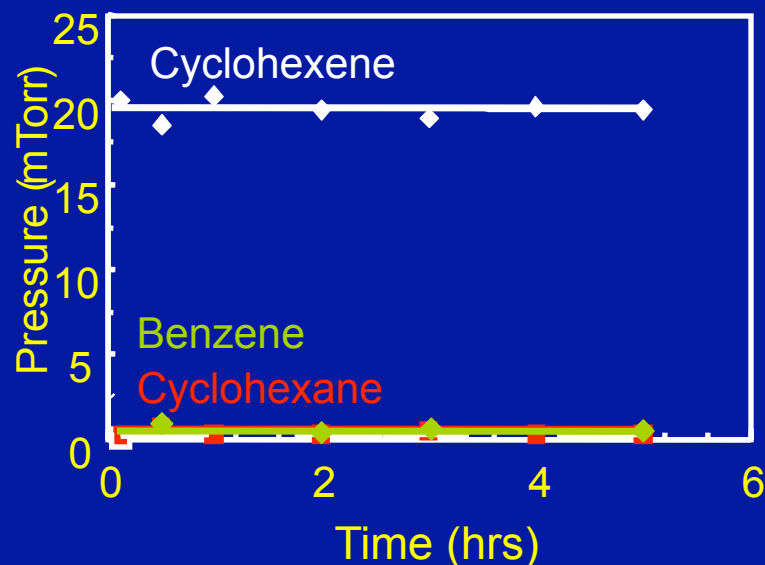
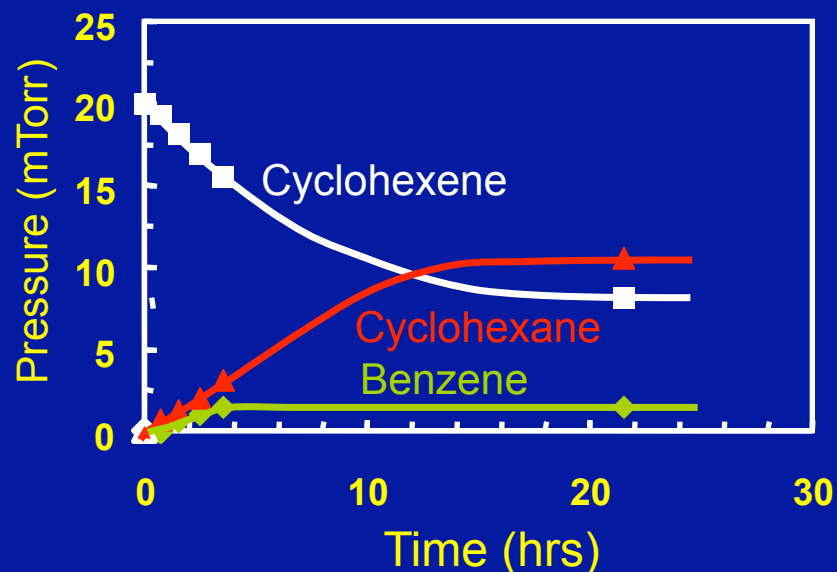
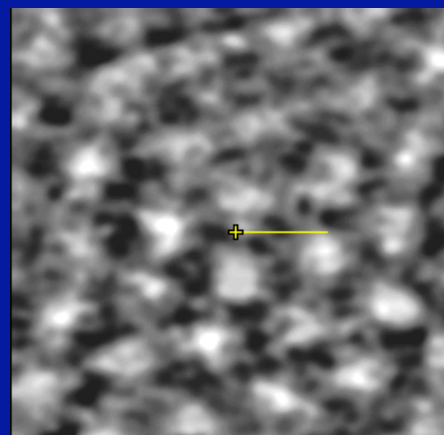
Adsorbate Mobility

High pressure STM Reaction Studies: the role of surface mobility

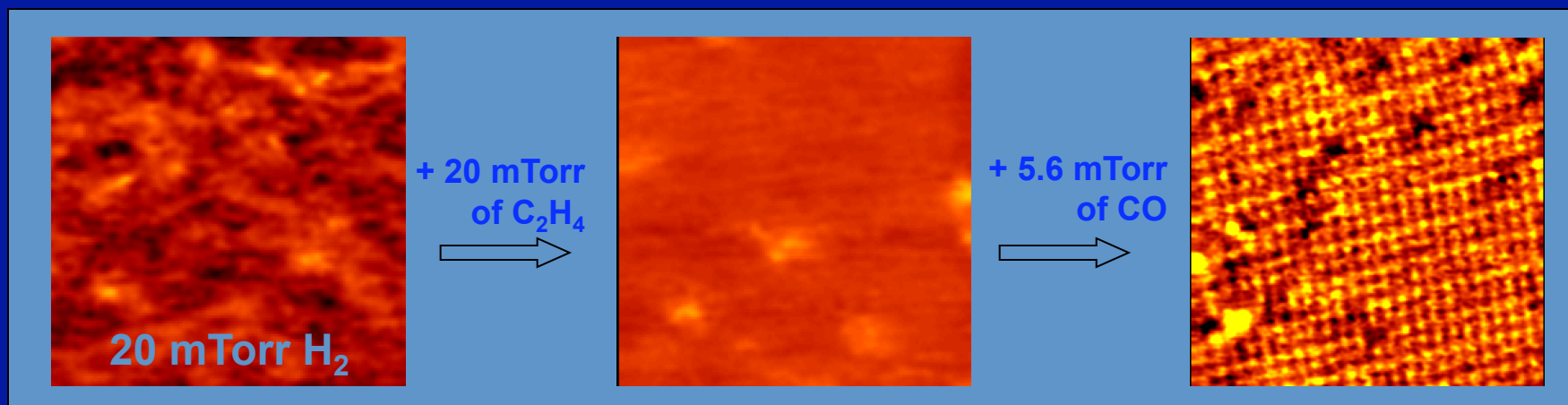
75Å x 75Å image of catalytically active Pt(111) at 25C. 200 mTorr H₂ and 20 mTorr cyclohexene



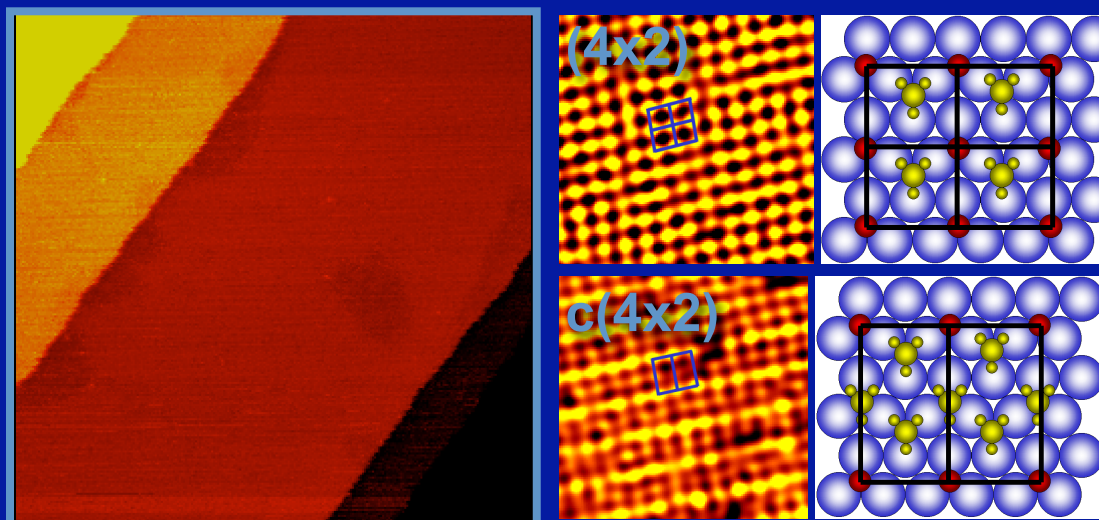
70Å x 70Å image of CO poisoned Pt(111) at 25C. 200 mTorr H₂, 20 mTorr of cyclohexene, and 5 mtorr CO



Blocking of adsorbate (C_2H_3 , H) mobility by CO poisons catalytic reaction on Rh and Pt(111)

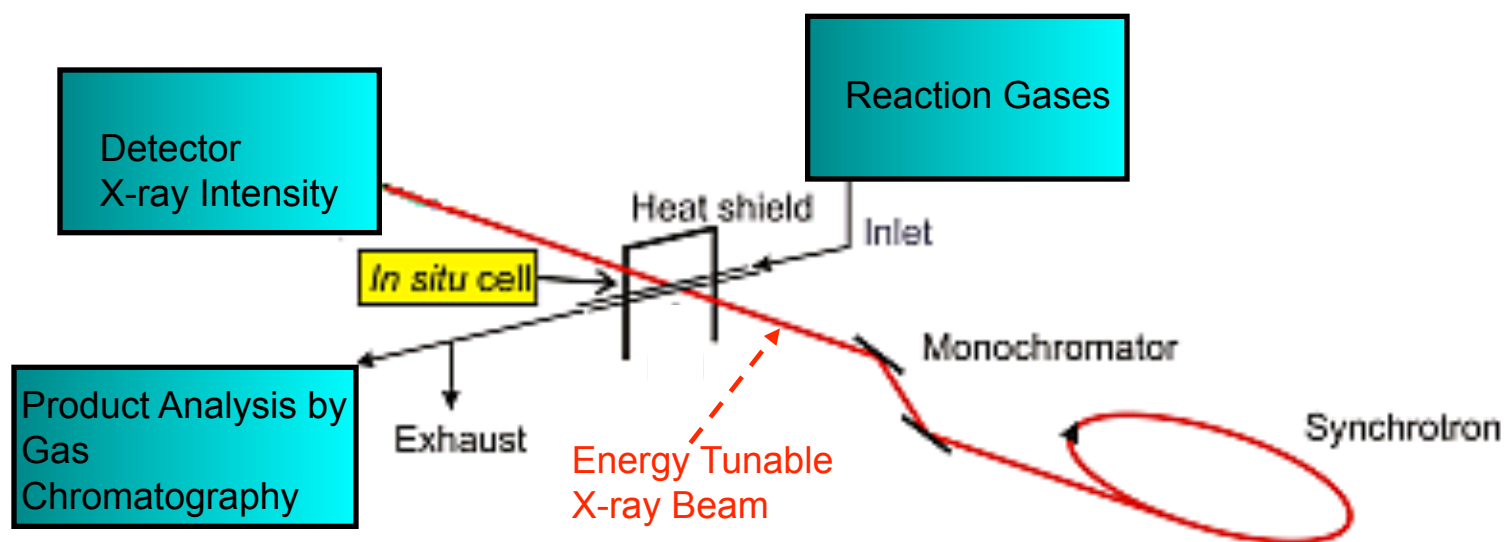


CO induces the formation of immobile crystalline coadsorbed structures



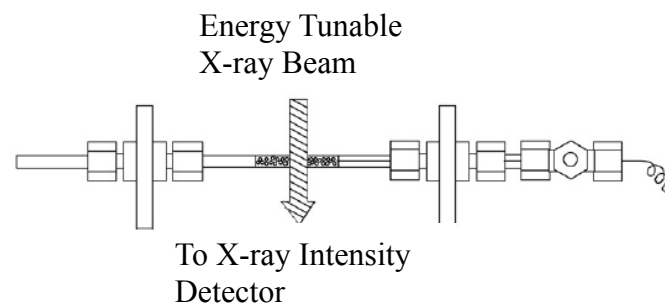
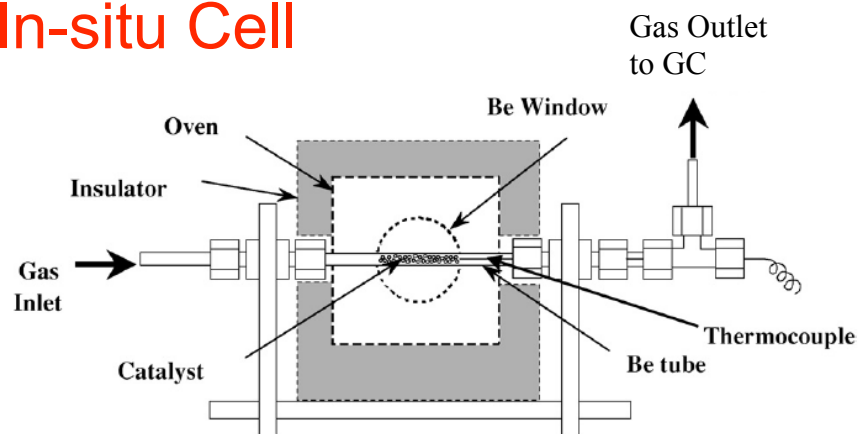
High pressure scanning tunneling microscopy study of CO poisoning of ethylene hydrogenation on Pt(111) and Rh(111) single crystals. D.C. Tang, K.S. Hwang, M. Salmeron and G.A. Somorjai. *J. Phys. Chem. B* 108,13300 (2004)

X-ray Absorption Spectroscopies (XAS)



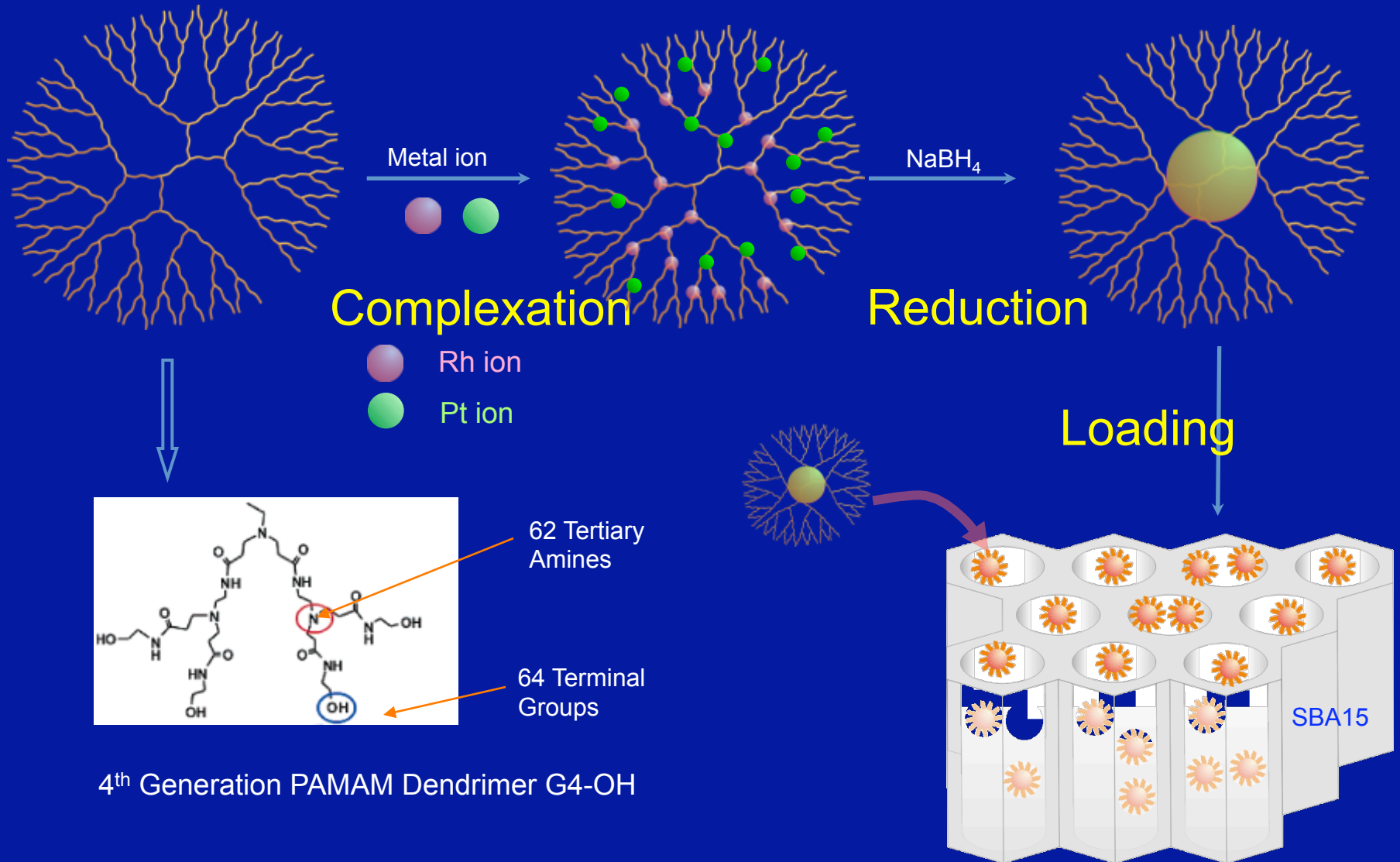
http://hasylab.desy.de/e77/e106/e122/e4410/e4413/fig11_eng.png

In-situ Cell

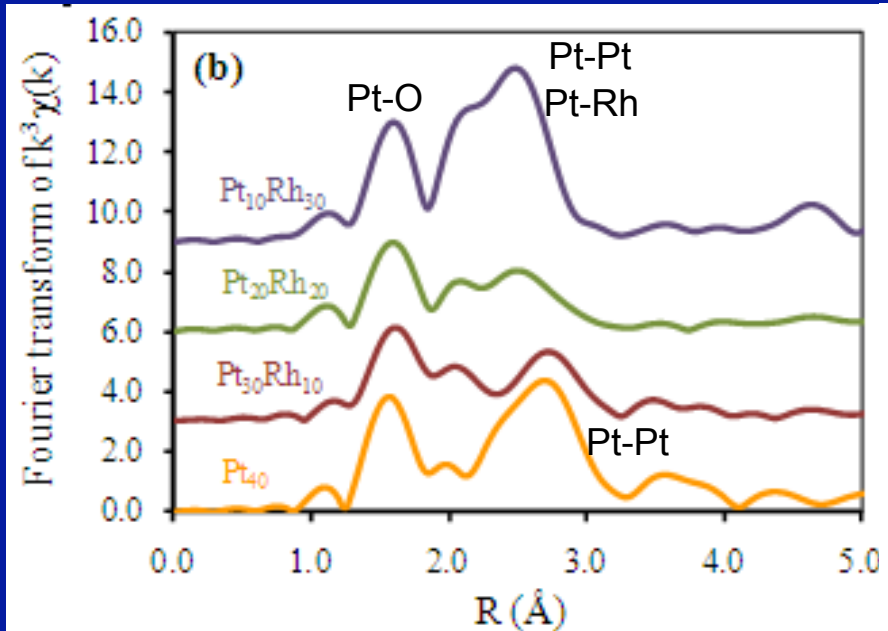


Bare, S. R. et al., *Catal. Today* 2007, 126, (1-2), 18-26.

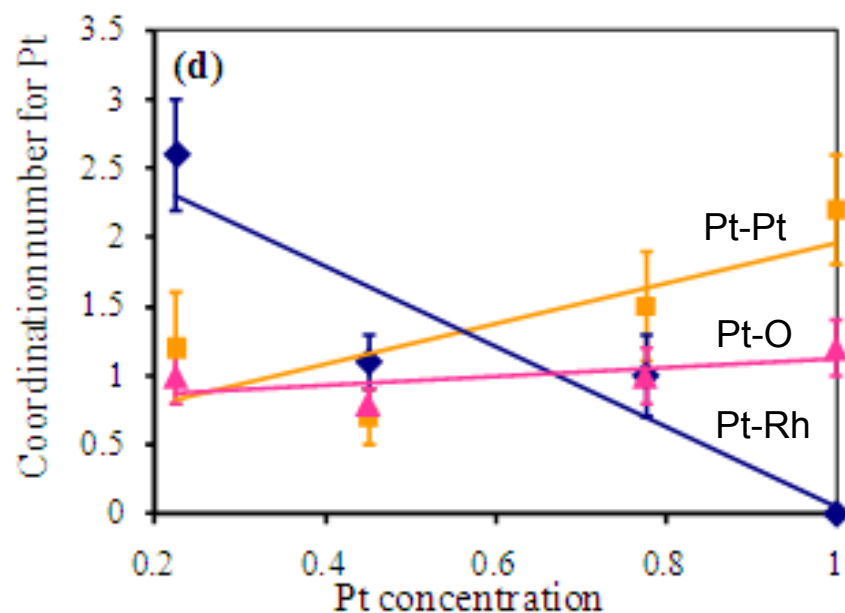
Synthesis and Immobilization of Dendrimer Encapsulated Bimetallic PtRh Nanoparticles



Coordination Environment of Dendrimer Encapsulated ~ 1 nm PtRh Bimetallic Nanoparticles Measured by EXAFS at Pt Edge

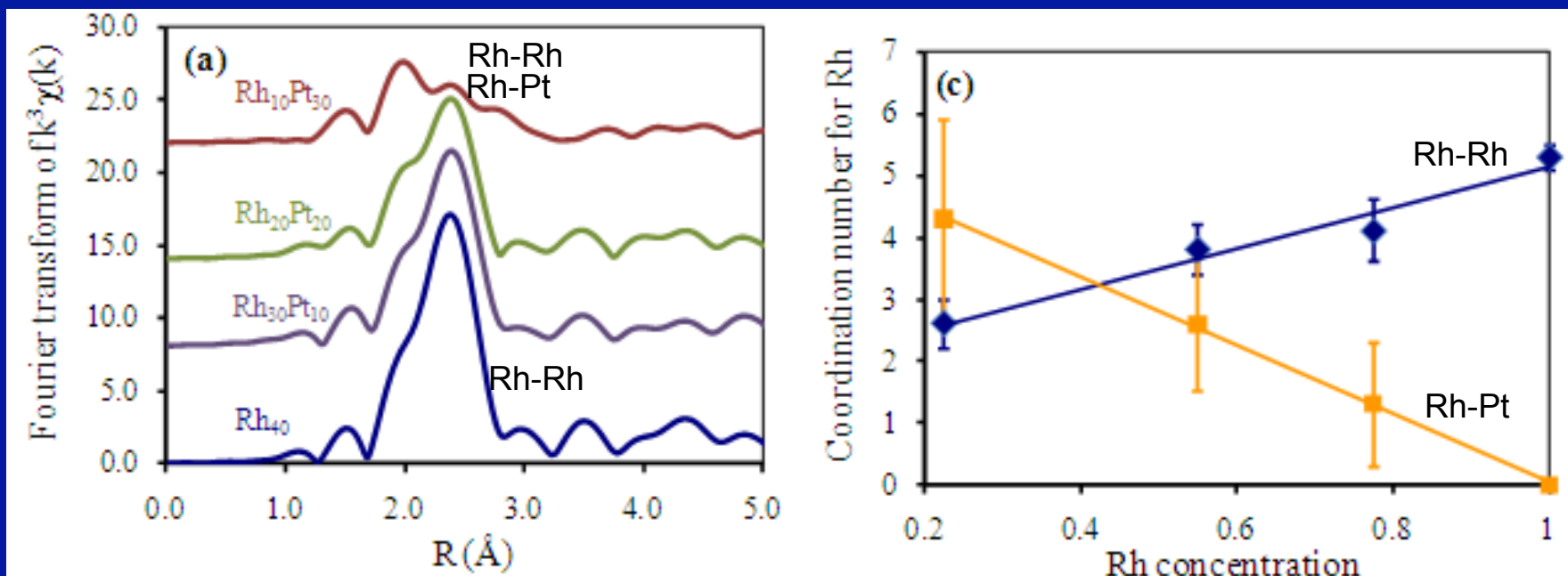


k^3 -weighted Fourier transform of Pt L_3 edge EXAFS spectra of the dendrimer Pt_xRh_{40-x} nanoparticles.



Local coordination numbers for Pt of the dendrimer bimetallic catalysts.

Coordination Environment of Dendrimer Encapsulated ~ 1 nm PtRh Bimetallic Nanoparticles Measured by EXAFS at Rh Edge



k^3 -weighted Fourier transform of Rh K edge EXAFS spectra of the dendrimer $\text{Pt}_x\text{Rh}_{40-x}$ nanoparticles.

Local coordination numbers for Rh of the dendrimer bimetallic catalysts.

Degree of Alloying in the $\text{Pt}_x\text{Rh}_{40-x}$ Nanoparticles

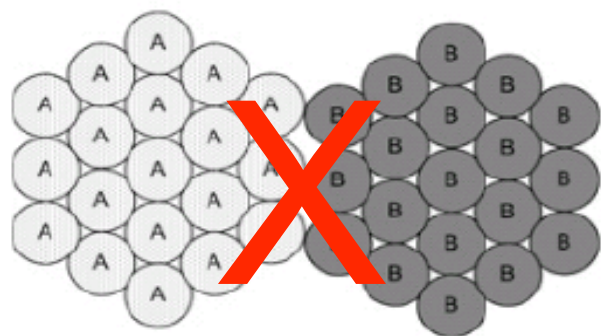
The two quantities determining the degree of alloying are given by

$$J_{\text{Pt}} = \frac{N_{\text{Pt-Rh}} / N_{\text{Pt,total}}}{c_{\text{Rh}}} \times 100\% \qquad J_{\text{Rh}} = \frac{N_{\text{Rh-Pt}} / N_{\text{Rh,total}}}{c_{\text{Pt}}} \times 100\%$$

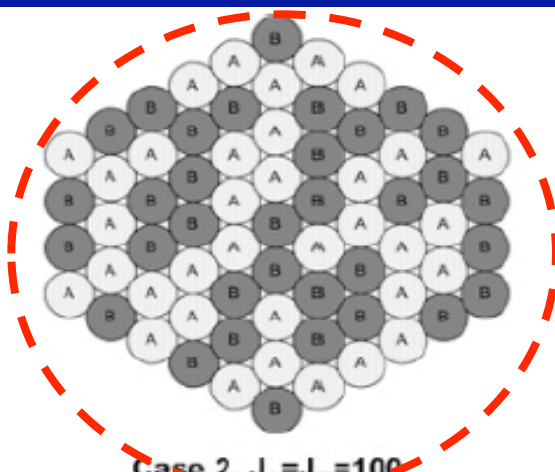
In above equations, c_{Pt} and c_{Rh} are the concentrations of Pt and Rh in the alloy nanoparticles, respectively. $N_{\text{Pt,total}}$ and $N_{\text{Rh,total}}$ are the total coordination numbers of the absorber atom Pt and Rh in the nanoparticles, respectively. The calculated J_{Pt} and J_{Rh} for the $\text{Pt}_x\text{Rh}_{40-x}$ samples are

	$J_{\text{Pt}} \%$	$J_{\text{Rh}} \%$
$\text{Pt}_{30}\text{Rh}_{10}$	128	80
$\text{Pt}_{20}\text{Rh}_{20}$	77	90
$\text{Pt}_{10}\text{Rh}_{30}$	70	107

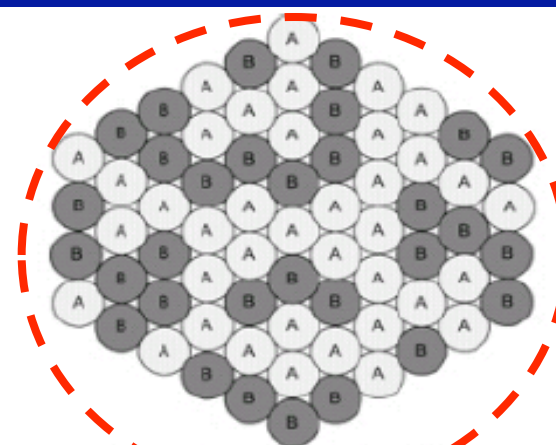
Schematics of bimetallic nanoparticles at various degrees of alloying



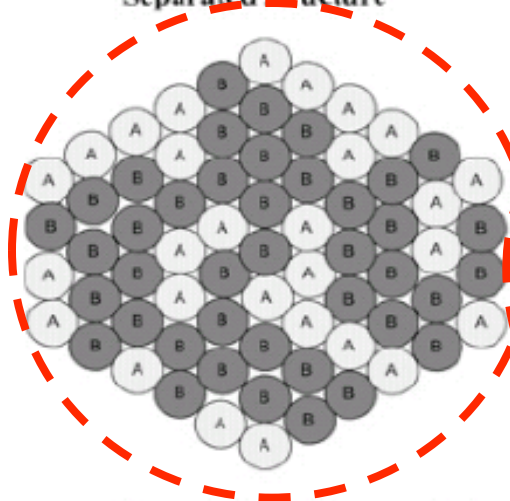
Case 1. $J_A=0, J_B=0$
 $H_{A-A} \& H_{B-B} \gg H_{A-B}$
 Separated structure



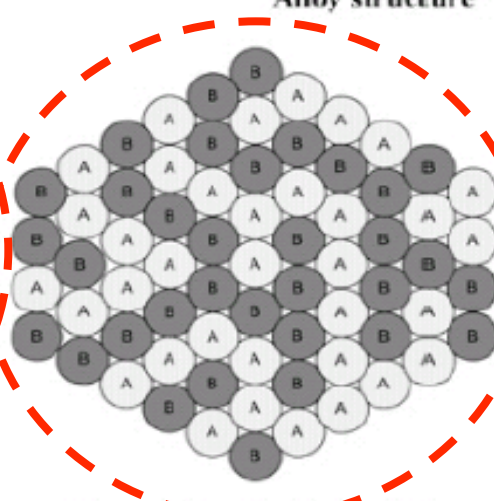
Case 2. $J_A=J_B=100$
 $H_{A-A}=H_{B-B}=H_{A-B}$
 Alloy structure



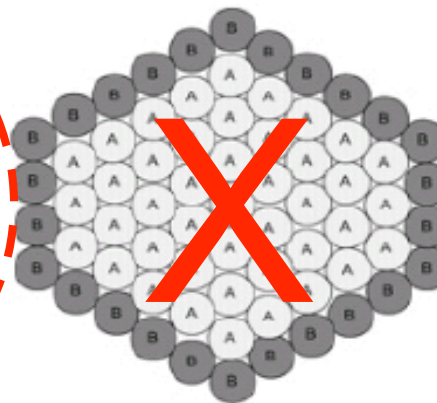
Case 3. $J_A < 100, J_B > 100$
 $H_{A-A} > H_{B-B} > H_{A-B}$
 Homo-philic structure



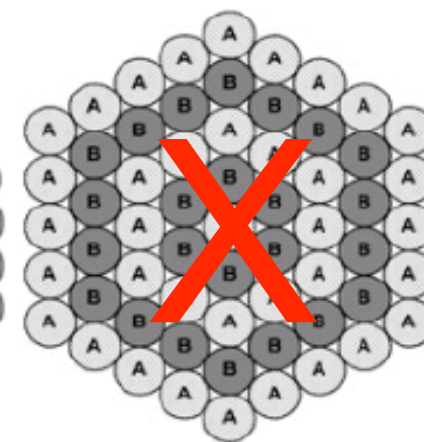
Case 4. $J_A > 100, J_B < 100$;
 $H_{B-B} > H_{A-A} > H_{A-B}$
 'B'-rich_{core}- 'A'-rich_{shell} structure



Case 5. $J_A > 100, J_B > 100$
 $H_{A-B} > H_{A-A}$ (or) H_{A-B}
 Heteratomic-rich structure

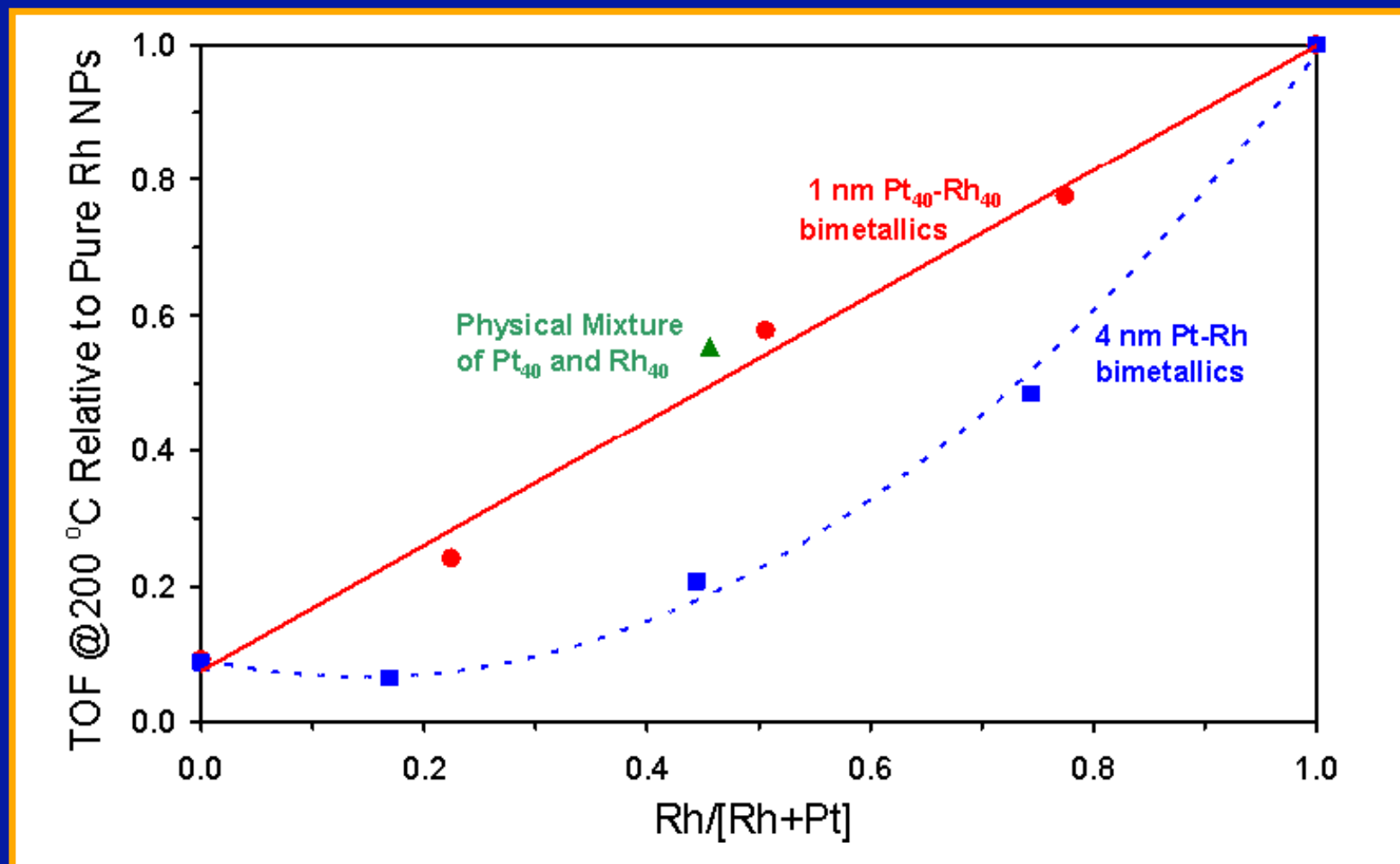


Case 6. $J_A < 50, J_B < 50$
 $H_{A-A} > H_{B-B} > H_{A-B}$
 $A_{core}-B_{shell}$ structure



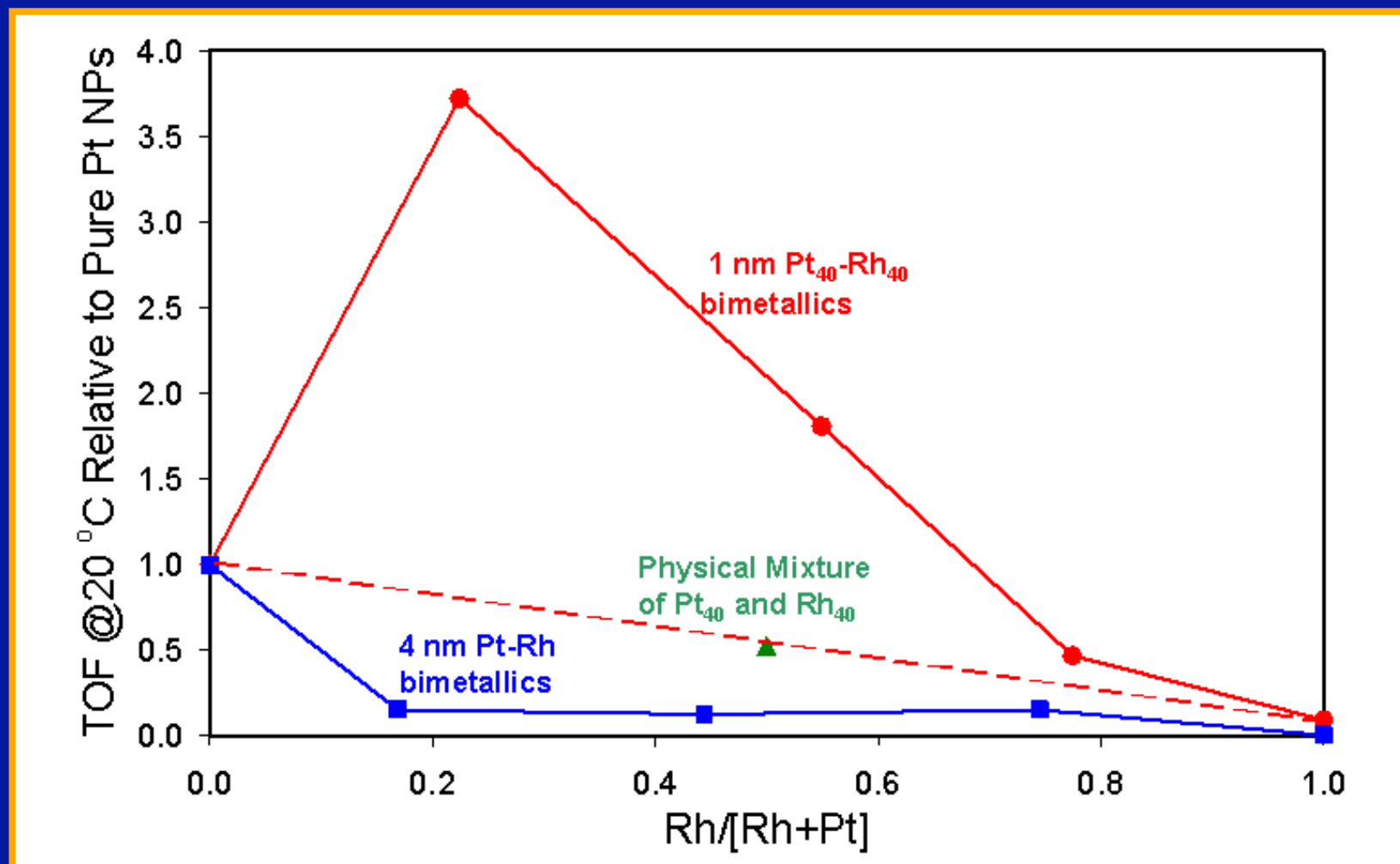
Case 7. $J_A = 200, J_B = 200$
 Onion-ring structure

CO Oxidation of Dendrimer Encapsulated 1 nm and PVP Capped 4 nm PtRh Bimetallic Nanoparticles



Reaction conditions were 10 Torr C₂H₄, 100 Torr H₂.
TOF was calculated based on 100 % metal dispersion.

Ethylene Hydrogenation of Dendrimer Encapsulated 1 nm and PVP Capped 4 nm PtRh Bimetallic Nanoparticles

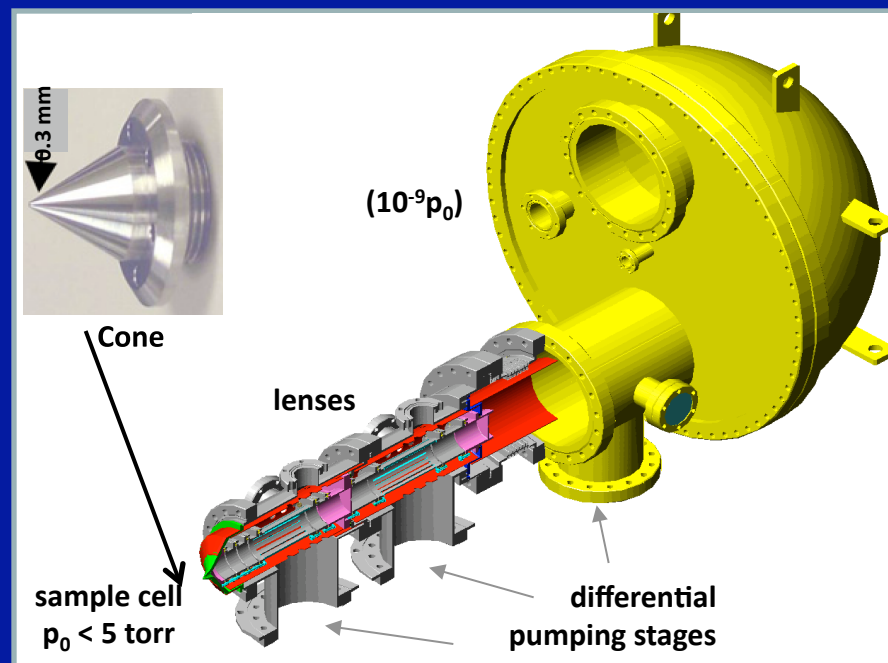
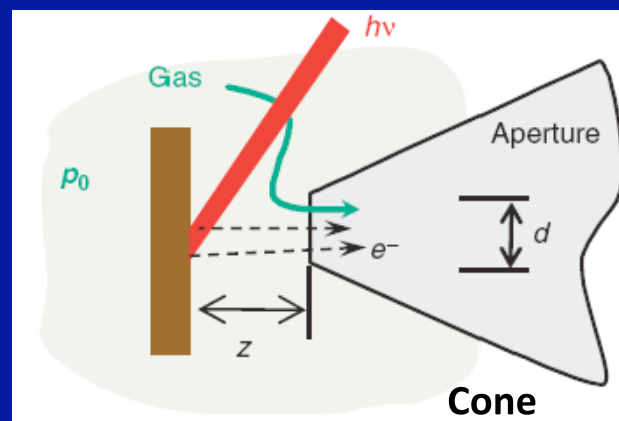
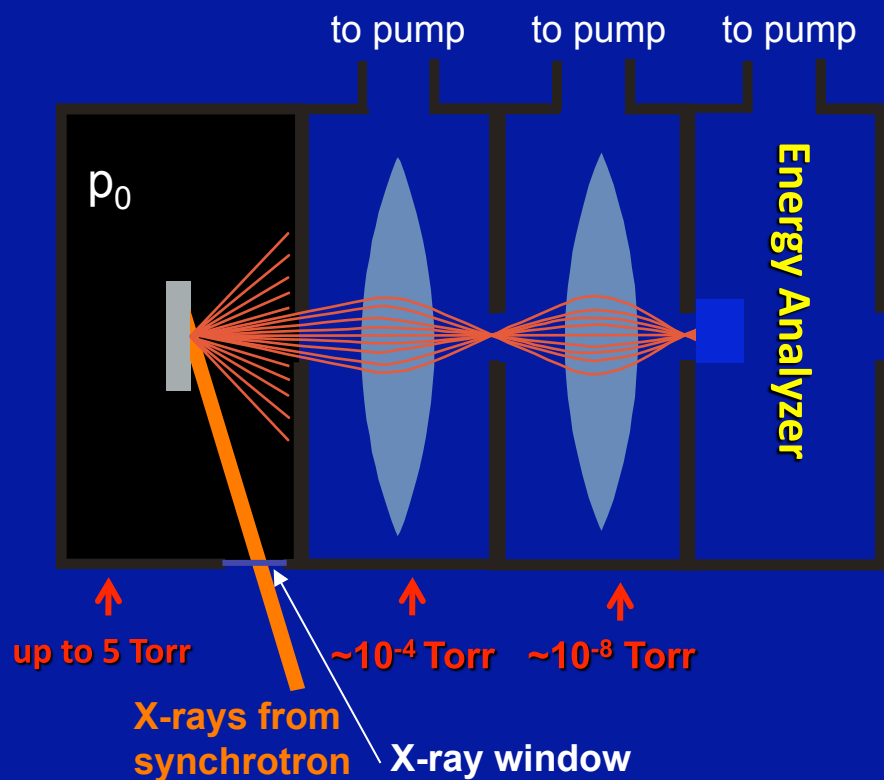


Reaction conditions were 10 Torr C₂H₄, 100 Torr H₂.
TOF was calculated based on 100 % metal dispersion.

Ambient Pressure X-Ray Photoelectron Spectroscopy

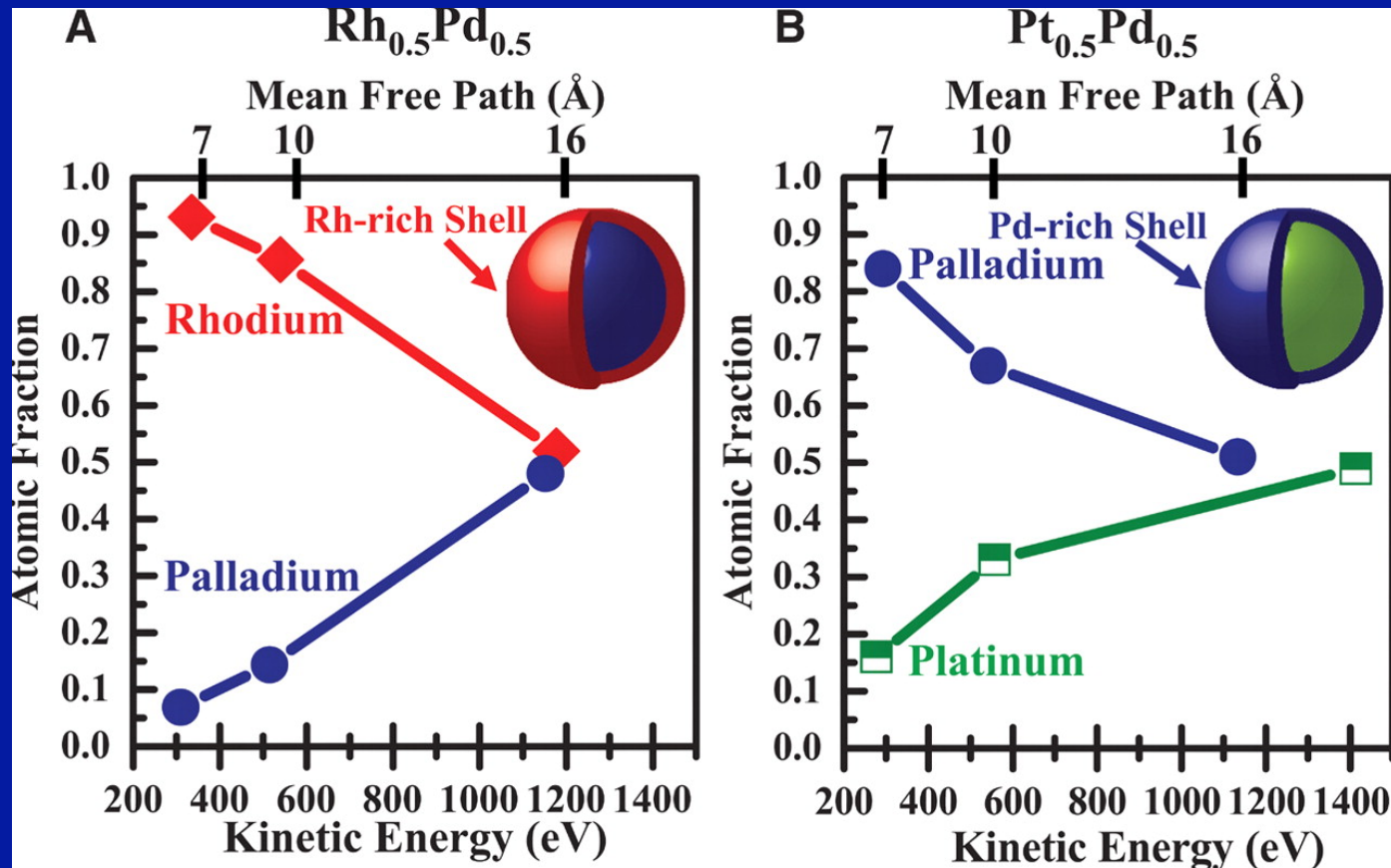
High Pressure XPS

Solutions: Capture electrons before they collide with gas molecules by means of differential pumping stages and focusing lenses



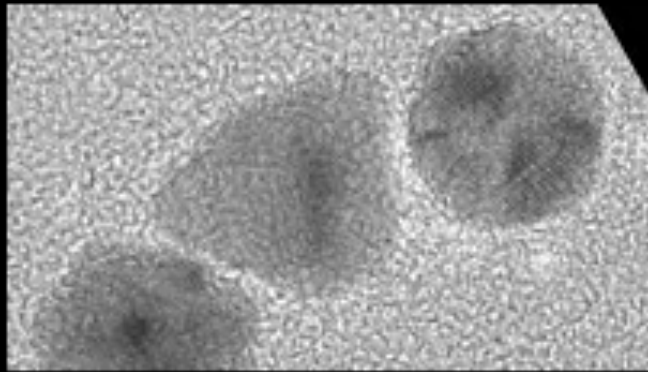
Surface Composition of Nanoparticles

Core-Shell Structure Probed by Synchrotron XPS

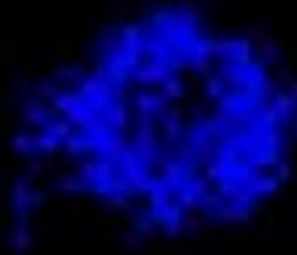


- 16 nm $\text{Rh}_{0.5}\text{Pd}_{0.5}$ nanoparticles form with a Rh rich shell
- 16 nm $\text{Pt}_{0.5}\text{Pd}_{0.5}$ nanoparticles form with a Pd rich shell
- XRD reveals only a single 50/50 alloy phase for both systems

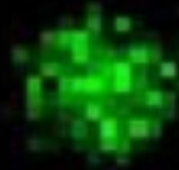
High Resolution TEM



Core-Shell Structured NPs



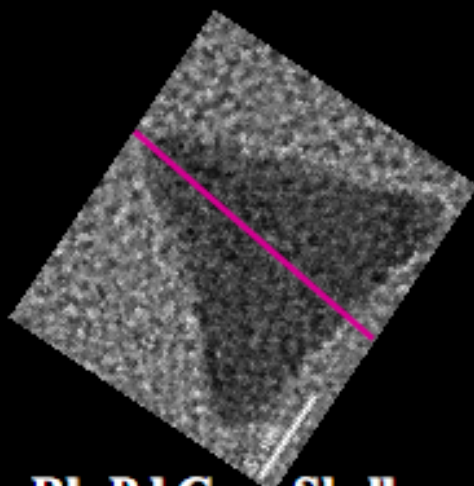
Rh K α 1



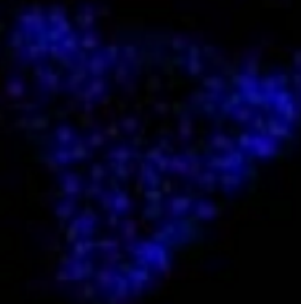
Pd K α 1



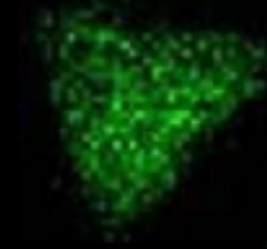
Core-Shell



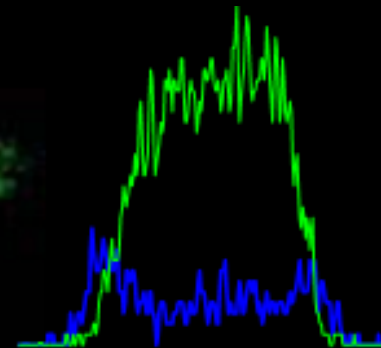
Rh-Pd Core-Shell



Rh K α 1



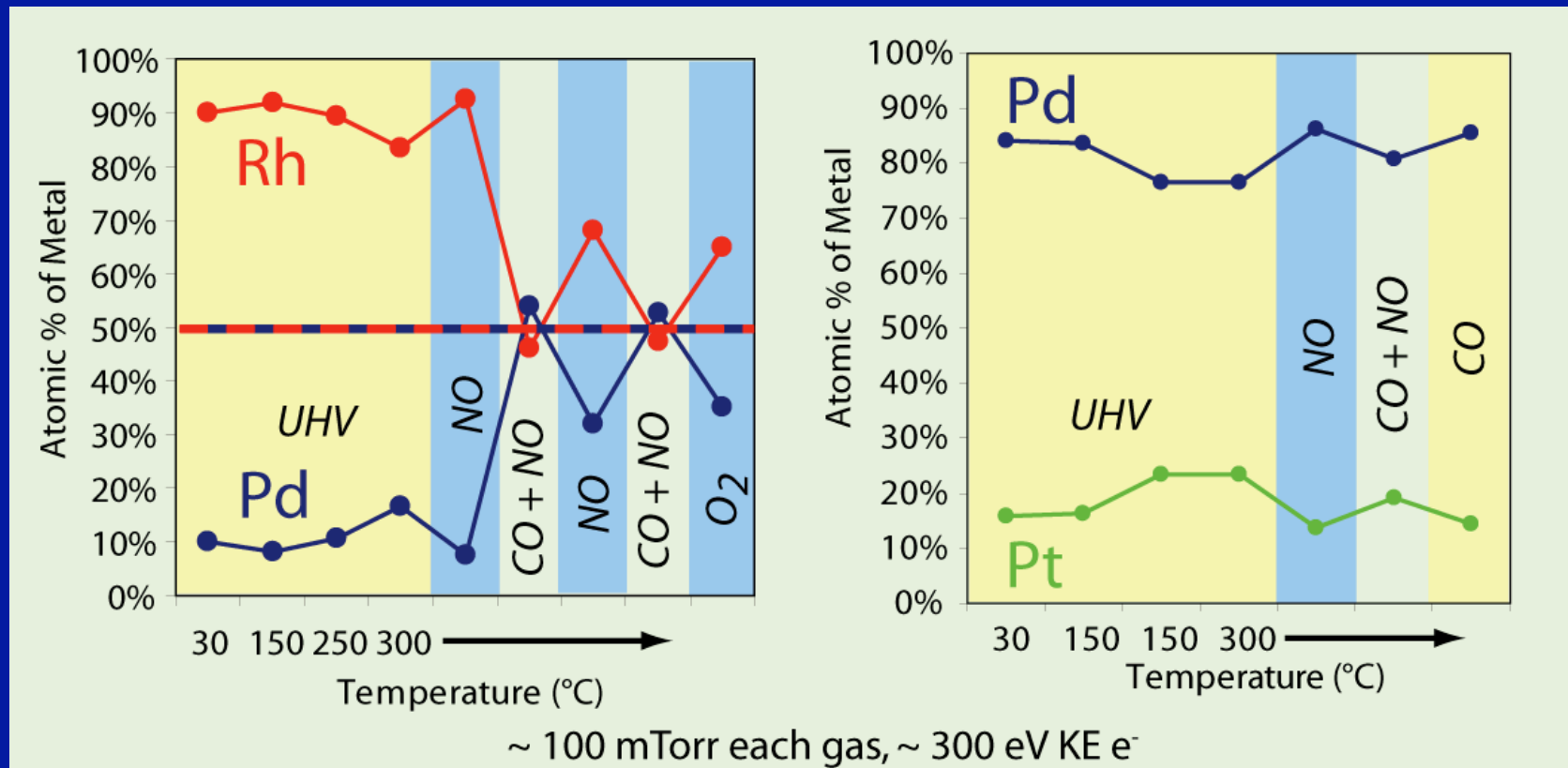
Pd K α 1



Line-scan

- Core-Shell structure confirmed with EDS mapping using STEM

Core-Shell Restructuring Probed by Ambient Pressure XPS



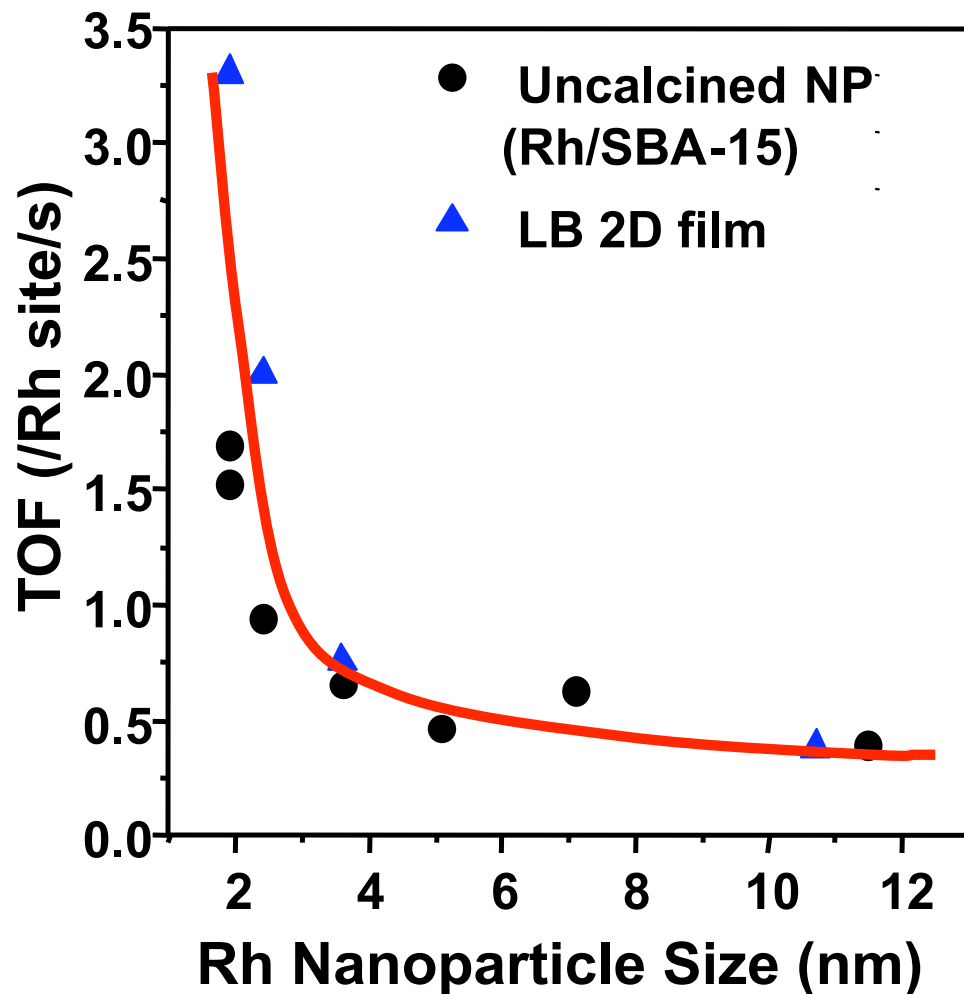
- Atomic diffusion within the nanoparticles results in surface composition changes as a function of ambient pressure
- Oxidation and Reduction at the nanoparticle surface is important

Molecular Factors of Catalytic Activity and Selectivity

- Surface Structure (Size, Shape)
- Surface Composition
- Reaction Intermediates
- Adsorbate-induced Restructuring
- Adsorbate Mobility
- Oxidation State
- Charge Transport

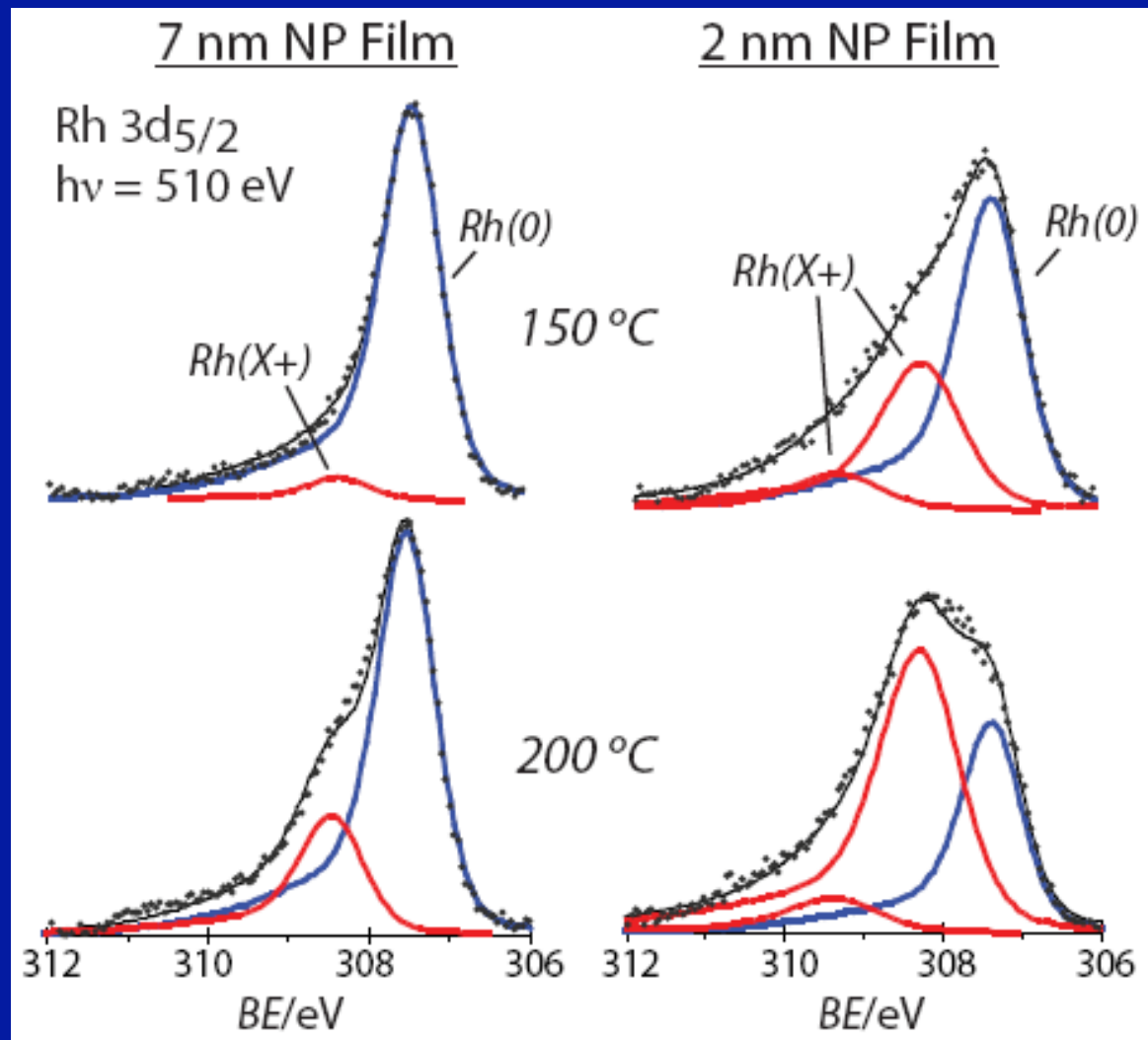
Size Dependence of CO Oxidation Activity

(100 Torr of O₂, 40 Torr of CO, and 443K)

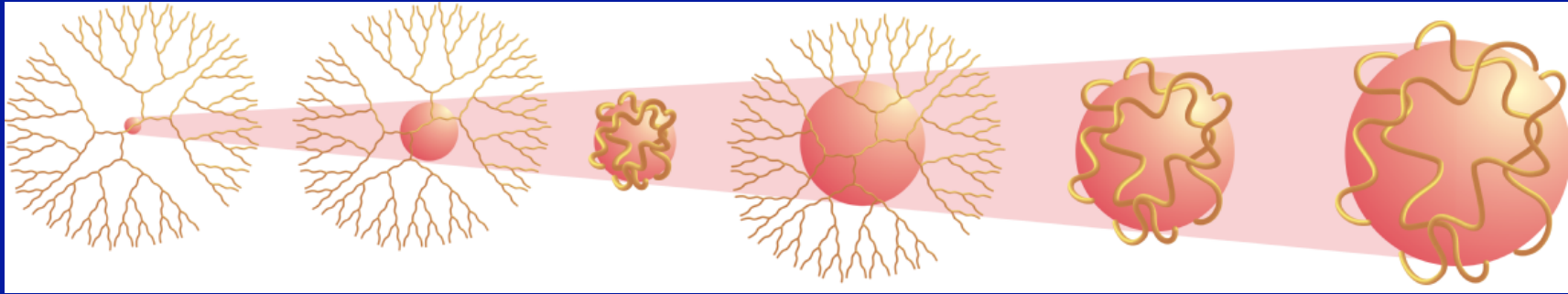


Rh Nanoparticles with size of 2-11 nm were used in this study

3D Rh nanoparticle catalysts (uncalcined Rh/SBA 15) exhibit particle size dependence, similar to Rh 2D LB (Langmuir-Blodgett) film



The Effect of Oxidation State Changes With the Size of Pt Nanoparticles



Size (nm):

0.8

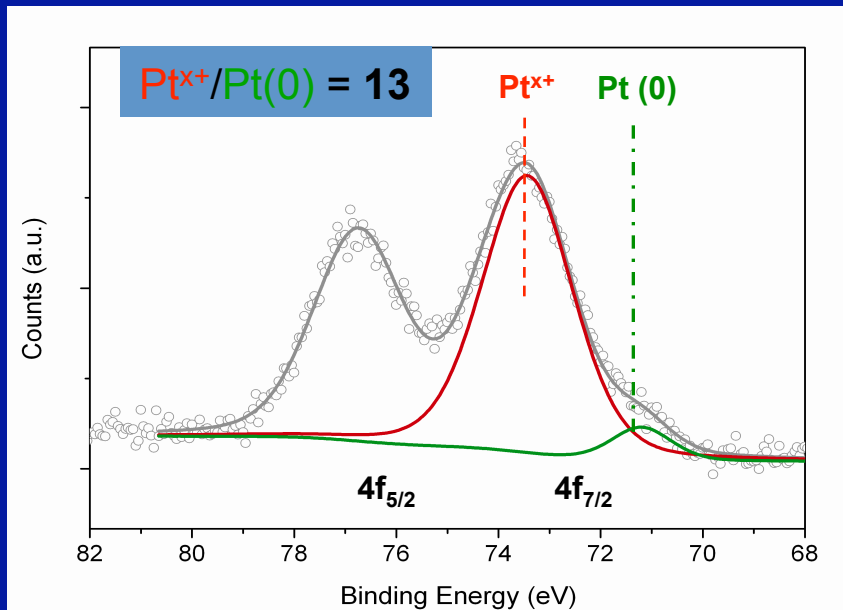
1.1

1.5

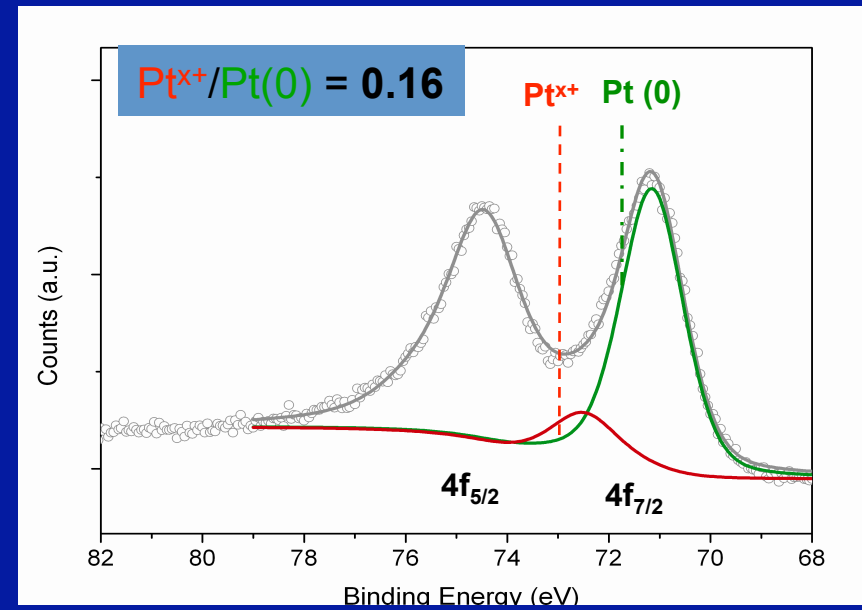
2.0

2.9

5.0



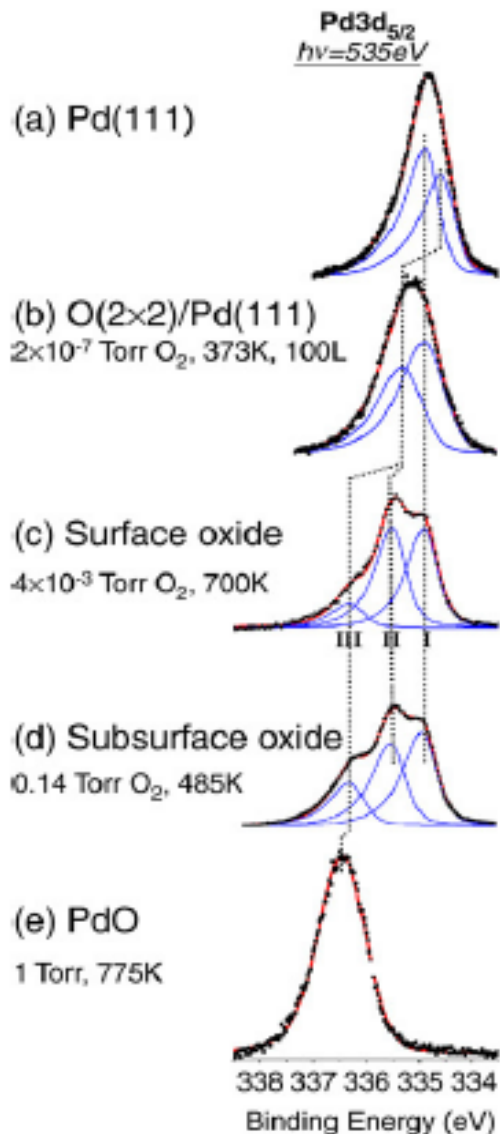
0.8 nm Pt Nanoparticles



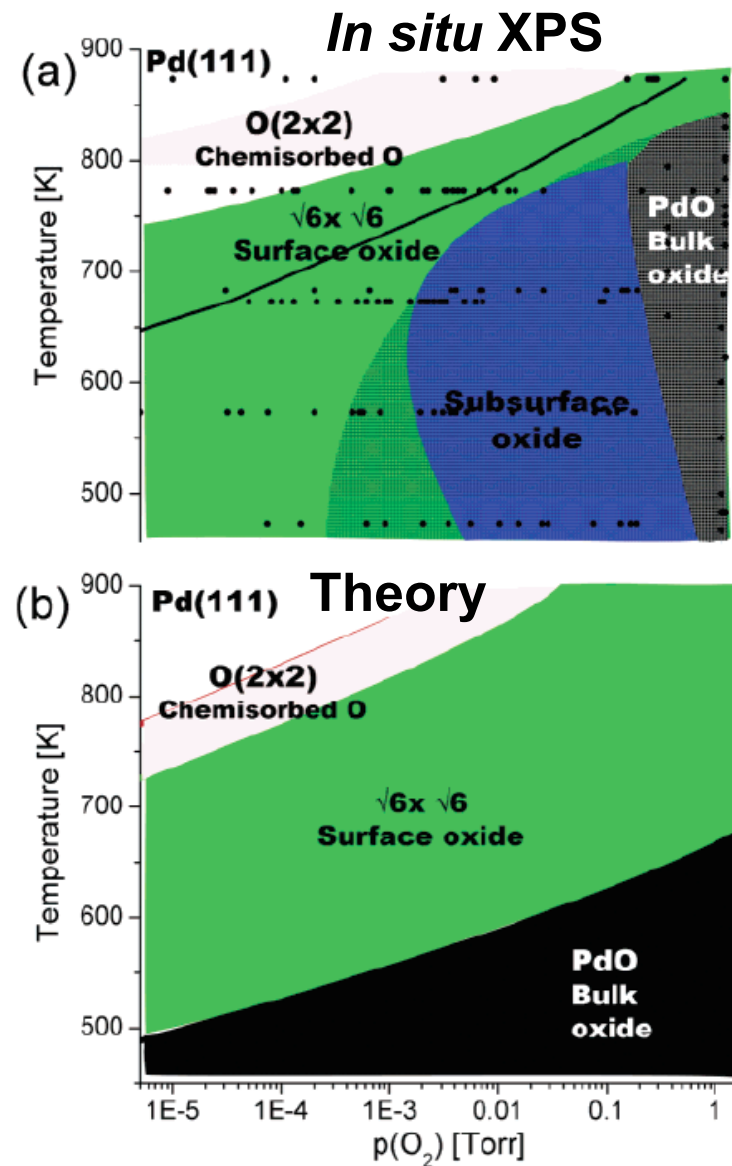
1.5 nm Pt Nanoparticles

For clarity, the deconvoluted peaks for Pt $4f_{5/2}$ are not shown in the XPS spectra.

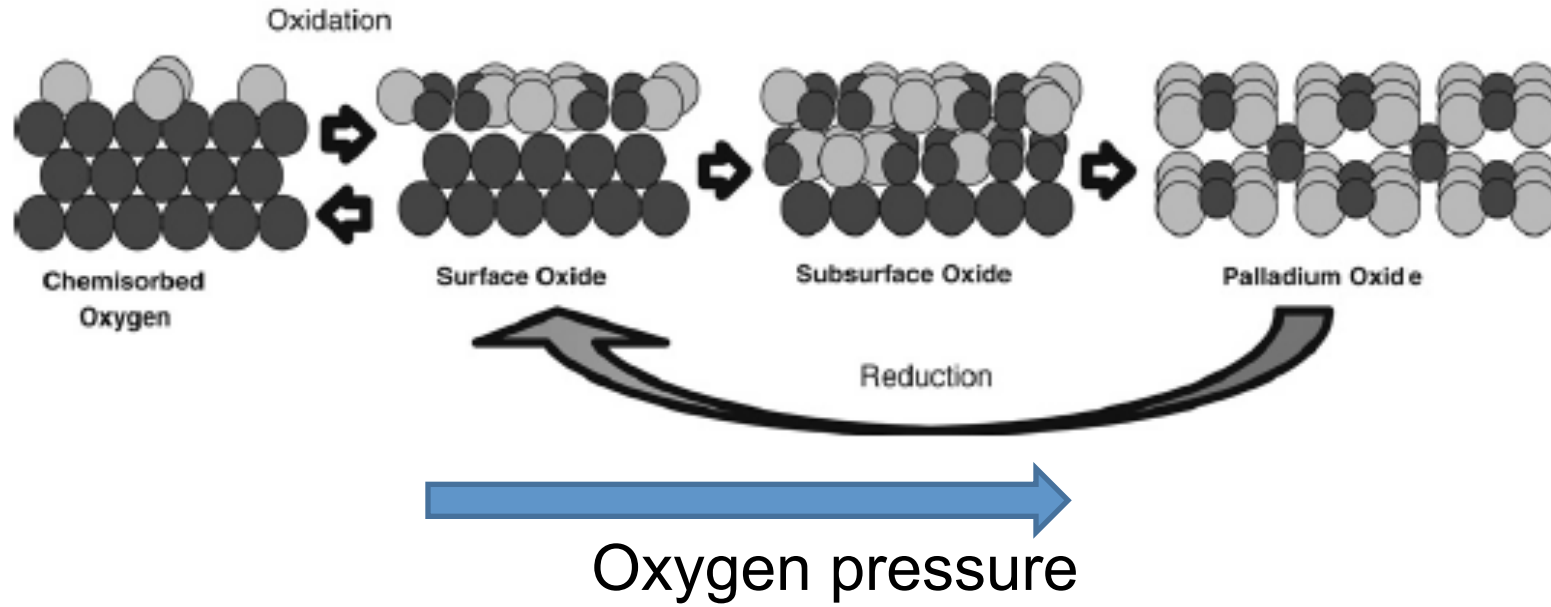
Oxidation of Pd(111)



- I. Bulk Pd
- II. Pd atom with two O neighbors
- III. Pd atom with four O neighbors



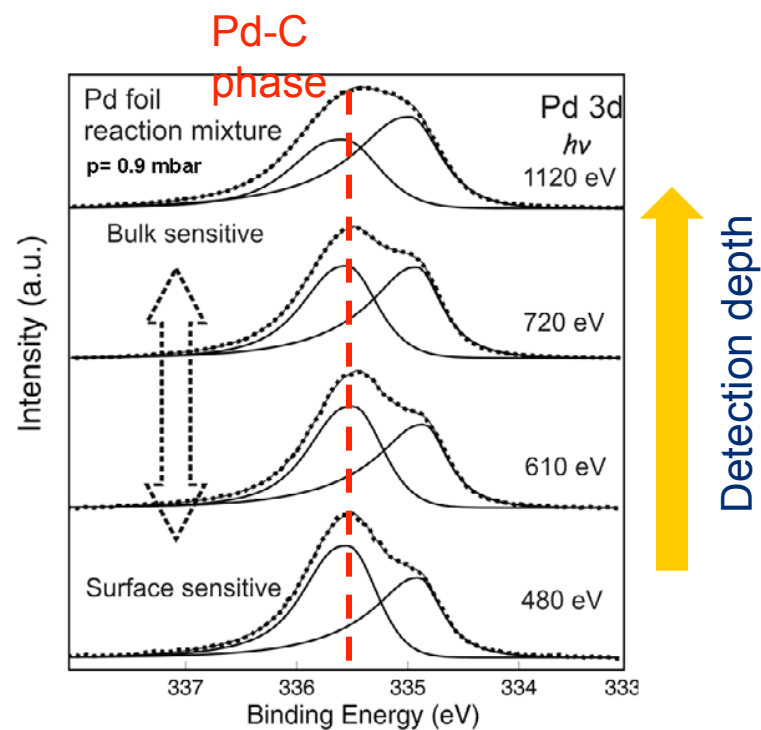
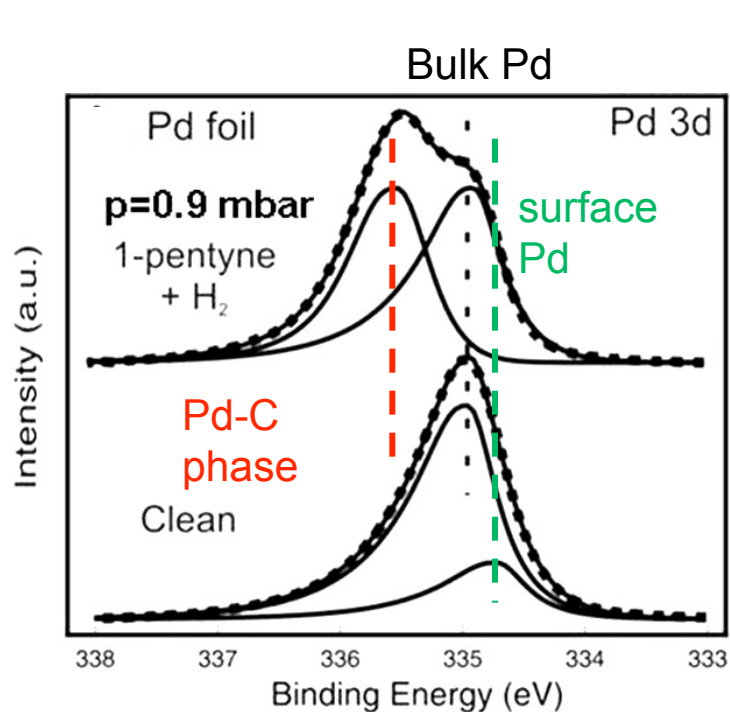
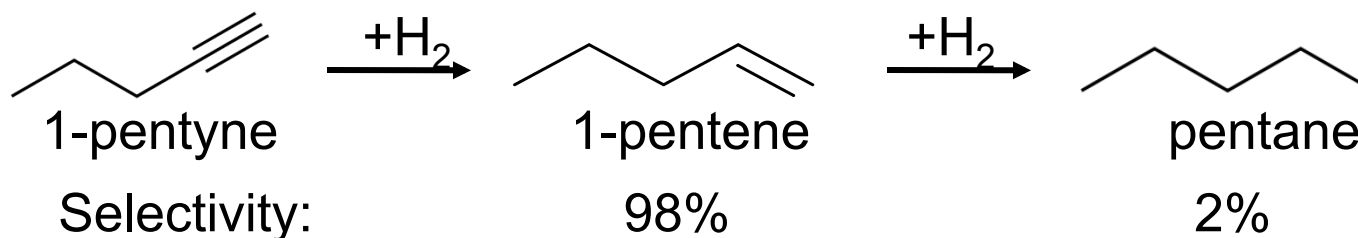
Oxidation of Pd(111) (Contd.)



The subsurface oxide is a metastable phase.

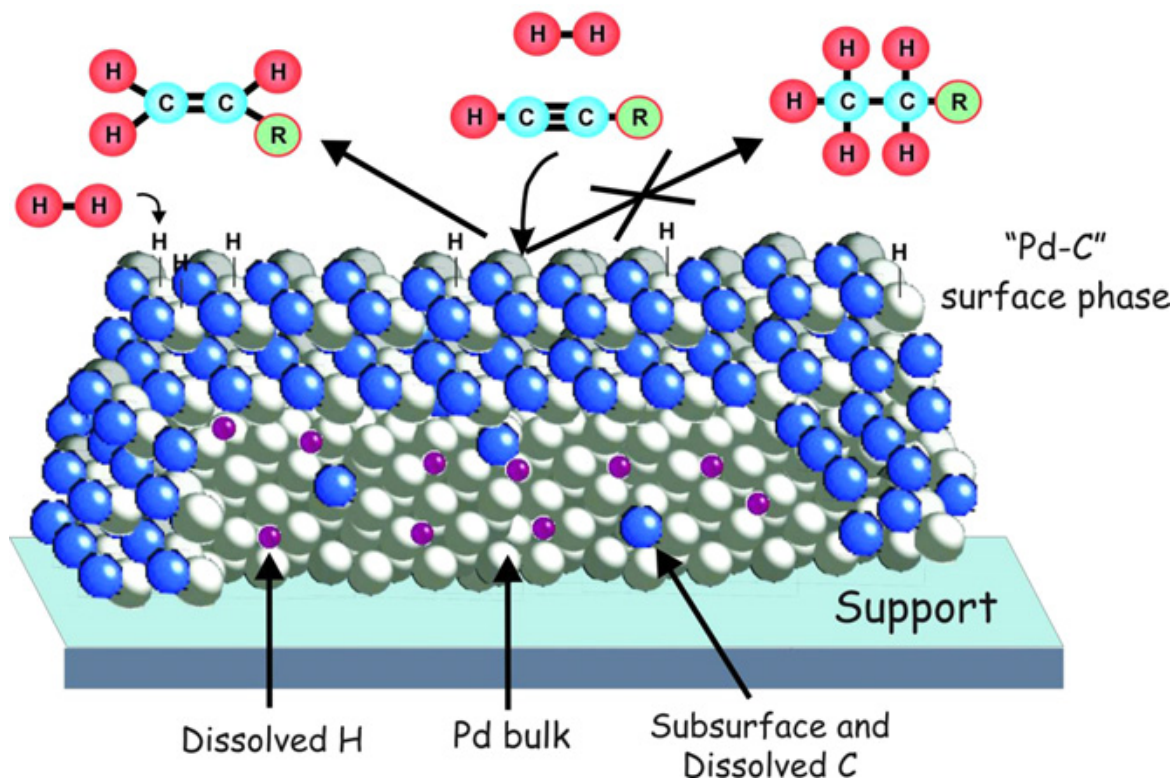
The role of Carbon Species in Heterogeneous Catalytic Processes

0.85 mbar H₂ + 0.05 mbar 1-pentyne at 358 K over Pd foil



Teschner D, et al, J. Catal. 242, 26 (2006)

The role of Carbon Species in Heterogeneous Catalytic Processes (contd.)



Formation of a carbon diluted Pd surface phase inhibited total hydrogenation of pentyne by the elimination of subsurface hydrogen participating in the reaction.

Molecular Factors of Catalytic Activity and Selectivity

- Surface Structure (Size, Shape)
- Surface Composition
- Reaction Intermediates
- Adsorbate-induced Restructuring
- Adsorbate Mobility
- Oxidation State
- Charge Transport

Metal-Semiconductor Nanodiode

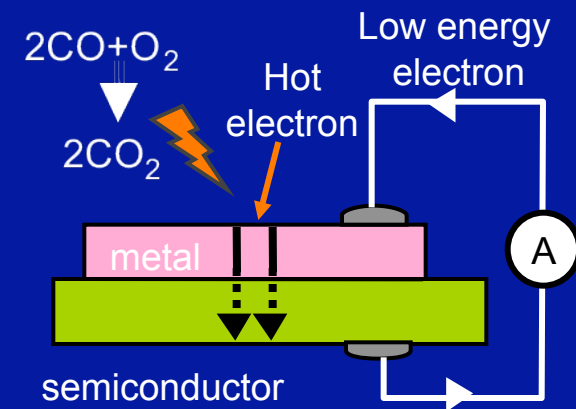
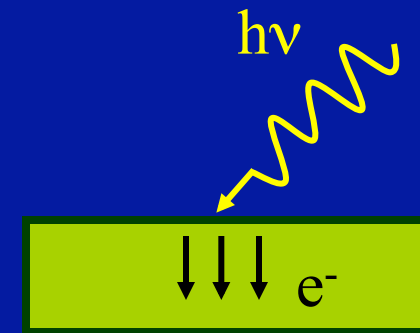
The Role of Hot Electrons in Catalysis Science

Hot Electron

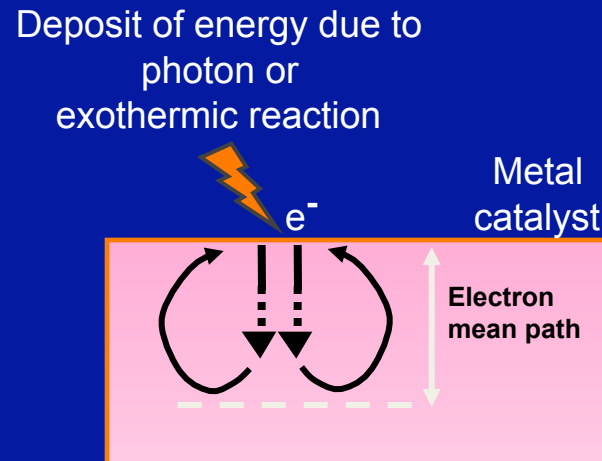
A hot electron is not in thermal equilibrium with the lattice

Creation of hot electrons

- Energy transfer from photon, energetic ions, exothermic chemical processes – through non-adiabatic energy dissipation
- Injection of hot electron with metal-insulator-metal junctions or STM tip



Mean Free Path of Hot Electrons in Metal Surfaces

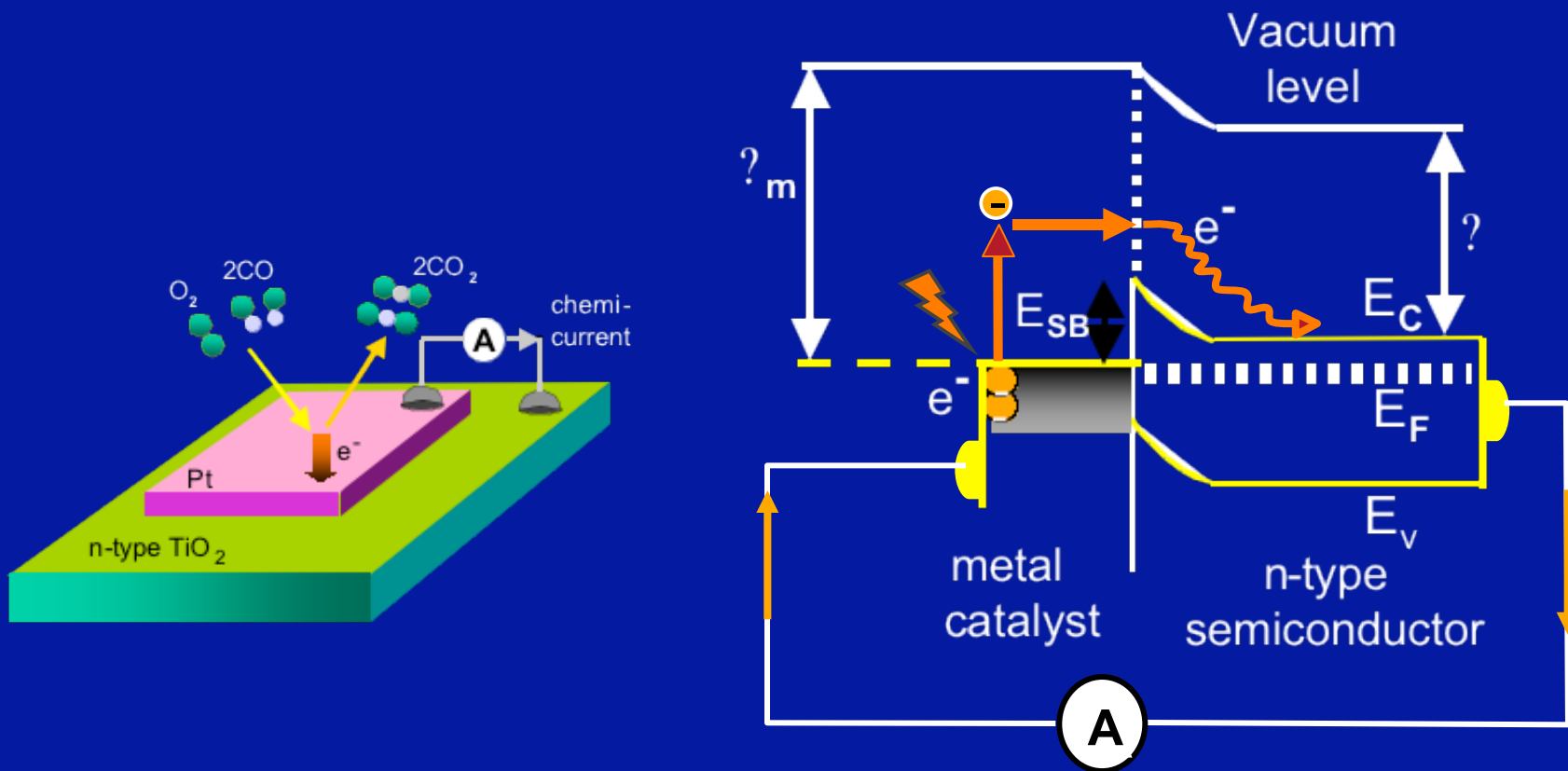


Ballistic Mean Free Path of Electrons at 1eV above E_f

- Gold 10-100 nm
- Copper 10-75 nm
- Palladium 3-9 nm
- Platinum 5-10 nm

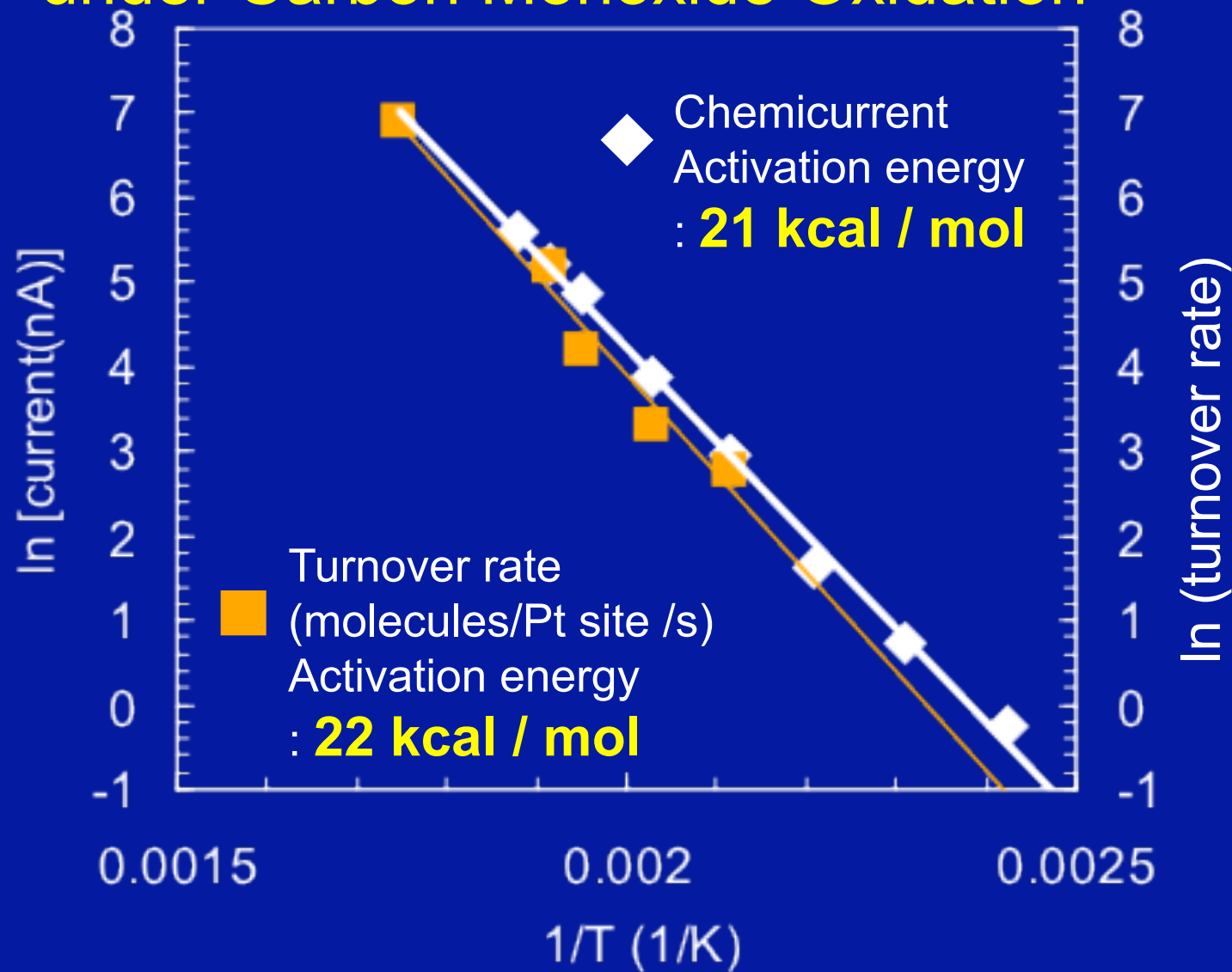
Inelastic mean free path at low energies given by $L \propto E^{-2}$

Hot electron generation by exothermic catalytic reactions (detection with Schottky diode under CO oxidation)



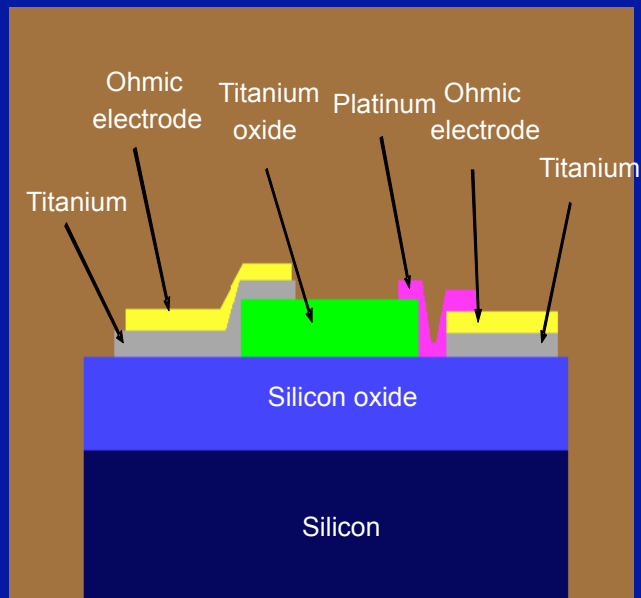
Schematic and energy diagram of catalytic nanodiode

Chemicurrent and Turnover Rate Measured under Carbon Monoxide Oxidation

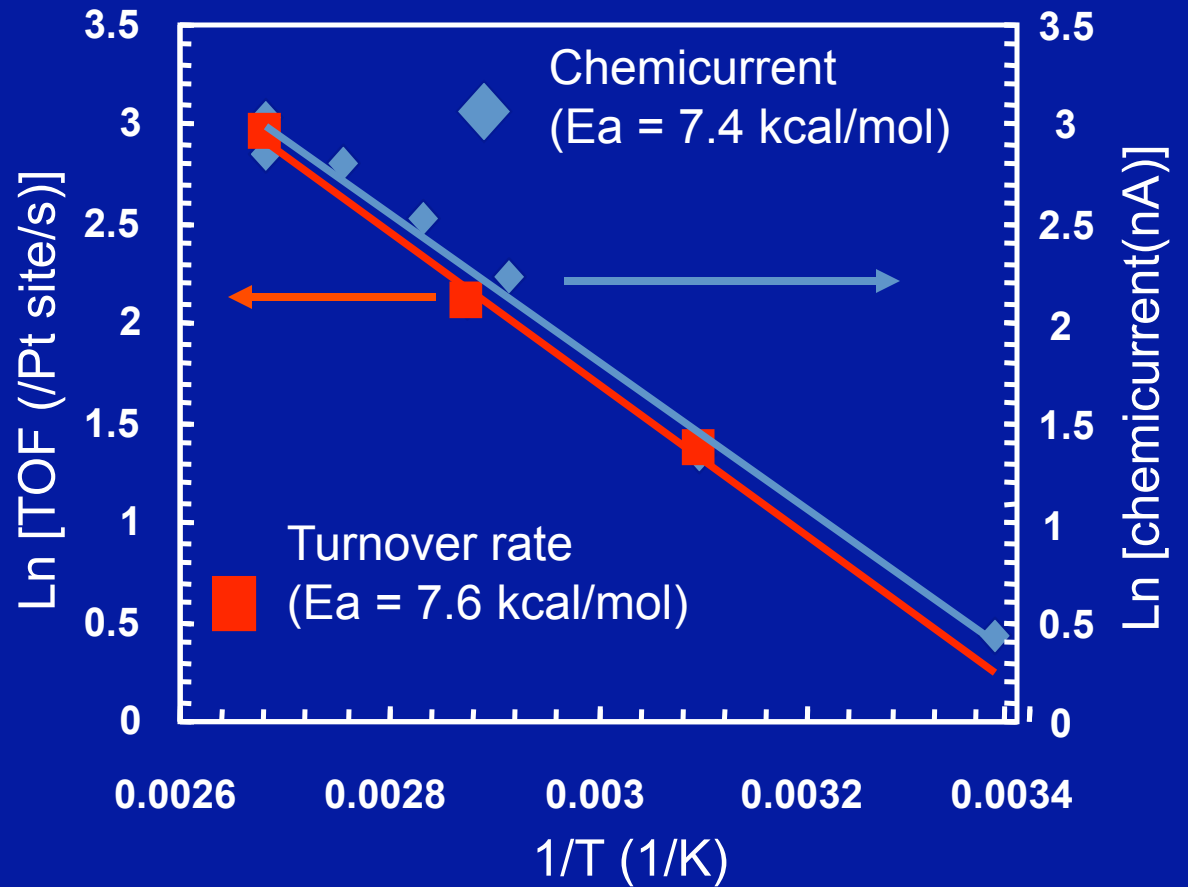


Chemicurrent and Turnover Rate Measured under Hydrogen Oxidation

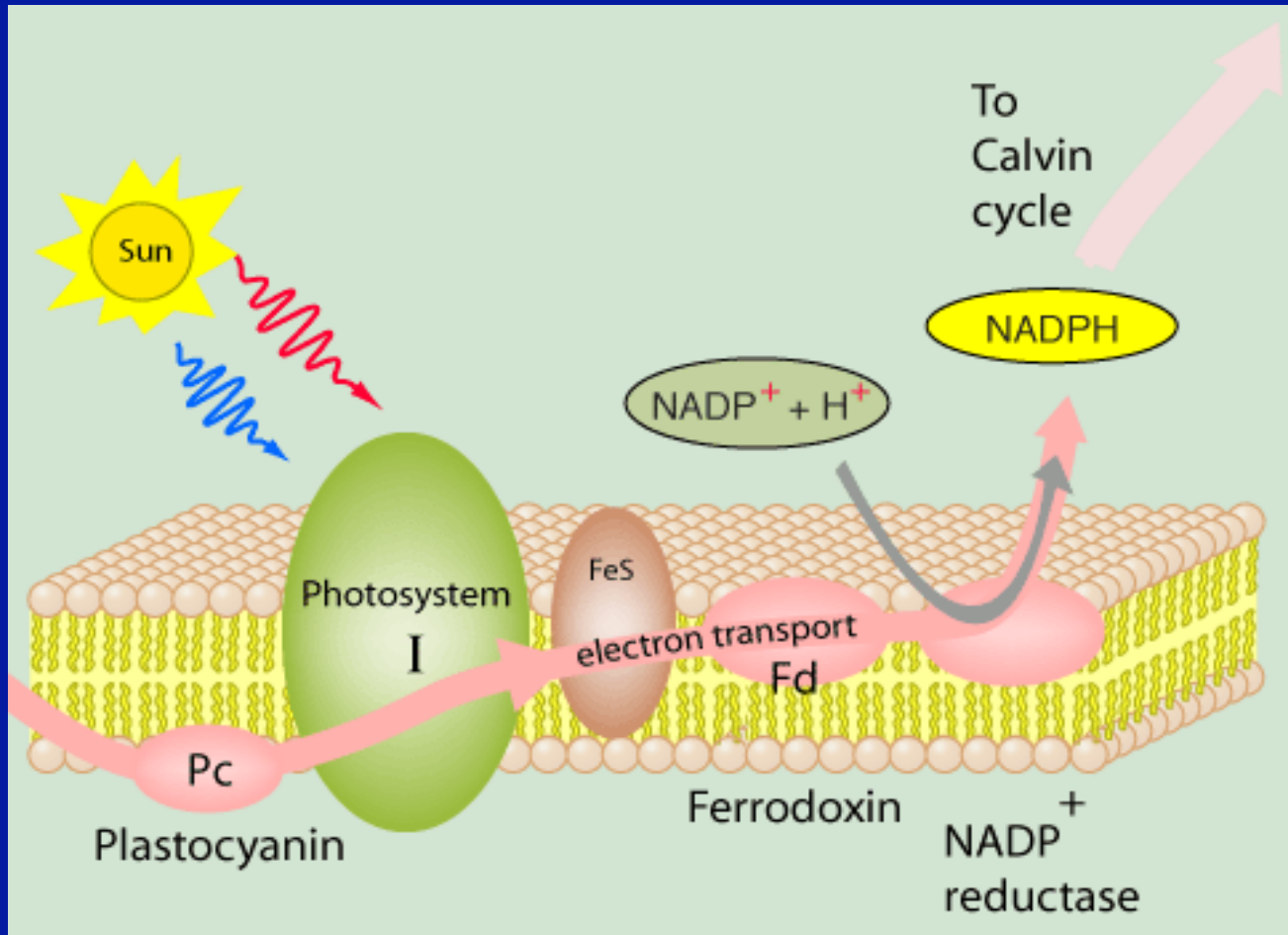
(with Pt/TiO₂ nanodiode and 700 Torr of O₂ and 6 Torr of H₂)



Scheme of Pt/TiO₂ nanodiode



Electron transport in Photosynthesis



<http://hyperphysics.phy-astr.gsu.edu/Hbase/Biology/psetran.html>

Moore R, Clark WD, Kingsley RS, and Vodopich D, Botany, Wm. C. Brown, 1995
Karp G, Cell and Molecular Biology, 5th Ed., Wiley, 2008

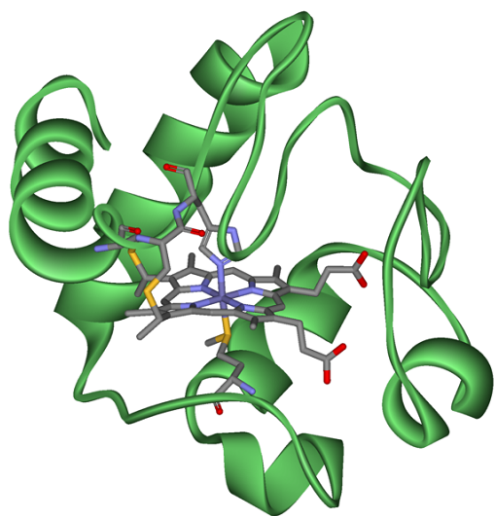
Molecular Factors of Catalytic Activity and Selectivity

- Surface Structure (Size, Shape)
- Surface Composition
- Reaction Intermediates
- Adsorbate-induced Restructuring
- Adsorbate Mobility
- Oxidation State
- Charge Transport

Future Challenges

Catalysts are Nanoparticles

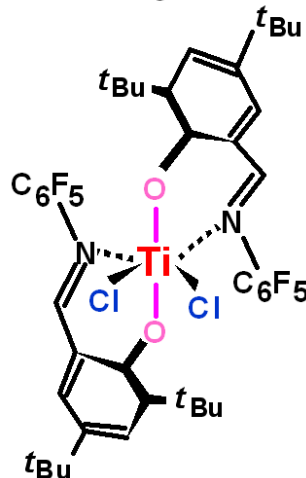
(a) Enzyme



Cytochrome C

Size: ~4 nm, 100 amino acids
Molecular weight: ~12,000 daltons

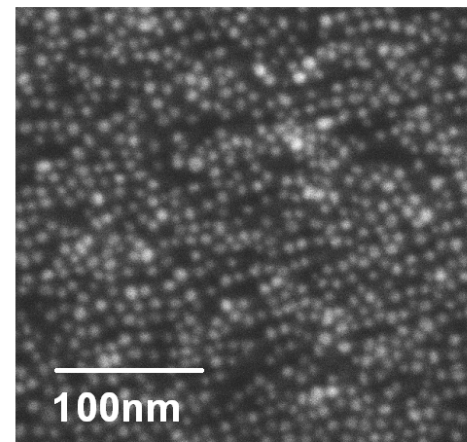
(b) Homogeneous catalysis



**Single-site olefin
polymerization catalyst**

Size : ~1.6 nm

(c) Heterogeneous catalysis



**Pt/Rh bimetallic
nanoparticles**

Size : 8 nm

Hybrid Systems

- Homogeneous – Heterogeneous
- Enzyme – Homogeneous
- Enzyme – Heterogeneous

Chemistry (Catalysis) of 10-40 Atom Clusters

(No Bulk Atoms)



Acknowledgement

Selim Alayoglu

Jim Krier

Cesar Aliaga

Hyun Sook Lee

Robert Baker

Yimin Li

Yuri Borodko

Russ Renzas

Derek Butcher

Hyungtak Seo

Antoine Hervier

Christoph Sprung

George Holinga

Feng Tao

Wenyu Huang

Chia-Kuang (Frank) Tsung

Sang Hoon Joo

Professor Dean Toste

Department of Energy